Technical Report HL-93-11
August 1993

US Army Corps
of Engineers
Waterways Experiment
Station

Grand and White Lakes Flood Control Project

Numerical Model Investigation

by Joseph V. Letter, Jr.
Hydraulics Laboratory

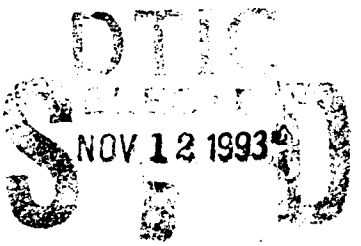

Prepared for U.S. Army Engineer District, New Orleans

Technical Report HL-93-11
September 1993

Grand and White Lakes Flood Control Project

Numerical Model Investigation

by Joseph V. Letter, Jr.
Hydraulics Laboratory

U.S. Army Corps of Engineers
Waterways Experiment Station
3909 Halls Ferry Road
Vicksburg, MS 39180-6199

Final report

Approved for public release; distribution is unlimited

Prepared for U.S. Army Engineer District, New Orleans
New Orleans, LA 70160-0267

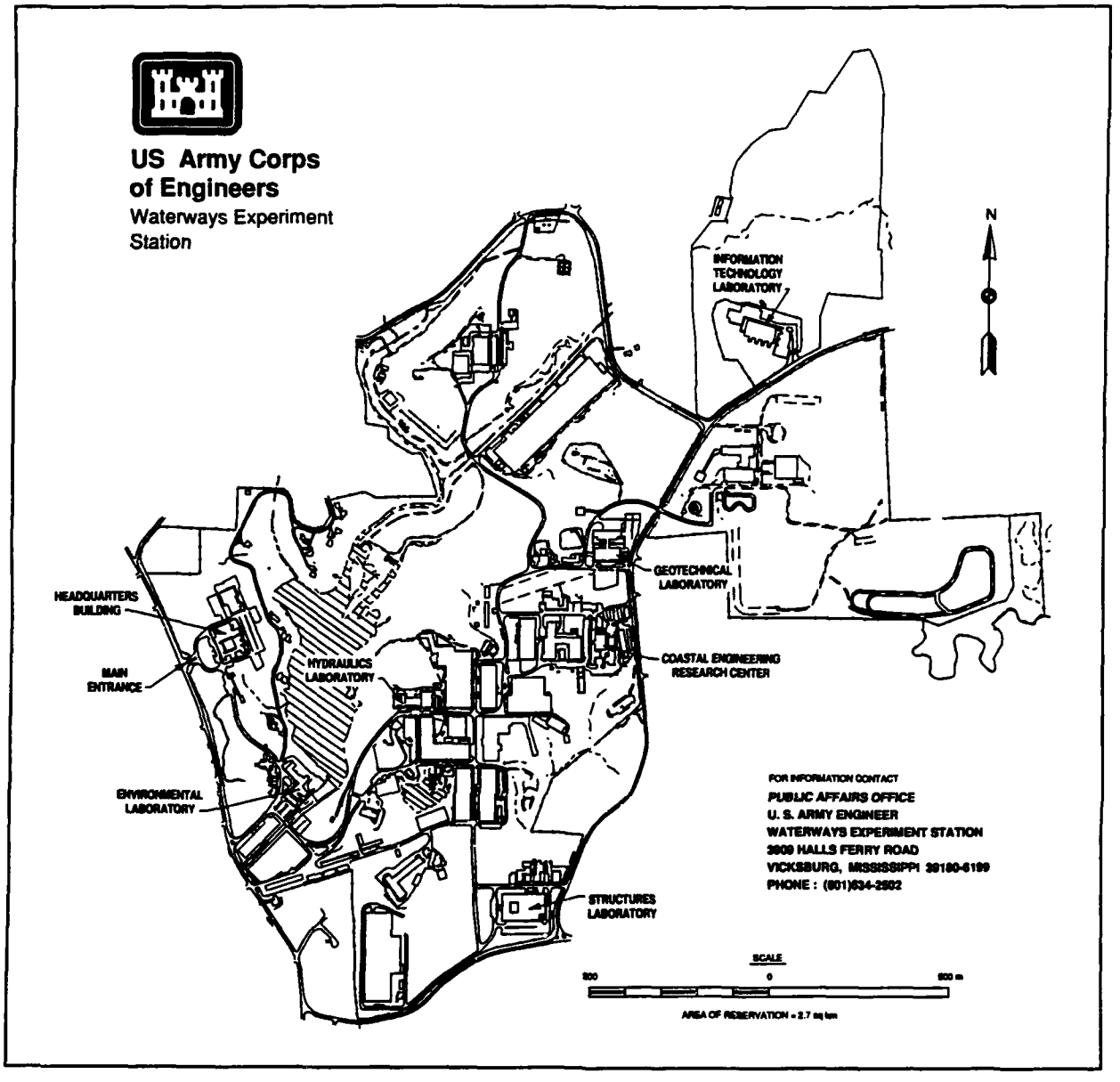

Waterways Experiment Station Cataloging-in-Publication Data

Letter, Joseph V.
Grand and White Lakes Flood Control Project: numerical model investigation / by Joseph V. Letter, Jr.; prepared for U.S. Army Engineer District, New Orleans.
124 p.: ill.; 28 cm. -- (Technical report; HL-93-11)
1. Flood control -- Louisiana -- Mathematical models. 2. Flood routing. 3. Saltwater encroachment -- Louisiana. 4. Wetland conservation -- Louisiana. I. United States. Army. Corps of Engineers. New Orleans District. II. U.S. Army Engineer Waterways Experiment Station. III. Title. IV. Series: Technical report (U.S. Army Engineer Waterways Experiment Station); HL-93-11.
TA7 W34 no.HL-93-11

Contents

Preface

The work reported herein was performed during the period 1986-1992 in the Hydraulics Laboratory (HL) of the U.S. Army Engineer Waterways Experiment Station (WES) for the U.S. Army Engineer District, New Orleans (LMN). Messrs. Cecil Soileau and Burnell Thibodeaux were the LMN Engineering Division liaisons during this study. Mr. Stan Green was the LMN Planning Division project manager for the overall study. This report presents the results of the numerical modeling work in support of the Grand and White Lakes flood control project.

The investigation was conducted under the direction of the following HL staff members: Messrs. F. A. Herrmann, Jr., Director; R. A. Sager, Assistant Director; W. H. McAnally, Jr. , Chief, Estuaries Division (ED); Joseph V. Letter, Jr., Former Chief, Estuarine Simulation Branch, ED; G. M. Fisackerly, Chief, Estuarine Processes Branch, ED; W. D. Martin, Chief, Estuarine Engineering Branch, ED; and project managers Mrs. *Tamsen Smith Dozier, for*merly of Estuaries Division, and Mr. Letter, Estuarine Processes Branch. The work was performed by Mrs. Dozier; Mr. Ben Brown, Estuarine Simulation Branch; Dr. Jerry Lin, Estuarine Engineering Branch; Mr. Letter; and Dr. Ian P. King, Resource Management Associates, Inc. (under contract). This report was prepared by Mr. Letter.

At the time of publication of this report, Director of WES was Dr. Robert W. Whalin. Commander was COL Bruce K. Howard, EN.

Conversion Factors, Non-SI to SI Units of Measurement

Non-SI units of measurement used in this report can be converted to SI units as follows:

Multiply	By	To Obtain
cubic feet	0.02831685	cubic meters
feet	0.3048	meters
inches	2.54	centimeters
miles (U.S. statute)	1.609347	kilometers
square miles	2.589998	square kilometers

1 Introduction

Background

The Mermentau River is the primary tributary to the Grand and White Lakes area of Louisiana, which provides fresh water for local agriculture for, livestock and for wildlife productivity (see Figure 1). Hydraulic control structures within the system prevent higher salinities from intruding into sensitive areas. These features also restrict the passage of flood flows from the lower Mermentau River basin to the Gulf of Mexico. Additional structural features are being considered to reduce flood stages.

Objective

The objective of this study is to evaluate the effectiveness of structural alternatives for providing flood control benefits. The study addresses the impact of proposed marine organism ingress structures on salinity intrusion. Quantitative evaluations are used to estimate project benefits.

Approach

A comprehensive numerical model of hydrodynamics and salinity intrusion in the study area and adjacent waterways was developed. This report describes the modeling tools and summarizes the results of the application of the models to the design alternatives.

2 Description of the System

The project area is located on the Louisiana coast southwest of Lafayette, Louisiana and south-southeast of Lake Charles, Louisiana. The primary study area spans 80 miles[1] in the east-west direction and 40 miles in the north-south direction (see Figure 1).

Wetland Characteristics

The wetland within the study area is quite variable. The areas north of and between Grand and White Lakes are covered with dense marsh grass. The regions southeast of White Lake are shallow intermittent grassy swamp, with low brush. South of the lakes the wetland is fragmented open water. High ridges support willow trees. Intermediate levels that intermittently wet support low brush that give way to grasses at lower elevations.

The wetlands are interlaced with natural meandering bayous and manmade canals. The canals are flanked by high ground, created during canal excavation, with higher vegetation type.

The wetlands are either storage areas adjacent to a primary channel, or open broad expanse with many smaller channels. The storage wetlands are filled when water overtops the primary channel as flood levels rise. The waters then drain back to the primary channel as the flood levels recede. The broad open wetlands are characteristic of the tidal portions of the system. Open wetlands also produce sheet flows in response to local rainfall.

Hydrology

The Mermentau River is formed at the confluence of several bayous (des Cannes, Nezpique and Plaquemine Brule) which drain a combined drainage area of approximately 2,800 square miles (see Figure 2) above the Intracoastal

[1] A table of factors for converting non-SI units of measurement to SI units is presented on page v.

Waterway. The average annual peak discharge is estimated to be 31,600 cfs at the Gulf Intracoastal Waterway (GIWW). The 50-year peak flow is 72,200 cfs.

To the east of the Mermentau River basin is the Vermilion River basin which has a drainage area of approximately 560 square miles. The Atchafalaya River is farther east with two primary outlets to the Gulf: Wax Lake Outlet and the Lower Atchafalaya River. Both enter the Atchafalaya Bay. Atchafalaya River freshwater has an influence on salinities for a considerable distance to the west, through East and West Cote Blanche Bays, Vermilion Bay and through the open Gulf of Mexico.

To the west of the study area is the Calcasieu River with a drainage area of approximately 3,800 square miles. The Calcasieu River flows through Calcasieu Bay and connects with the Gulf via a confined channel through the shoreline ridges.

Flood events on the Mermentau basin are associated with local rainfall. The average annual rainfall for the basin is approximately 60 inches. Short-term storms produce up to 20 inches in a single day (US Army, 1987). Most of the extreme flood events on record are associated with tropical storms and hurricanes.

Annual low flows occur in the late summer to fall, with October having the lowest monthly flows. The lowest mean monthly flows are 397 cfs for Bayou Nezpique and 122 cfs for Bayou Des Cannes. (The period of record for these statistics is 1971 - 1985). The mean low flows for October during that period were only 156 cfs for Bayou Nezpique and 39 cfs for Bayou Des Cannes.

For the needs of the current study there was insufficient gaging data to adequately estimate a flood-frequency curve for the basin. This information is important for accurately estimating the benefits associated with possible design alternatives. This problem is addressed by applying a rainfall runoff model.

Tidal Influences

The Mermentau River is tidal downstream of the Catfish Point control structure. During low river flows the system upstream of the closed control structures can be viewed as a large storage basin with no tidal influence. At higher river flows when the structures are opened tidal effects are temporarily reduced in a local portion of the system. When Gulf water levels are abnormally high tidal influences and salinity intrude through the myriad of small bayous and canals. This intrusion has a minor influence on the primary lakes and inland waterways.

The mean tide range at the Gulf coast is approximately 2.0 ft. The average spring tide range is 2.9 ft. The mean tide range in Vermilion Bay is 1.5 ft. The lower Mermentau River mean tide is amplified to 2.5 ft.

Regional and seasonal rises in the mean Gulf level increase tidal water levels in the lower portions of the system. The existing control structures are then unable to maintain water levels in the upper basin and fail to control salinity intrusion.

Meteorology

Meteorology has a significant influence on the hydrologic, hydraulic and salinity conditions of the system. The influence of rainfall on the hydrology has been mentioned as well as the influence of changes in the mean Gulf level. The variations in Gulf level are typically in response to regional weather patterns. Wind stresses move large volumes of water in the shallow coastal zone. These variations can be very dramatic in response to frontal passages which have rapid changes in wind direction with relatively high wind speeds. East-west winds influence water levels within the upper basin. Wind shear in the wetland areas is reduced by local vegetation and other barriers to flow.

The average wind speed at Lake Charles, La. is southerly at 8.7 mph. Hurricane gusts may exceed 100 mph.

Waterways

There are numerous navigable waterways of importance to the hydraulics of the system. The Gulf Intracoastal Waterway (GIWW) channel runs east-west with a channel dimension of 12 ft by 125 ft (Figure 1). The GIWW is flanked on the north side by storage wetland, while the south side is flanked by open wetland. The Vermilion River channel (9 ft by 100 ft) runs from Vermilion Bay up the Vermilion River to Lafayette, La. The Freshwater Bayou channel (10 ft by 125 ft) connects the Gulf of Mexico with the GIWW at Intracoastal City. The Inland Waterway (5 ft by 40 ft), sometimes called the Old GIWW, runs from near the intersection of the Mermentau River and the GIWW southwest through Grand and White Lakes and then Schooner Bayou to connect with Freshwater Bayou east of White Lake. Calcasieu River and Pass Ship Channel is 42 ft by 800 ft from deep water in the Gulf to protected waters and 40 ft by 400 ft through Calcasieu Lake and River to Lake Charles, La (mile 34.1). From mile 34.1 to 36.0 the project is 35 ft by 250 ft.

The Mermentau River navigation channel is 9 ft by 100 ft from the Gulf through Grand Lake and the Mermentau River to Mermentau La. The channel then branches and extends up Bayou Nezpique to near Panchoville, and up Bayou Des Cannes to north of Evangeline, La. A side channel of the Mermentau River, with 9 ft by 100 ft dimensions, runs up Bayou Queue de Tortue to Riceville. A channel 8 ft by 60 ft runs from Bayou Plaquemine to Crowley, La. In addition the Mermentau River Project provides for a 3000 ft^2 channel cross-section for flood control.

The Warren Canal, provides freshwater for local irrigation although a navigation channel is not maintained here. It provides a conveyance path for salinity intrusion at extremely low river flows.

Barriers to Flow

There are many natural and man-made barriers to flow within the study area. The old barrier island ridges run east-west along the Gulf shoreline. These ridges are staggered inland from the Gulf. Examples are Little Cheniere Ridge just west of Grand Lake and Grand Lake Ridge on the northeast side of Calcasieu Lake.

There are a number of highways which restrict flows. Highway 82 runs east-west along most of the Grand Cheniere Ridge, crosses the Mermentau River at Grand Cheniere and turns northward on the eastern side of White Lake. This highway creates a significant barrier to sheet flow through the marshes. Midway between Grand Lake and Calcasieu Lake, Highway 27 runs north-south restricting the east-west flow of water. There are periodic culverts and canals under the highways. Canals created during the construction of the roads enhance the flow of water parallel to the roadway.

Control Structures

There are five major structures in the study area (Figure 3). These structures control the intrusion of saline waters into the upper basin and produce water levels suitable for irrigation and wildlife productivity. Two of the structures are locks on the GIWW. These structures are located at Intracoastal City just east of the Vermilion River (Leland Bowman Lock) and the Calcasieu Lock located on the north side of Calcasieu Lake near Highway 384. The third lock is located on Freshwater Bayou about a mile from the Gulf of Mexico.

In addition to the locks there are two flow control structures. The Catfish Point control structure is located on the southwest side of Grand Lake on the Mermentau River. Schooner Bayou control structure is located east of White Lake on the Inland Waterway through Schooner Bayou. The control structures are used to maintain water levels in Grand and White Lakes and adjacent wetlands at optimum seasonal levels.

The pertinent design dimensions of the control structures are presented in Table 1. The structures are closed during low flow periods to reduce salinity intrusion. The locks operate during those periods in a normal locking mode of operation. When flood flows are occurring the structures are opened for unimpeded passage of flood waters. All operations of the structures are coordinated to optimize water levels within the upper basin.

Salinity Intrusion

Salt water intrusion into the study area reduces the availability of freshwater for irrigation, livestock and wildlife productivity. Salinity intrusion can occur through surface water and groundwater. Generally, the waters downstream of the control structures are brackish. During low river flows tidal exchange increases salinities on the downstream side of the structures. Operation of the structures for navigation then results in measurable salinity levels in the upper basin.

3 Technical Approach

Field Data Collection

To support the numerical model study a field data collection effort was undertaken. The data collection included water surface elevations, salinities, water temperature and current speed and direction. Water surface elevations were monitored at 10 locations and velocities, salinities, and temperatures at 11 stations (Figure 4). The monitoring program covered the period of November 1986 through December 1987. A full description of the field data collection and data is presented by Benson (1993).

Modeling Needs

Accurate estimate of project benefits for design alternatives requires evaluation of their hydraulic and salinity intrusion performance. This quantitative expectation combined with the complex physical setting led to the need for a numerical model study.

The complexity of the system geometry influences the selection of an appropriate numerical model. A link-node model was considered during the formulation of the technical approach. However, its inability to handle complex geometric features and two-dimensional aspects of sheet flow with realism made it a poor choice. Because of the extremely large geographical area to be modeled a conventional two-dimensional (2D) model would create a large numerical mesh that could prove intractable from a computational requirement.

Many of the system features can be represented as one-dimensional channels (1D) or as 1D channels with off-channel storage. This includes most of the Mermentau River, GIWW and most of the major canals. Open bodies of water and marshes require a 2D evaluation, particularly when wind influences are considered and at higher flood stages. There was believed to be no need for a three-dimensional (3D) evaluation within the study area in order to achieve project study goals.

The TABS-MD numerical modeling system was selected for this study. This system uses multi-dimensional spatial discretization, a marsh porosity

formulation, and control structure formulations which are useful for describing features of the Grand and White Lakes project. Special improvements made to the hydrodynamic model RMA2 which were utilized in this study are documented in (King, 1988). These modeling features will be briefly discussed here. For a full description of these features and the TABS-MD system refer to the system documentation (Thomas and McAnally, 1991).

Multidimensional Model Approach

Multidimensional spatial discretization allows for 1D and 2D (or 3D) representations of the geometry in a single numerical model mesh. The approach removes the need to match boundary conditions between 1-D and 2-D models. The interfaces between different levels of discretization are handled automatically in a consistent manner.

The 1D formulation assumes a trapezoidal channel cross-section with the width, depth and side slopes varying along the channel length. In addition, off-channel storage is provided for the 1D channels, which is accounted for in the balance of water mass and salt mass, but has no direct influence on the momentum within the 1D channels. The 2D formulation is fully flexible.

The advantages of the multidimensional approach are several. A larger domain of simulation can be accommodated for a given level of discretization. The model boundaries can be located at convenient locations where field data is available. More rigorous numerical simulation can be performed with moderate computational costs.

Marsh Porosity

The first impression of the complexity of the wetlands in the study area, with hundreds of small bayous and canals, is that it is not possible to explicitly model the flows and salinity intrusion in all of these small features and still hope to address the regional goals of the project. However, it is not be necessary to model all the small features to get an accurate estimate of the influence of these fine features on regional flood control.

The marsh porosity capability is analogous to calculating flow in a porous medium, as in groundwater simulation (Roig and King, 1992). When calculating groundwater flows bulk parameters such as porosity are used to define via a continuous medium, the finer details on the broader flow characteristics. In fact, the bulk parameters are spatially averaged descriptors of the finer subscale media properties.

The parameters of interest in a wetland, relative to the hydraulic response, relate the area of flow to the water surface elevation. In addition, the effective roughness of the wetland is important. The roughness depends upon the type

of vegetation present and the depth of flow. These parameters can be viewed as bulk parameters which are actually spatially averaged descriptors of the wetland geometry over some chosen characteristic scale.

The characteristic length scale for bulking of the wetland properties varies itself over the domain of the model. The local bulking length scale depends first on the level of spatial resolution needed in that particular area to meet the overall study objectives and then on the local heterogeneity of the wetland.

If one were to walk out into a wetland in the Grand and White Lakes system the impression of the system would be dramatically different depending on which type of wetland was entered. Furthermore, the impression of the system could vary dramatically in the same general area if the path taken were shifted by only 100 ft. The size of the zone of impression for a person on foot is only on a scale of about 100 ft. If he were to gather statistical parameters in that zone he could make a good attempt at representing the hydraulics of the wetland locally. However, if he had moved some distance in any direction he might have found quite different statistics. This can be visualized as the differences between standing on the bank of a major natural bayou versus moving off into adjacent marsh grass.

If instead of walking into the wetland the person had chosen an airboat to get an impression of the wetland he would perhaps have come away with a different perspective. Assume that the airboat lets him ride high so he gets a broader view and can go pretty fast so he sees a larger area zoom past him as he motors through the wetland. Now the impression obtained is less likely to be biased by some local feature. The zone of impression and for compiling statistical information about the wetland is now say approximately 1000 ft.

At this scale of statistical summary (1000 ft) the influence of moving some distance in any direction begins to become less important to the statistics, as long as we stay in the same general type of wetland.

Finally, had one chosen to go out in a helicopter rather than by foot or airboat the impression gained would begin to take on a regional scale. The zone of impression may now be about 10,000 ft and the impression of the wetland becomes clearer at first glance. The statistics that one might develop from such a scale would be generally accurate if applied to the zone as a whole. As the helicopter moves from one area of the system to another the statistical parameters will now change primarily because the character of the wetland is changing. The dependence of these parameters on the scale of measurement takes on some aspects of fractals and self-similarity. Self-similarity of the statistics at scales much larger or much smaller than considered here probably exists; but those concepts can currently provide no guidance in the development of parameters for the present study.

Looking more explicitly now at the statistical variables of significance, consider the zone of wetland depicted in Figure 5. The wetland consists of generally grassy marsh with a few high ridges and some small feeder channels.

As the water level fluctuates within this marsh the wetland area varies. Another way of quantifying the variability is to measure the incremental volume of the zone that is wet as a function of water surface elevation. This fraction will then vary from 0.0 when the water level falls to the bottom of the deepest feeder channel to 1.0 when it rises higher than the highest ridge. This distribution function is presented in Figure 6. Although this general shape may be applicable to many wetland types, it is not universally applicable.

Once the relationship (Figure 6) between fractional volume, K, and water surface elevation is defined, the water volume for any water level is calculated as

$$V = \int_{a_{\min}}^{Z_s} K \, dz \tag{1}$$

where

V = volume of water in the zone of interest

a_{min} = elevation of bottom of deepest feeder channel

Z_s = water surface elevation

K = fractional volume = $\frac{\partial V}{\partial z}$

z = vertical coordinate

An effective depth for the cross-section is then computed as

$$h_\sigma = V/A \tag{2}$$

where A is the surface area of the zone. The numerical model uses this effective depth in its computations.

The numerical model uses a schematized representation of the distribution function K as shown in Figure 7. The deep feeder channels are represented by a finite percentage of the width that remains wet when the water level falls below a bank-full elevation (A_B). There is a linear transition zone over which the water leaves the feeder channels and floods the shallow marsh until at the maximum elevation in the wetland (A_T), the wetland is totally submerged.

The zone of influence of the statistical marsh porosity parameters is assumed to be the area of the numerical computational mesh associated with a single computational node. That area will depend on the size of the finite elements used to discretize the wetland.

These marsh porosity parameters may be varied in space over the mesh. However, at a single point the porosity is assumed to be isotropic. Preferential conveyance pathways for water flow may be influenced by variation in the marsh porosity parameters in the direction perpendicular to the dominant pathway.

For the specification of the wetlands in the Grand and White Lakes system, the scale of spatial averaging was defined over characteristic length scales varying from 500 to 15,000 ft. High altitude aerial photography was used to classify wetland type and extent. Vegetation maps for coastal Louisiana provided indicators for general topography. It was not feasible to physically measure the details of the topographic and bathymetric variations over the entire domain of this modeling effort.

Control Structures

The TABS-MD system has the ability to represent hydraulic control structures within 1D portions of the mesh. This is accomplished by providing a series of generic relationships between the water surface elevations on either side of the control structure and the discharge through the structure.

The optional relationships available include a weir equation, pumped source or sink, irreversible head difference versus discharge, reversible head difference versus discharge or discharge versus head difference relationships. These *options* provide the capability of addressing most types of hydraulic structures.

The model makes no attempt to simulate details of the flow through the structures, but relies upon the design characteristics of the structure to simulate the impact of the structure on the far-field hydrodynamics and salinity intrusion. The model equations used for the control structures are dramatically different in the open condition than for the closed condition.

Open Control Structures

The design equation supplied by CELMN that was used for all of the structures in the system for the open condition was

$$Q = 4.46\ W\ (H_1 - H_2)^{0.5} \left[1.71\ D - (H_1 - H_2)\right] \tag{3}$$

where

Q = discharge through the structure

W = width of control structure

H_1 = water surface elevation on the upstream side

H_2 = water surface elevation on the downstream side

D = depth of water over the sill

For all of the structures, D is relatively large compared to the expected head difference, so that the farthest right term of Equation 3 can be replaced by a constant, and

$$Q = 4.46\ W\ D_1\ (H_1 - H_2)^{0.5}$$

where

$$D_1 = 1.71\ D - (H_1 - H_2)'$$

or

$$Q = B\ (H_1 - H_2)^{0.5} \tag{4}$$

Now B is a nearly constant parameter which can be computed for each control structure

$$B = 4.46\ W \left[1.71\ D - (H_1 - H_2)'\right] \tag{5}$$

The primed head difference above is an estimated value. Equation (4) above is the form for specification in TABS-MD control structure representation as a discharge versus head-difference structure. Preliminary tests of the model showed that for small head differences the equation became numerically unstable. Therefore, the relationship was expressed as a function of flow

$$(H_1 - H_2) = (1/B)^2\ Q^2 = C\ Q^2 \tag{6}$$

The coefficient C or $(1/B)^2$ for each structure was specified as presented in Table 2.

Closed control structures

The closed condition for the structures was developed for the low-flow testing and was dependent on the operational schedule for the structure. For locking operations the volume of exchange of water through the structure for a single locking is the product of the surface area of the lock chamber and the head difference through the structure. For the long-term impact the locking frequency must be included.

$$Q_L = \alpha\ W\ L\ (H_1 - H_2) \tag{7}$$

where

α = locking frequency (per sec)

W = width of lock

L = length of lock

This relationship was designed to be applicable to the time scales of the numerical model time step. The locking frequency can therefore be modified for each timestep through the simulation to reflect changes in the frequency with either phases of the tide or time of day.

For the control structures the closed condition is more difficult to define because the structures are occasionally (instead of periodically) opened for the passage of navigation. The typical opening of the structure is estimated to be five minutes. The frequency of opening is then defined. The volume of water that passes the control structure during an opening was estimated by CELMN to last five minutes. The frequency of opening is then defined. The flow rate passing the control structure during an opening was estimated to be

$$Q_s = c\ W\ (H_1 - H_2)/\ 2 \tag{8}$$

where

c = celerity of a gravity wave

g = acceleration of gravity (32.2 ft/sec^2)

The actual relationship specified in the model included the frequency of opening the structure and the average time of the opening operation.

Whether for the locks or control structures, the form of the relationship for flow at the structure takes the form

$$Q = B_1\ (H_1 - H_2) \tag{9}$$

where B_1 is a coefficient dependent only on the size and type of structure. The coefficients for the closed condition of the structures are presented in Table 3.

The specification of the conditions at the structures for the salinity model were only of concern for the closed condition since the salinity computations were not run for high flow conditions when the structures would be open.

For locking operations the salt flux at the lock was specified based on the volume of the lock, the salt concentration difference across the lock and the locking frequency. Keulegan (1957) conducted experiments on the movement of salt water through locks in a physical scale model and found that the mixing

in the lock chamber itself was independent of the density differences across the lock and that after a locking procedure the salt concentration remaining in the chamber was the average of those upstream and downstream of the lock. The salt flux for a locking operation is computed as

$$S_L = \alpha V (C_2 - C_1) \quad (10)$$

where the lock volume, V, and the locking frequency, α, are specified.

For control structures the specification of the salinity conditions is simpler mathematically, yet more difficult for proper modeling. In the nominal closed condition the saline waters are free to move through the structure, when opening the structure for navigation. For this case, the concentrations are set equal across the structure and the full convective-diffusion equation is solved at the structure. The difficulty arises in defining the diffusion coefficient at the structure. This was computed based on a mixing zone associated with the structure, and the frequency of openings of the structure for navigation.

$$D_{xx} = \alpha A_m \quad (11)$$

where

A_m = mixing zone area (ft^2)

Freshwater Inflows

As stated earlier, no accurate estimates existed for the flood flow frequencies needed for reliable development of a testing program. Therefore, a 1D flood routing model was developed for the Mermentau River and Vermillion River basins using HEC-1. The pertinent parameters used in the model are presented in Table 4.

The model used the rainfall records at Lake Charles and Lafayette to develop hydrographs for 1986 and 1987 during the period of field monitoring. This information was used for the selection of the verification periods and for specification of the model boundary conditions for the verification runs. The model was also used to develop boundary conditions for the production testing program, which involve the 2-, 5-, 10-, 25- and 50-year flood events.

Tidal Boundary Conditions

The tidal boundary conditions for the numerical simulations were taken from field observations and from tidal harmonic analysis of that data and from harmonic analyses performed during the study of the Atchafalaya Bay delta study (Donnell, et al., 1991).

Computational Mesh

The finite element mesh for the study was developed in two phases; a low-flow mesh and a high-flow mesh. The mesh developed for the low-flow verification is presented in Figure 8. The design of the mesh was based on characteristics of wetlands as discussed in paragraphs 5-7. Primary channels and waterways were represented by 1D elements and open water and broad marshes by 2D elements. Note that the 1D elements are represented as lines, but each 1D element had a width and off-channel storage defined.

The low-flow mesh was also used for the high-flow verification, which had a peak flow of 9000 cfs on the Mermentau River. The estimated 50-year flood has a peak flow of 72,200 cfs. At that level, additional 2D wetland becomes important, primarily north of White Lake. Therefore, a high-flow mesh was developed to handle these extreme conditions (see Figure 9).

4 Verification

Verification Conditions

Model verification was performed, for a high-flow period during November 1987 and for a low-flow period during October 1987. The high flow verification was performed under contract (Rachiele and King, 1989) to the numerical mesh developed at WES. The low-flow verification period was used to verify tidal propagation and salinity intrusion, while the high-flow period was used to verify flood routing and stages.

The estimated Mermentau River discharge for 1987 from the HEC-1 model are presented in Figure 10. The period chosen for the low-flow verification was mid to late October 1987, when the flows were below 1000 cfs for a prolonged period of time. The high-flow verification period was selected as the period 18-20 November 1987, when a moderately high flow was coincident with good data return from the monitoring program.

High-flow Verification

The high-flow verification began with steady-state simulation using approximate discharges to develop an appropriate initial condition at the start of the verification period. Then a one-day dynamic simulation applying the known tidal, flow and wind conditions was performed to establish approximate flow and tidal equilibrium. Finally, a two-day simulation for 19-20 November was performed using the appropriate boundary conditions to constitute the verification run. This verification was performed on the low-flow mesh (Figure 8).

Boundary conditions

The location of flow and tidal boundary conditions are presented in Figure 11. There were five tidal boundary conditions; four along the open Gulf of Mexico and one at the Vermilion Bay boundary. The recorded tidal data on the downstream side of the Freshwater Bayou lock was used for the Gulf

boundaries (see Figure 12). The Vermilion Bay boundary condition is shown in Figure 13.

The estimated daily freshwater inflows to the system from the hydrologic model for the Mermentau River and Lacassine Bayou are presented in Figure 14. These flows were interpolated to hourly values and distributed 90 percent to the Mermentau River and 10 percent to Lacassine Bayou, based on drainage areas. No discharges were available for the Calcasieu River. For the verification simulation the Calcasieu River flows were set to match those of the Mermentau River and Bayou Lacassine. Trial runs suggested that the Grand and White lakes system is insensitive to flows on the Calcasieu River. However, this approach provides only estimates of the river discharge and these boundary conditions have a large degree of uncertainty.

Wind forcings

The wind forcings for the verification period were taken from the Lake Charles NOAA climatological data station. Daily resultant wind speed and direction are presented in Table 5. The winds were generally from the north around 10 miles per hour during the verification period.

Control structures

The primary influence on the water levels and current velocities for the verification period was the operation of the control structures. The specification of the control structures for the open conditions are presented in Table 2 and for the closed condition in Table 3. The operational schedule of the control structures during the verification period is presented in Table 6.

Results

The results of the high-flow verification are presented in Figures 15 through 19. The location of the current velocity verification stations are presented in Figure 4. The current meters at stations 17 and 23 showed no response to flow during the verification period; probably due to meter fouling.

The modeled current velocities at station 16 follow the pattern observed in the field with regard to magnitude of flow and direction when the currents are strong. At lower velocities the directions do not always agree but the field data also exhibits ambiguity in flow direction (see hour 23 of the simulation).

The results at station 19 show general agreement in the flow direction and magnitude with the model exhibiting more variability than the observed data. The variability suggests that the model is getting too great a tidal influence during periods of open operation of the Leland-Bowman Lock and Schooner Bayou Control Structure.

At station 20, at the western side of White Lake, the model and observed currents are always flowing toward the gulf, with the simulated currents slightly lower than the observed currents. The observed currents during the first 6 hours of the simulation appear to fall below the threshold of the current meters.

The comparisons between simulated and observed water surface elevations at the western end of the Schooner Bayou control structure and the north end of the Freshwater Bayou Lock are presented in Figures 18 and 19. The overall trends in the water surface elevations are similar, but short-term variations do not match well, given the complexity of the system response to control structure operation, wind forcings and tidal effects. With the uncertainties in the discharge boundary conditions used it is believed that the verification is acceptable.

Low-Flow Verification

The month of October 1987 was the lowest discharge period during the CEWES field data collection effort. The estimated flow on the Mermentau River fell below 1000 cfs on 27 September and remained below 1000 cfs until 27 October. The average flow for that period was 230 cfs, but from October 12 through October 26 the flow was below 100 cfs.

Hydrodynamic verification

Boundary Conditions. The model was run with a constant Mermentau River flow of 200 cfs and a Bayou Lacassine flow of 100 cfs, based on ratios of drainage basin areas. The Calcasieu River discharge was also estimated to be about 100 cfs. The Vermilion River was not explicitly specified, but its influence was assumed to be dominated by the influence of the Atchafalaya system which was incorporated into the salinity boundary condition in Vermilion Bay.

The tidal boundary condition used was generated from the tidal harmonic constituents, correcting the phases for the October 1987 period. The Gulf boundaries were based on the harmonic analysis of tide data from the Calcasieu entrance channel, and the Vermilion Bay boundary from a tide station inside Southwest Pass from a previous study (Table 7).

Wind Forcing. The wind forcings were developed from the NOAA data at Lake Charles, Louisiana. The wind data are summarized in Table 8, and were interpolated to generate a time series with one-hour interval.

The approach for the low-flow verification was similar to that of the high-flow in that a steady-state simulation was used to establish the initial water elevations throughout the system and then a dynamic simulation performed

until the tides reached a dynamic equilibrium. The resulting tidal results were then used to drive the transport model for the salinity verification.

Results. The results of the low-flow hydrodynamic verification are presented in Figures 20 through 30. Figures 20 through 26 present the verification of the model to water surface elevations. Variations in water surface elevations for stations downstream of the control structures are shown in Figures 20 and 21 for stations 4267 and 4255, at Leland-Bowman Lock (east) and Schooner Bayou Lock (east). Both of these stations exhibit significant wind influence in the field data; however, the model did not show those effects, primarily due to the fact that the model boundary conditions do not include any wind influences.

The verification of water surface elevations for stations upstream of the control structures are shown in Figures 22 through 26. The upstream side (west end) of Leland-Bowman Lock is shown in Figure 22, indicating good agreement in water surface elevation and in the general response of the water levels to the wind forcings. The western side of Schooner Bayou Lock (Figure 23) shows similar agreement in water levels, but the variations due to the wind are not as evident in the model.

The comparison of water surface elevations in White Lake (station TG21; Figure 24) is good, with the timing of the wind influences in quite good agreement, but with the range of response slightly less in the model. Farther west along the GIWW, west of Grand Lake, the response of the model to the wind matches the field data generally very well (Figure 25). The station at the east end of Calcasieu Lock is presented in Figure 26, and indicates basic agreement in the overall water surface elevation, but the short term responses to the winds did not agree well with the field data.

Verification of the model to current velocities for the low flow condition is presented in Figures 27 through 30. Figure 27 presents the currents at station V16, on the Lower Mermentau River. This was the only data available that had a significant tidal influence, which is evident in both the model and the field data. The general magnitude of the model velocities are in agreement with the field data, with some deviations associated with the wind effects.

The remaining three stations of velocity data are for stations upstream of the control structures, where the current magnitudes are quite low, often below current meter threshold values, making the field data susceptible to noise from wave action and other interference.

In spite of these limitations, the currents in the model were in reasonable agreement with two of the three stations upstream of the control structures. At station V17, in the mouth of the upper Mermentau River where it enters Grand Lake, the model had very low velocities, generally less than 0.1 fps (Figure 28). The field data there was also generally below 0.1 fps but had some periods when the flows are higher.

At station V19 (Figure 29), located in the GIWW north of White Lake, the comparison was good with the field data again exhibiting considerable noise. However, the magnitude of the underlying velocity trends in response to the winds was in good agreement.

The greatest response of velocities to the wind forcing at the stations upstream of the control structures was seen at station V20, located on the western end of White Lake in the mouth of the Old GIWW (see Figure 30). The model velocities are in good agreement with the observed currents with regard to the general trends in direction and magnitude. The observed currents do exhibit a greater variability, but the model wind forcings were based on interpolation of daily average conditions, so loss of some variability could be expected.

The overall performance of the hydrodynamic model for the low-flow condition was believed to be acceptable for the purpose of driving the salinity transport model for the evaluation of the marine ingress structures.

Salinity verification

Boundary Conditions. The boundary conditions for the salinity model were required at all open boundaries. The Gulf boundaries all had a concentration of 30 ppt specified, and the Vermillion Bay boundary was set at 25 ppt. These boundary conditions were only used when the flow entered the model on flood currents. Upon outflow, concentration is unconstrained. The river inflows were set to an inflow concentration of 0.2 ppt.

Initial Conditions. The initial salinity conditions for the low flow verification were developed from field measurements and were interpolated over the model using the model in a steady-state salinity simulation with internal boundary conditions. The run durations provided time for transient conditions created by the initial valves to subside.

Results. The number of stations of salinity data available for the low flow verification was somewhat limited with only four stations operational. Three of the four stations were located upstream of the control structures and consequently the salinities were close to zero. The only station with measurable salinity was Station V16 on the lower Mermentau River, where the salinities ranged from 8 to 25 ppt during the verification period. The model salinities were generally within this range (8 to 22 ppt) as shown in Figure 31.

5 Description of Testing

The numerical models developed for this project were used for flood event testing and salinity intrusion testing. These testing programs were designed to address flood control structure design and the design of marine ingress structures.

Flood Control Testing

The testing program for the flood control plans was designed to allow the sponsor to construct flood elevation frequency curves throughout the system for each of the plans. This approach included simulations of a series of flood events of various return periods.

River discharges

The primary difficulty with designing the testing program was, as discussed in paragraph 13, the estimation of the flood flows for various return intervals on the Mermentau River, the primary tributary. The period of record for the Mermentau River did not allow for an accurate estimation of the longer return period flows. Therefore, the HEC-1 model was utilized to synthesize the flood hydrographs.

The HEC-1 model was driven with 2- year, 5-year, 10-year, 25-year and 50 year rainfall events (Hershfield, 1961). These rainfall events resulted in discharge hydrographs from the HEC-1 model for each return interval. These time series hydrographs were used as the boundary condition for the Grand and White Lakes TABS-MD finite element model of the lower basin.

The flood control plans were all tested with the same upstream Mermentau River discharge boundary conditions for each test. These tests were designated as the F02, F05, F10, F25 and F50 flood flow tests, for the 2-, 5-, 10-, 25- and 50-year flood hydrographs, respectively. The peak Mermentau River discharges for each flood event are provided in Table 9.

For the other tributaries into the general study area mean river discharges were prescribed as the inflows. These included the Calcasieu River, Bayou Lacassine and Vermilion River.

Tidal boundary conditions

The flood control tests were performed with a repetitive mean tide as the Gulf tidal boundary condition. Although spring-neap tidal variations are considered to be important for flood wave progression, these tests were concerned with the relative impacts of each alternative. A repetitive tide is adequate to evaluate relative system response to the different management alternatives.

The Gulf of Mexico tides were prescribed with a 1.9 ft mean tide range and the tide in Vermilion Bay had a reduced tide range of 1.5 ft. There was no tidal phase lag prescribed between any of the Gulf boundaries. The Vermilion Bay tide was lagged behind the gulf boundaries by 4 hours, based on harmonic analysis of the tides.

Test duration

The duration of the tests was determined by the length of time needed for the flood wave to pass through the system. This is generally associated with the return of the water levels in the upper basin to 2 ft above mean low Gulf (MLG). This duration was approximately 1200 hours (50 days). An operational constraint placed on the simulations was the size of the model output file that could be archived on a single magnetic backup tape (after compression for storage efficiency). This arbitrary restriction limited the model simulations to 1177 hours. This proved to be quite satisfactory.

Salinity Intrusion Testing

For the evaluation of salinity intrusion plans, a series of tests was designed to evaluate the response of the salinities in the system to a number of factors. These factors included river flows, tide level, tide range and wind stress.

The test designations and the values of the tidal factors for each test are presented in Table 10. The test designations were developed with either a "W" prefix or an "S" prefix to signify either a wildlife (W) test or a general salinity intrusion (S) test. Wildlife tests were conceived to evaluate long-term average trends. The number following the letter is arbitrary, based on the list of proposed tests that were considered. These tests will be discussed individually below.

Test W3

Test W3 was designed to provide screening of the various plans under conditions typical of when salinity intrusion will be of concern. For this test the Mermentau River and all tributaries had approximately the average annual low discharge. A mean sea level and a repetitive mean tide range were used for the Gulf boundary conditions. No wind was applied to the model.

Test S1

To address increased salinity intrusion associated with prolonged southeasterly winds, Test S1 was developed. This test also had low river discharges, the same as Test W3, but had the mean Gulf level raised by 0.5 ft in response to the prolonged wind stress from the southeast, which was also applied to the model at a steady speed of 20 mph.

Test S2

This test was designed to assess impacts during periods when prolonged southeasterly winds are not coincident with low river discharges. This test is the same as Test S1, except that mean river discharges were used for each of the tributaries.

Test W4

This test was developed for the evaluation of the marine organism bypass structures and was designed to assess the salinity intrusion response to fortnightly variations in the tidal levels in the Gulf of Mexico. The river discharges were kept at the average low flows, as for Tests W3 and S1, but the tidal boundary conditions varied in both mean elevation and tide range.

The mean daily water level in the Gulf can vary dramatically in a relatively short period of time in response to wind. When these fluctuations in water level occur the salinity regime response is equally dramatic. Therefore, Test W4 was designed to start with the mean water level at mean sea level. The astronomical tidal boundary condition was reconstituted from tidal harmonic constituents developed from field measurements, providing the time-varying tidal range between neap and spring tides. The tidal constituent amplitudes and phases are provided in Table 7.

After 200 hours into the simulation the mean tide level was gradually raised by 0.5 ft over the next 100 hours. After 600 total hours of simulation the mean water level was then lowered back to mean sea level over the next 100 hours. The simulation was continued for a total time of 1177 hours, as discussed above. No wind was applied in Test W4. The Gulf boundary

condition forcing is presented in Figure 32 and the Vermilion Bay boundary condition in Figure 33.

Test W5

Test W5 was designed for the evaluation of the impact of the varying tidal conditions with mean river discharges and a wind forcing. The tidal boundary conditions were the same as described for Test W4. However, mean river discharges were used. Wind forcing was applied during the same period of time that the mean tide level was elevated above mean sea level (hours 200 through 700 of the simulation).

Salinity simulations

After the hydrodynamics for each of the salinity tests described above were completed, salinity transport simulations were performed using the plan-test hydrodynamics. The salinity model used boundary conditions of 30 ppt in the Gulf of Mexico and 25 ppt in Vermillion Bay. The results of the salinity model were used for the evaluation of plan performance.

6 Description of Plans Tested

The alternative plans evaluated in the modeling effort were in two groups: flood control plans, generally designed to provide greater flow capacity between the upstream portion of the system and the Gulf, and salinity intrusion plans. The salinity intrusion plans were designed to limit salinity intrusion while providing for migration of marine organisms.

Plan designations (Plan 1, Plan 2, etc.) used within this report are arbitrary and hold no significance relative to other studies. Figure 34 shows the location of the plan alternatives tested.

Flood Control Plans

The flood control plans all consisted of increasing flow capacity between the upper part of the system and the lower portion of the system. The plans differed in the design, size and location of the new structures.

Plan 1

The Plan 1 structure was located just south of the GIWW west of Grand Lake, just west of Highway 27. This structure was a 2,000-ft-long overflow weir, allowing flows to enter the marsh to the southwest. The floodwaters would then be evacuated to the west through lower Calcasieu Lake.

Plan 2

Plan 2 was of the same design as Plan 1 but located further west on the GIWW, in the vicinity of Sweet Lake as the GIWW turns toward the northwest. This plan was accompanied by channelization through the marsh downstream of the structure to accommodate the diverted waters as they flow toward upper Calcasieu Lake.

Plan 3

A diversion structure on the south side of White Lake of the same basic design and capacity as the Catfish Point structure is the primary feature of Plan 3. The diverted flows would flow through the marshes around the east end of Rockefeller wildlife refuge toward the Gulf.

Plan 4

Plan 4 had a diversion structure at the same location as Plan 3 on the south shore of White Lake, but with only half the flow capacity of the Catfish Point structure. In addition, this plan included a canal capable of efficiently carrying that flow to the Gulf along the eastern edge of Rockerfeller refuge.

Plan 8

Plan 8 doubled the capacity of the flows diverted at Catfish Point by the addition of a new structure of equal capacity.

Plan 9

Plan 9 was the same as Plan 8, but with the added feature of enlarging the capacity of the lower Mermentau River to handle the increased flow from the structures. This was generally accomplished within the model by increasing the channel width, but at critical sections depth was increased instead, using Manning's equation to estimate proportionality of capacity prior to model testing.

Plan 10

Plan 10 was the same as Plan 9 in all aspects except that the increase in capacity was to bring the total flow capacity at Catfish Point to three times that of the existing structure.

Plan 11

Plan 11 was the same in principle as Plan 4 except that the capacity of the new structure on the southern side of White Lake and the canal to the Gulf were equal in capacity to the Catfish Point control structure.

Plan 16

Plan 16 was the same as Plan 11 but with the added feature of improved capacity for flow between Grand and White Lakes by enlarging the channel.

Plan 17

The addition of additional flow capacity at the location of Calcasieu Lock was the primary element of Plan 17. The capacity of the structure was to be whatever the GIWW could carry. However, the plan did not call for any improvement to the flow capacity of the GIWW to carry flood flows toward the Calcasieu structures.

Salinity Intrusion Plans

Plan 5

Plan 5 called for a closure dam in Warren Canal at its downstream end where it joins Schooner Bayou. For the purposes of the low-flow salinity testing the elevation of the dam was not a factor, and the canal was disconnected at that location. The purpose of this plan was to provide reduced salinities for rice farmers who use Warren Canal waters for irrigation.

Plan 6

Plan 6 included the closure dam on the southern end of Warren Canal and the construction of a new canal from Warren Canal, approximately 3000 feet north of the closure dam westward to connect with White Lake. The dimensions of the new canal were 100 feet wide by 5 feet deep.

Plan 7

Auxiliary structures for the passage of juvenile marine organisms past the existing flow control structures were the basis for Plan 7. These structures would be permanently open but designed for passing near surface waters to minimize the impact on salinity intrusion. The plan specifications called for structures at both Catfish Point and Schooner Bayou with dimensions as described by Alternative 4 (CELMN, 1987). The flow capacity response for these structural systems is shown in Figure 35. The structure consisted of ten 4-ft diameter round culverts with invert elevations ranging from -4 ft NGVD to 0.5 ft NGVD at 0.5 ft increments. The numerical model discretization of the response of the system was accomplished by two separate head-discharge relationships; one for flooding flows and one for ebbing flows to represent the

nonsymmetrical response of the culverts. The flow through the Catfish Point structure, Q, was modeled as

$$Q = A\ (H_n - H_S)^B \qquad \textit{for ebb}$$

and

$$Q = C\ (H_S - H_n)^D \qquad \textit{for flood}$$

These response curves match Figure 35 if A = 1150, B = 0.5 , C = 1340, and D = 0.7. H_n is the water surface elevation north of the structure and H_S is the elevation south of the structure. For the Schooner Bayou structure the north/south references would be replaced with west/east head differences.

Plan 12

Plan 12 involved the construction of a marine organism passage structure of much lower capacity than Plan 7. It consisted of 4-ft wide vertical slots with bottom elevation of the slots at -4 ft NGVD. The plan called for two slots at Catfish Point control structure and one slot at Schooner Bayou control structure. For a reduction in the number of slots the flow-head difference relationship was proportioned linearly to the total width of all of the slots.

Plan 13

Plan 13 was the same as Plan 12 but with the omission of the single additional marine organism passage structure at Schooner Bayou. This would leave just two vertical slots at Catfish Point.

Plan 14

Plan 14 evaluated the combined effects of Plans 5 and 12. It included both the Warren Canal closure dam and the marine organism passage structures (slots) at both Catfish Point and Schooner Bayou control structures.

Plan 15

Plan 15 included the marine organism slots and the Warren Canal closure dam, but also included the new canal between Warren Canal and White Lake (combination of Plans 12 and 6).

Plan 18

Plan 18 was essentially an operational test for Catfish Control Structure for the purposes of marine ingress. The plan called for opening the control structure gates by 1 ft to allow for marine ingress. The operational scenario tested was to leave the gates with a 1 ft opening throughout the test. This would obviously only be operated at low flows when salinity intrusion was not a problem. This plan used the full discharge relationship of the structure (Equations 4 and 5) with a 1 ft width.

7 Results

The volume of information generated from the numerical model study was approximately 14 gigabytes of data. This volume of data has been summarized in a number of ways for use by CELMN for the development of project benefits. The summarized data filled ten large-ring binders which were provided separately. The model results presented here are representative of the full data analysis performed. The most significant results are presented in tabular form.

The flood control plan that has been given the greatest probability of implementation is Plan 16 (see paragraph 127). Therefore, the results for that plan will be presented in some detail for a number of representative locations to demonstrate the system response to the plan. For the marine ingress concerns, Plan 18 provides a general response of the system typical of most of the alternatives as illustration.

Flood Control

The response of flood stages in the system is dependent largely on the location in the system relative to the control structures, either existing or planned. Figure 36 presents the station locations for presentation of model results. Figures 37 through 42 present the water surface elevation response to the 50-year flood for Base conditions and Plan 16. Figure 37 presents the results at Station 1870, the upstream side of the Catfish Point control structure. The base condition elevation peaks at 6.0 ft after approximately 305 hours into the simulation. Plan 16 elevations peak at 5.6 ft after 295 hours. The length of time that flood stages were above the 2 ft (MLG) level was reduced by approximately 250 hours by Plan 16 for Station 1870.

The analysis of the flood testing also included a graphical display of the length of time that a certain critical water level was exceeded during a particular test. The exceedance interval curves for the Plan 16 test for the 50-year flood event is presented relative to existing structural configuration in Figure 38. The periods of time that a particular elevation is flooded is of value to various interests within the study area.

Figure 39 presents the response of water levels for the 50-year flood at Station 1090, at the west end of White Lake, close to the entrance to the Old GIWW. The Base test showed a peak flood stage of 3.9 ft after approximately 515 hours of simulation. Plan 16 test showed a peak elevation of 3.5 ft after only 320 hours, occurring significantly earlier. The response at Station 1090 shows the benefits from the added structure on the southern shore of White Lake and the increased capacity of the Old GIWW channel between Grand and White Lakes. The reduction in the period of time of flood stages above the 2 ft level was about 300 hours at Station 1090. The elevation exceedance curves for Station 1090 are presented in Figure 40.

The response of the western part of the system was similar, as indicated at Station 1998 (Figure 41). The Base and Plan responses both show tidal influence from the Calcasieu system, even at the peak flood stages. The Plan condition showed a reduction in peak stages from 4.8 ft to 4.5 ft with the time of peak flood levels changed from 315 hours to 295 hours into the simulation. The length of time for which the flood stages remained above the 2.0 ft level was reduced by approximately 200 hours at Station 1998. Figure 42 presents the exceedance curves for Station 1998, which show less dramatic reductions with the Plan than seen to the east.

The results for all of the flood control plans tested for the flood return intervals of 2-, 5-, 10-, 25-, and 50-years are presented in Tables 11 through 19. The stations presented in each of the tables are located in Figure 36 and the changes shown are computed as Plan levels minus Base levels. A positive change indicates that the Plan flood level was higher than for the Base conditions.

Salinity Intrusion

The tests conducted for the facilitation of the migration of marine organisms were, as discussed earlier, salinity intrusion tests. There were several different testing scenarios developed, all of which were not tested for every plan. Early in the testing program, the tests with repeating mean tides were used as a screening tool. The later developed plans were tested primarily using tests W4 and W5 due to their more realistic tidal forcings.

The results of a single plan-test will be presented here to illustrate the model capability and typical response. The results for all plans and tests are presented in tabular form for that subset of station locations. Station locations are shown in Figure 36. The plan presented here is Plan 18, which was simply to open the Catfish Point control structure to a 1 ft gap for allowing organisms to pass.

The hydrodynamic results for the Plan 18 Test W4 (see Table 10 for a summary of the test conditions) are presented in summary in order to provide insight into the salinity response. Figures 43 through 45 show the general characteristics of the hydrodynamic response. Figure 43 shows the water

surface elevation at Station 1905, on the Lower Mermentau River. There is no discernable difference between the Base and Plan conditions at that location, which is dominated by the Gulf boundary condition.

At the upstream end of the Catfish Point control structure (Figure 44) there is a drop in the water level associated with the opening of the gates, of about 0.17 ft initially, and diminishing as the test continues. Notice that even with the gates opened by 1 ft there is no dramatic rise in the water levels upstream of the control structure due to the vast expanse of storage area upstream of the structure.

At other upstream stations far removed from the control structure (Catfish Point) the response is similar to that seen just upstream of the structure. Figure 45 shows the response at Station 1090, at the western end of White Lake. This indicates that for low flow conditions, when the structures are generally closed, the system above the structures is like a bathtub with a slow leak.

The salinity results of the Plan 18 testing for Test W4 are presented in Figures 46 through 48. The response of the model at Station 1905 is presented in Figure 46, located on the lower Mermentau River. The salinities ranged from 14.2 to 23.9 ppt for the Base test with a general downtrend in salinities that is interrupted by an increase in salinity associated with the increased water levels between hours 200 and 600 of the test. The Plan 18 response is qualitatively the same as the base test, but with faster response to the changes. That is, the reduction in salinities early in the test (hours 0-200) is greater for the Plan; however, the rebound when the water levels rise is also faster, so that by hour 600 of the test the salinities are approximately the same. After the water levels have returned to normal the influence of the increase is felt for a greater period of time for the Plan due to a greater influx of salinity upstream of the Catfish control structure. The range of salinities for the Plan was 15.6 to 23.9 ppt, with no change in maximum salinity.

The response of the system at the upstream end of the Catfish control structure (Station 1870) is presented in Figure 47 for Test W4 for Base and Plan 18. The influence of the opened gate is evident at this station. The initial salinity is much lower for the Plan due to the diluting effect of the water that is discharged through the small opening in the gate. Once the Gulf level starts to rise both the Base and the Plan tests show an increase in salinity at the control structure. The Base test shows a maximum salinity of 8.6 ppt after about 650 hours of simulation. The Plan maximum salinity occurs at the same time as the base, but at a maximum of 14.2 ppt. The gap in the structure does allow a slug of salt water to intrude upstream, but after the Gulf level falls the system is flushed back to levels lower than for the Base test, again due to the net effect of release of fresh water.

The salinity response for upstream stations far removed from the Catfish Point structure is illustrated by Figure 48, Station 1090 at the west end of White lake. At that location there is little difference between the Base and Plan tests, with the Plan salinity slightly lower (0.1 ppt) than the Base.

The results of the Plan testing for other design alternatives are summarized in Tables 20 through 24, organized by test scenario. Table 20 presents the results of the Base and Plans 5 and 6 tested with Test S1 conditions. Both of these plans included a closure dam in the south end of the Warren canal, and Plan 6 also included a new canal connecting Warren canal with White Lake. Both plans achieved the desired goal of reducing salinities in Warren Canal (Station 432), with Plan 6 showing a greater reduction in salinity. Both plans also indicated a slight increase in salinity for Schooner Bayou upstream of the control structure (Stations 2545 and 805) in response to reduced freshwater supply with the closure dam in place.

Table 21 presents the results of the Test S2 simulations, on Plans 5 and 6. These results are consistent with those observed in Test S1, but show less salinity reduction in the Warren Canal due to the lower Base salinities there with the higher river discharges. The results of Test W3 (Table 22) were qualitatively the same as for Tests S1 and S2, being performed again for Plans 5 and 6.

The results of Test W4 are presented in Table 23, and was performed on six plans; Plans 7, 13, 14, 15, 16, and 18. With the exception of Plan 16, all of the plans involved varying scenarios of adapting either or both Catfish Point and Schooner Bayou control structures for passage of marine organisms. Plan 16 was simulated for sensitivity of the low-flow salinity regime to the major revision in flow conveyance between Grand and White Lakes.

Test W4 showed that the Plan 7 alternative would have an unacceptable impact on salinity intrusion, with a 15.4 ppt increase just upstream of the Catfish Point control structure (Station 1870), and a 4.2 ppt increase at Schooner Bayou structure (Station 2545). Generally, Plan 7 increased salinities throughout the model.

Plans 14 and 15 showed reductions in salinity in Warren Canal with reduced levels of impact at the auxiliary structures as compared with Plan 7. Plan 16 did not show dramatic changes in the salinity regime upstream of the control structures.

Table 24 presents the results of Test W5, which involved mean river discharges and wind forcings. This test was performed on Plans 7, 12, 13, 14, 15 and 18. The impact of Plan 7 on salinities is shown to be unacceptable. The influence of the wind is dependent on the combination of the auxiliary structures and the circulation circuits defined by possible closed loops in the system which can develop net flows in response to the wind forcing.

8 Conclusions

This study represents a major advancement in environmental fluid dynamics. This study was undertaken at a time when state-of-the-art hydrodynamic modeling was insufficient to address the questions posed. New model developments were required to achieve the results reported herein. The primary reasons for the technology gap were:

a. The physical size of the study area was large. Contradictory demands of project scale and computational refinement lead to extravagant computational requirements for a numerical model with a rigorous formulation.

b. The geometric complexity of the wetlands in the study area required schematization of the small scale geomorphic features in order to comprehensively model the entire system.

c. Myriad manmade canals and waterways suggested the usefulness of a one-dimensional model formulation, but a simple one-dimensional model could not address the complex routing of flood flows when the wetlands are submerged.

d. Hydraulic control structures within the system required special treatment that would allow for direct coupling of the flow through the structures with the hydrodynamics of the wetlands.

e. Complex hydrodynamic interactions over the large study area required that all of these special features be addressed in a single hydrodynamic model.

f. The modeling approach required incorporation of salinity transport simulation consistent with all of these concerns.

The technical choices at the outset of this study included a fully 1D approach or a 2D approach, with modified capability to address the large spatial limits. It was felt that the complexity of the wetland hydrodynamics required a dynamic 2D approach, while large portions of the system could be handled in 1D. Therefore, the TABS-MD system was chosen because of its ability to include both 1D and 2D formulations in a nonlinear dynamic

solution. The models were modified to incorporate the hydraulic control structures and to address the wetland hydrodynamics in a spatially averaged manner (Roig and King, 1992).

The results of this effort have shown the technical approach taken to have been fully successful at accomplishing the technical goals of the study. The quality of the verification for hydrodynamics in a spatially averaged salinity intrusion was appropriate for giving confidence in the model's predictions.

Flood Control

The flood control testing program provided several conclusions about the potential design of alternative structural improvements:

a. The structural modifications must be combined with appropriate improvements in the channel carrying capacity to route the flows diverted from the structures.

b. Structural improvements on the far western end of the system were less effective in providing flood control benefits than those in the vicinity of Catfish Point or White Lake. This is in part due to the limit on the efficiency of the GIWW to deliver flood waters to those western structures.

c. The testing program identified several alternatives that can provide reduced flood stages locally in excess of 1.0 ft for the 50-year flood, with general flood level reductions of several tenths of a foot.

d. Because of the extremely flat topography of the system, a small reduction in flood stage can result in large areas of reduced flooding.

Salinity Intrusion

The plans for reduction in salinities along the Warren Canal and upstream (Plans 5 and 6) were shown to reduce but not eliminate salinity intrusion. The reductions in salinity along Warren Canal were in the range of 25 percent for Plan 5 (closure dam) and 33 percent for Plan 6 (closure dam plus new canal).

The testing of the marine ingress structural plans showed that, in general, these plans will increase salinity intrusion. The model results suggest that in order to keep these effects to a minimum the number and size of the openings for organism migration should be as small as possible. The option of slightly opening the gates at Catfish Point (Plan 18) for marine organisms seems to provide an alternative that can be controlled or eliminated easily when salinity levels become undesirable.

The Plan 18 test was conducted as a severe condition of having the gates always slightly opened. In reality the gates would probably only be opened periodically. Therefore, the Plan 18 results presented here are highly conservative.

The testing Plan (Test W4) illustrated that several plans can provide migration enhancement for marine organisms while limiting the level of salinity intrusion, both in magnitude and spatial extent. Plans 13, 14, 15 and 18 provide for passage without increasing salinity levels dramatically at the structures, while limiting the effects to little or no change at upstream stations far from the structure.

References

Donnell, Barbara P., J. V. Letter, Jr. and A. M. Teeter, May 1991, "The Atchafalaya River Delta; Report 11, Two-Dimensional Modeling," Technical Report HL-82-15, Waterways Experiment Station, Vicksburg, MS.

Hershfield, David M., May 1961, "Rainfall Frequency Atlas of the United States; for Durations from 30 Minutes to 24 Hours and Return Periods from 1 to 100 years," U. S. Department of Commerce Technical Paper No. 40, Washington, DC.

Keulegan, Garbis H., March 1957, "An Experimental Study of the Motion of Saline Water from Locks into Fresh Water Channels," Thirteenth Progress Report on Model Laws for Density Currents, National Bureau of Standards Report 51687.

King, Ian P., December 1988, "Program Documentation: RMA2 - Two-Dimensional Finite Element Model for Flow in Estuaries and Streams; Version 4.2," Resource Management Associates, Lafayette, Ca.

Rachiele, Richard R. and Ian P. King, November 1989, "Verification of the Grand and White Lakes High-Flow Case Model," Resource Management Associates, Lafayette, CA.

Roig, Lisa C. and Ian P. King, 1992, "Continuum Model for Flows in Emergent Marsh Vegetation," Proceedings of the 2nd International Conference on Estuarine and Coastal Modeling, ASCE, Tampa, FL.

U.S. Army Corps of Engineers, New Orleans, October 1987, "Water Control Plan, Mermentau River Basin, Louisiana, Water Resources Projects," New Orleans, LA.

U.S. Army Engineer District, New Orleans, 1987, "Reconnaissance Report for the Grand and White Lakes Flood Control Project", New Orleans, LA.

Thomas, William A. and McAnally, W. H., Jr. July, 1991, "User's Manual for the Generalized Computer Program System: Open-Channel Flow and Sedimentation, TABS-2; Main Text", Instruction Report HL-85-1, Waterways Experiment Station, Vicksburg, MS.

Table 1
Control Structure Dimensions

Control Structure	Width (ft)	Sill Depth (ft)	Lock Length (ft)
Leland Bowman Lock	110	15	1200
Calcasieu Lock	75	14	1200
Freshwater Bayou Lock	84	16	600
Catfish Point C.S.	3 x 75	15.3	-
Schooner Bayou C.S.	2 x 75	14	-

Table 2
Control Structure Parameters High Flow Verification

Control Structure	Open Operation	
	Equation Used	Coefficient $((1/B)^2$ or C)
Leland Bowman Lock	6	2.82×10^{-8}
Calcasieu Lock	6	1.57×10^{-8}
Fresh Water Bayou Lock	6	8.49×10^{-9}
Catfish Point C.S.	6	1.46×10^{-9}
Schooner Bayou C.S.	6	3.93×10^{-9}

Table 3
Control Structure Parameters High Flow Verification

Control Structure	Closed Operation	
	Equation Used	Coefficient(B_1)
Leland Bowman Lock	9	2.82×10^{-8}
Calcasieu Lock	9	1.57×10^{-8}
Fresh Water Bayou Lock	9	8.49×10^{-9}
Catfish Point C.S.	9	1.46×10^{-9}
Schooner Bayou C.S.	9	3.93×10^{-9}

Table 4
Parameter Specification for HEC-1

River Basin	Tp	Cp	CNSTL
Mermentau	86.54	0.31	0.0225
Lacassine Bayou	56.27	0.31	0.0229
Vermilion	69.18	0.31	0.0200

Tp = Snyders standard lag (hours)
Cp = Snyders peak coefficient
CNSTL = uniform rainfall loss (inch/hour)

Table 5
NOAA Wind Data for Lake Charles, La.
November 18-20, 1987

Date	Resultant Direction (Deg from N)	Resultant Speed (mph)
November 18	50	9.3
November 19	360	10.7
November 20	350	7.4

Table 6
Lock and Control Structure Operation Used in High-Flow Verification Simulation

Control Structure	Hours of Simulation								
	1	6	12	18	24	30	36	42	48
Leland Bowman Lock	+++++ ++++				+++++++++++++++++++++++++++				
Calcasieu Lock									
Freshwater Bayou Lock				++++++++		+++++++++		++++++++	
Catfish Point C.S.		+++++++++			++++++++++				
Schooner Bayou C.S.		++++++++			+++++++++++++++++++++++++++				

+ = Open operation of lock or control structure

Table 7
Tidal Constituents for Test W4 and W5 Boundary Conditions

Constituent	Period (Hr)	Gulf of Mexico		Vermilion Bay	
		Amplitude (Ft)	Phase (Hr)	Amplitude (Ft)	Phase (Hr)
M2	12.42	0.41	2.59	0.11	6.59
S2	12.66	0.09	9.09	0.03	0.84
N2	12.00	0.10	7.45	0.04	1.58
K2	11.97	0.12	9.90	0.02	2.56
K1	23.93	0.42	0.80	0.15	5.39
O1	25.82	0.37	14.92	0.14	19.73
P1	24.07	0.19	3.86	0.11	5.98
SO3	8.21	0.011	2.53	0.004	0.74
M4	6.21	0.001	4.14	0.005	6.21

Table 8
Low Flow Verification Wind Data for Lake Charles, Louisiana
October 1987

Day	Resultant		Average Speed (mph)	Fastest 1-min		Peak Gust	
	Dir (°N)	Speed (mph)		Speed (mph)	Dir (°N)	Speed (mph)	Dir (°N)
1	20	3.0	6.1	9	60	16	NE
2	260	3.8	4.9	14	230	17	SW
3	20	11.5	12.1	18	20	28	NE
4	40	5.2	6.8	14	50	17	NE
5	180	2.5	4.6	10	190	14	S
6	340	6.9	8.1	15	10	20	N
7	350	5.2	7.4	12	360	20	N
8	130	4.1	6.9	12	170	16	S
9	130	5.3	6.6	14	100	14	NE
10	60	5.9	6.3	12	90	18	E
11	10	7.7	8.3	14	20	22	N
12	10	10.3	10.6	15	340	23	N
13	40	7.3	7.6	13	40	20	NE
14	110	3.1	6.3	12	210	16	SE
15	110	5.0	6.6	12	170	17	S

Table 9
Peak Mermentau River Flows

Flood Return Interval (Years)	Peak Discharge (cfs)
2	31,600
5	42,200
10	51,200
25	60,700
50	72,200

Table 10
Grand and White Lakes Low Flow Testing

Testing Conditions				
Test ID	River Flow	Tide Level	Tide Range	Wide
W3	Low	Mean	Mean	None
S1	Low	+0.5 ft	Mean	SE
S2	Mean	+0.5 ft	Mean	SE
W4	Low	Vary	Vary	None
W5	Mean	Vary	Vary	SE

Table 11
Plan 1 Summary of High-flow Test Results

	Maximum Flood Stages[1] and Differences[2] From Base (ft)									
	2-Year		5-Year		10-Year		25-Year		50-Year	
Station	Plan	Diff	Plan	Diff	Plan	Diff	Plan	Diff	Plan	Diff
354	1.9	0.0	1.9	0.0	1.9	0.0	2.0	0.0	2.0	0.0
432	2.4	-0.1	2.7	-0.1	3.0	-0.2	3.7	0.2	4.0	0.0
805	2.5	-0.1	2.8	-0.2	3.1	-0.3	3.5	-0.3	3.9	-0.4
1375	3.3	0.0	3.8	-0.2	4.3	-0.3	4.9	-0.3	5.5	-0.4
1744	2.6	0.0	2.9	-0.2	3.3	-0.1	4.0	0.2	4.3	0.0
1870	3.3	0.0	3.8	-0.2	4.3	-0.3	5.5	0.3	5.9	-0.1
1906	2.0	0.0	2.1	0.0	2.1	0.0	2.2	0.1	2.2	0.0
1998	2.2	-0.5	2.3	-1.0	2.4	-1.3	2.6	-1.6	4.8	0.0
2024	1.9	0.0	1.9	-0.1	1.9	-0.3	1.9	-0.5	2.7	0.0
2276	1.9	0.0	1.9	0.0	1.9	0.0	1.9	0.0	1.9	0.0
2545	2.0	-0.1	2.2	0.0	2.3	-0.1	2.6	0.1	2.7	0.0
3050	3.2	-0.1	3.8	-0.2	4.3	-0.3	4.9	-0.3	5.5	-0.4
3194	3.2	-0.1	3.7	-0.3	4.2	-0.4	4.8	-0.4	5.5	-0.4
3479	2.0	0.1	2.3	0.4	2.5	0.6	2.7	0.5	2.8	0.9

[1] Stages are in ft above mean low gulf (MLG).
[2] Differences are Plan minus Base.

Table 12
Plan 2 Summary of High-flow Test Results

	Maximum Flood Stages[1] and Differences[2] From Base (ft)									
	2-Year		5-Year		10-Year		25-Year		50-Year	
Station	Plan	Diff	Plan	Diff	Plan	Diff	Plan	Diff	Plan	Diff
354	1.9	0.0	1.9	0.0	1.9	0.0	1.9	-0.1	2.0	0.0
432	2.5	0.0	2.8	0.0	3.1	-0.1	3.4	-0.1	3.8	-0.2
805	2.6	0.0	2.9	-0.1	3.3	-0.1	3.7	-0.1	4.1	-0.2
1375	3.4	0.1	4.0	0.0	4.5	-0.1	5.1	-0.1	5.8	-0.1
1744	2.7	0.1	3.0	-0.1	3.4	0.01	3.7	-0.1	4.2	-0.1
1870	3.4	0.1	4.0	0.0	4.5	-0.1	5.1	-0.1	5.8	-0.2
1906	2.0	0.0	2.1	0.0	2.1	0.0	2.1	0.0	2.2	0.0
1998	2.4	-0.3	2.6	-0.7	2.8	-0.9	3.0	-1.2	3.2	-1.6
2024	1.9	0.0	1.9	-0.1	1.9	-0.3	1.9	-0.5	1.9	-0.8
2276	1.9	0.0	1.9	0.0	1.9	0.0	1.9	0.0	1.9	0.0
2545	2.1	0.0	2.2	0.0	2.3	-0.1	2.5	0.0	2.7	0.0
3050	3.2	-0.1	3.9	-0.1	4.4	-0.2	5.1	-0.1	5.7	-0.2
3194	3.3	0.0	3.9	-0.1	4.5	-0.1	5.1	-0.1	5.7	-0.2
3479	1.9	0.0	1.9	0.0	1.9	0.0	1.9	0.0	2.0	0.1

[1] Stages are in ft above MLG
[2] Differences are Plan minus Base.

Table 13
Plan 3 Summary of High-flow Test Results

	Maximum Flood Stages[1] and Differences[2] From Base (ft)									
	2-Year		5-Year		10-Year		25-Year		50-Year	
Station	Plan	Diff	Plan	Diff	Plan	Diff	Plan	Diff	Plan	Diff
354	1.9	0.0	1.9	0.0	1.9	0.0	2.0	0.0	2.0	0.0
432	2.5	0.0	2.8	0.0	3.2	0.0	3.5	0.0	4.0	0.0
805	2.5	-0.1	2.9	-0.1	3.3	-0.1	3.7	-0.1	4.2	-0.1
1375	3.3	0.0	4.0	0.0	4.6	0.0	5.2	0.0	5.9	0.0
1744	2.6	0.0	3.1	0.0	3.4	0.0	3.8	0.0	4.3	0.0
1870	3.3	0.0	4.0	0.0	4.6	0.0	5.2	0.0	5.9	-0.1
1906	2.0	0.0	2.1	0.0	2.1	0.0	2.1	0.0	2.2	0.0
1998	2.7	0.0	3.3	0.0	3.7	0.0	4.2	0.0	4.8	0.0
2024	1.9	0.0	2.0	0.0	2.2	0.0	2.4	0.0	2.7	0.0
2276	1.9	0.0	1.9	0.0	1.9	0.0	1.9	0.0	1.9	0.0
2545	2.1	0.0	2.2	0.0	2.3	-0.1	2.5	0.0	2.7	0.0
3050	3.3	0.0	4.0	0.0	4.6	0.0	5.2	0.0	5.9	0.0
3194	3.3	0.0	4.0	0.0	4.6	0.0	5.2	0.0	5.9	0.0
3479	1.9	0.0	1.9	0.0	1.9	0.0	1.9	0.0	1.9	0.0

[1] Stages are in ft above MLG.
[2] Differences are Plan minus Base

Table 14
Plan 8 Summary of High-flow Test Results

	Maximum Flood Stages[1] and Differences[2] From Base (ft)									
	2-Year		5-Year		10-Year		25-Year		50-Year	
Station	Plan	Diff	Plan	Diff	Plan	Diff	Plan	Diff	Plan	Diff
354	1.9	0.0	1.9	0.0	1.9	0.0	2.0	0.0	2.0	0.0
432	2.5	0.0	2.8	0.0	3.2	0.0	3.5	0.0	4.0	0.0
805	2.6	0.0	3.0	0.0	3.4	0.0	3.8	0.0	4.3	0.0
1375	3.3	0.0	4.0	0.0	4.6	0.0	5.2	0.0	5.9	0.0
1744	2.6	0.0	3.1	0.0	3.4	0.0	3.8	0.0	4.3	0.0
1870	3.3	0.0	4.0	0.0	4.6	0.0	5.2	0.0	5.9	-0.1
1906	2.0	0.0	2.1	0.0	2.1	0.0	2.1	0.0	2.2	0.0
1998	2.7	0.0	3.3	0.0	3.7	0.0	4.2	0.0	4.8	0.0
2024	1.9	0.0	2.0	0.0	2.2	0.0	2.4	0.0	2.7	0.0
2276	1.9	0.0	1.9	0.0	1.9	0.0	1.9	0.0	1.9	0.0
2545	2.1	0.0	2.2	0.0	2.4	0.0	2.5	0.0	2.7	0.0
3050	3.3	0.0	4.0	0.0	4.6	0.0	5.2	0.0	5.9	0.0
3194	3.3	0.0	4.0	0.0	4.6	0.0	5.2	0.0	5.9	0.0
3479	1.9	0.0	1.9	0.0	1.9	0.0	1.9	0.0	1.9	0.0

[1] Stages are in ft above MLG.
[2] Differences are Plan minus Base.

Table 15
Plan 9 Summary of High-flow Test Results

	Maximum Flood Stages[1] and Differences[2] From Base (ft)									
	2-Year		5-Year		10-Year		25-Year		50-Year	
Station	Plan	Diff	Plan	Diff	Plan	Diff	Plan	Diff	Plan	Diff
354	1.9	0.0	1.9	0.0	1.9	0.0	1.9	-0.1	2.0	0.0
432	2.3	-0.2	2.6	-0.2	2.8	-0.4	3.1	-0.4	3.5	-0.5
805	2.3	-0.3	2.6	-0.4	2.9	-0.5	3.3	-0.5	3.7	-0.6
1375	3.0	-0.3	3.6	-0.4	4.1	-0.5	4.6	-0.6	5.3	-0.6
1744	2.4	-0.2	2.8	-0.3	3.1	-0.3	3.4	-0.4	3.9	-0.4
1870	3.0	-0.3	3.5	-0.5	4.0	-0.6	4.6	-0.6	5.2	-0.8
1906	2.0	0.0	2.1	0.0	2.1	0.0	2.1	0.0	2.2	0.0
1998	2.4	-0.3	2.9	-0.4	3.3	-0.4	3.7	-0.5	4.3	-0.5
2024	1.9	0.0	1.9	-0.1	2.0	-0.2	2.2	-0.2	2.4	-0.3
2276	1.9	0.0	1.9	0.0	1.9	0.0	1.9	0.0	1.9	0.0
2545	2.0	-0.1	2.1	-0.1	2.2	-0.2	2.3	-0.2	2.5	-0.2
3050	2.8	-0.5	3.4	-0.6	4.0	-0.6	4.5	-0.7	5.2	-0.7
3194	2.9	-0.4	3.5	-0.5	4.0	-0.6	4.6	-0.6	5.2	-0.7
3479	1.9	0.0	1.9	0.0	1.9	0.0	1.9	0.0	1.9	0.0

[1] Stages are in ft above MLG.
[2] Differences are Plan minus Base.

Table 16
Plam 10 Summary of High-flow Test Results

	Maximum Flood Stages[1] and Differences[2] From Base (ft)									
	2-Year		5-Year		10-Year		25-Year		50-Year	
Station	Plan	Diff	Plan	Diff	Plan	Diff	Plan	Diff	Plan	Diff
354	1.9	0.0	1.9	0.0	1.9	0.0	1.9	-0.1	1.9	-0.1
432	2.2	-0.3	2.5	-0.3	2.7	-0.5	3.0	-0.5	3.3	-0.7
805	2.2	-0.4	2.5	-0.5	2.7	-0.7	3.0	-0.8	3.4	-0.9
1375	2.9	-0.4	3.4	-0.6	3.8	-0.8	4.3	-0.9	4.9	-1.0
1744	2.4	-0.2	2.7	-0.4	2.9	-0.5	3.2	-0.6	3.6	-0.7
1870	2.8	-0.5	3.3	-0.7	3.8	-0.8	4.3	-0.9	4.9	-1.1
1906	2.0	0.0	2.1	0.0	2.1	0.0	2.1	0.0	2.2	0.0
1998	2.3	-0.4	2.7	-0.6	3.1	-0.6	3.5	-0.7	4.0	-0.8
2024	1.9	0.0	1.9	-0.1	1.9	-0.3	2.1	-0.3	2.3	-0.4
2276	1.9	0.0	1.9	0.0	1.9	0.0	1.9	0.0	1.9	0.0
2545	2.0	-0.1	2.0	-0.2	2.1	-0.3	2.2	-0.3	2.4	-0.3
3050	2.6	-0.7	3.2	-0.8	3.7	-0.9	4.3	-0.9	4.9	-1.0
3194	2.7	-0.6	3.3	-0.7	3.8	-0.8	4.3	-0.9	4.9	-1.0
3479	1.9	0.0	1.9	0.0	1.9	0.0	1.9	0.0	1.9	0.0

[1] Stages are in ft above MLG.
[2] Differences are Plan minus Base.

Table 17
Plam 11 Summary of High-flow Test Results

	Maximum Flood Stages[1] and Differences[2] From Base (ft)									
	2-Year		5-Year		10-Year		25-Year		50-Year	
Station	Plan	Diff	Plan	Diff	Plan	Diff	Plan	Diff	Plan	Diff
354	1.9	0.0	1.9	0.0	1.9	0.0	1.9	-0.1	1.9	-0.1
432	2.4	-0.1	2.7	-0.1	3.0	-0.2	3.4	-0.1	3.8	-0.2
805	1.9	-0.7	1.9	-1.1	2.1	-1.3	2.3	-1.5	2.5	-1.8
1375	3.3	-0.0	4.0	-0.0	4.6	0.0	5.2	0.0	5.9	0.0
1744	2.6	0.0	3.0	-0.1	3.4	0.0	3.8	0.0	4.3	0.0
1870	3.3	0.0	4.0	0.0	4.6	0.0	5.2	0.0	5.9	-0.1
1906	2.0	0.0	2.1	0.0	2.1	0.0	2.1	0.0	2.2	0.0
1998	2.7	0.0	3.2	-0.1	3.7	0.0	4.2	0.0	4.8	0.0
2024	1.9	0.0	2.0	0.0	2.2	0.0	2.4	0.0	2.7	0.0
2276	1.9	0.0	1.9	0.0	1.9	0.0	1.9	0.0	1.9	0.0
2545	1.8	-0.3	1.9	-0.3	2.0	-0.4	2.1	-0.4	2.3	-0.4
3050	3.2	-0.1	3.9	-0.1	4.5	-0.1	5.2	0.0	5.9	0.0
3194	3.3	0.0	3.9	-0.1	4.5	-0.1	5.2	0.0	5.9	0.0
3479	1.9	0.0	1.9	0.0	1.9	0.0	1.9	0.0	1.9	0.0

[1] Stages are in ft above MLG.
[2] Differences are Plan minus Base.

Table 18
Plan 16 Summary of High-flow Test Results

	Maximum Flood Stages[1] and Differences[2] From Base (ft)									
	2-Year		5-Year		10-Year		25-Year		50-Year	
Station	Plan	Diff	Plan	Diff	Plan	Diff	Plan	Diff	Plan	Diff
354	2.0	0.1	2.0	0.1	2.0	0.1	2.0	0.0	2.0	0.0
432	2.4	-0.1	2.7	-0.1	3.0	-0.2	3.3	-0.2	3.7	-0.3
805	2.0	-0.6	2.3	-0.7	2.6	-0.8	2.9	-0.9	3.3	-1.0
1375	3.2	-0.1	3.8	-0.2	4.3	-0.3	4.9	-0.3	5.6	-0.3
1744	2.5	-0.1	2.9	-0.2	3.2	-0.2	3.6	-0.2	4.1	-0.2
1870	3.2	-0.1	3.8	-0.2	4.3	-0.3	4.9	-0.3	5.6	-0.4
1906	2.0	0.0	2.1	0.0	2.1	0.0	2.1	0.0	2.2	0.0
1998	2.6	-0.1	3.1	-0.2	3.5	-0.2	4.0	-0.2	4.5	-0.3
2024	1.9	0.0	1.9	-0.1	2.1	-0.1	2.3	-0.1	2.5	-0.2
2276	1.9	0.0	1.9	0.0	1.9	0.0	1.9	0.0	1.9	0.0
2545	1.9	-0.2	2.1	-0.1	2.2	0.24	2.3	-0.2	2.5	-0.2
3050	3.0	-0.3	3.7	-0.3	4.3	-0.3	4.9	-0.3	5.6	-0.3
3194	3.1	-0.2	3.7	-0.3	4.3	-0.3	4.9	-0.3	5.6	-0.3
3479	1.9	0.0	1.9	0.0	1.9	0.0	1.9	0.0	1.9	0.0

[1] Stages are in ft above MLG.
[2] Differences are Plan minus Base.

Table 19
Plan 17 Summary of High-flow Test Results

	Maximum Flood Stages[1] and Differences[2] From Base (ft)									
	2-Year		5-Year		10-Year		25-Year		50-Year	
Station	Plan	Diff	Plan	Diff	Plan	Diff	Plan	Diff	Plan	Diff
354	2.0	0.1	2.0	0.1	2.0	0.1	2.0	0.0	2.0	0.0
432	2.5	0.0	2.8	0.0	3.2	0.0	3.5	0.0	3.9	-0.1
805	2.6	0.0	3.0	0.0	3.4	0.0	3.8	0.0	4.3	0.0
1375	3.3	0.0	4.0	0.0	4.6	0.0	5.2	0.0	5.9	0.0
1744	2.6	0.0	3.0	-0.1	3.4	0.0	3.8	0.0	4.3	0.0
1870	3.3	0.0	4.0	0.0	4.6	0.0	5.2	0.0	5.9	-0.1
1906	2.0	0.0	2.1	0.0	2.1	0.0	2.1	0.0	2.2	0.0
1998	2.6	-0.1	3.1	-0.2	3.6	-0.1	4.1	-0.1	4.7	-0.1
2024	1.9	0.0	1.9	-0.1	1.9	-0.3	1.9	-0.5	2.0	-0.7
2276	1.9	0.0	1.9	0.0	1.9	0.0	1.9	0.0	1.9	0.0
2545	2.1	0.0	2.2	0.0	2.3	-0.1	2.5	0.0	2.7	0.0
3050	3.3	0.0	4.0	0.0	4.6	0.0	5.2	0.0	5.9	0.0
3194	3.3	0.0	4.0	0.0	4.6	0.0	5.2	0.0	5.9	0.0
3479	1.9	0.0	1.9	0.0	1.9	0.0	1.9	0.0	1.9	0.0

[1] Stages are in ft above MLG.
[2] Differences are Plan minus Base.

Table 20
Results of Low Flow Salinity Test S1

Station	Base Salinity (ppt)	Plan 5		Plan 6	
		Salinity (ppt)	Change (ppt)	Salinity (ppt)	Change (ppt)
354	19.5	19.5	0.0	19.5	0.0
432	8.0	6.2	-1.8	5.4	-2.6
805	1.7	2.0	0.3	1.9	0.2
1375	1.3	1.3	0.0	1.3	0.0
1744	6.5	6.3	-0.2	6.0	-0.5
1870	4.8	4.8	0.0	4.7	-0.1
1906	19.0	19.0	0.0	19.0	0.0
1998	3.0	2.9	-0.1	3.0	0.0
2024	5.3	5.3	0.0	5.3	0.0
2276	14.2	14.2	0.0	14.2	0.0
2545	13.6	13.9	0.3	13.8	0.2
3050	3.4	3.4	0.0	3.4	0.0
3194	1.1	1.1	0.0	1.1	0.0
3479	14.1	14.1	0.0	14.1	0.0

Table 21
Results of Low Flow Salinity Test S2

Station	Base Salinity (ppt)	Plan 5		Plan 6	
		Salinity (ppt)	Change (ppt)	Salinity (ppt)	Change (ppt)
354	17.5	17.6	0.1	17.5	0.0
432	4.4	3.3	-1.1	3.0	-1.4
805	1.4	1.7	0.3	1.6	0.2
1375	0.7	0.7	0.0	0.7	0.0
1744	3.4	3.3	-0.1	3.2	-0.2
1870	1.0	1.0	0.0	1.0	0.0
1906	1.5	1.5	0.0	1.5	0.0
1998	2.0	2.0	0.01	2.0	0.0
2024	4.0	4.0	0.0	4.0	0.0
2276	13.5	13.5	0.0	13.5	0.0
2545	9.0	9.4	0.4	9.2	0.2
3050	1.0	1.0	0.0	1.0	0.0
3194	1.0	1.0	0.0	1.0	0.0
3479	13.5	13.5	0.0	13.5	0.0

Table 22
Results of Low Flow Salinity Test W3

Station	Base Salinity (ppt)	Plan 5		Plan 6	
		Salinity (ppt)	Change (ppt)	Salinity (ppt)	Change (ppt)
354	18.7	18.7	0.0	18.7	0.0
432	6.7	5.1	-1.6	4.4	-2.3
805	1.5	1.8	0.3	1.8	0.3
1375	0.9	0.9	0.0	0.9	0.0
1744	5.4	5.2	-0.2	5.0	-0.4
1870	1.0	1.0	0.0	1.0	0.0
1906	7.3	7.3	0.0	7.3	0.0
1998	2.8	2.8	0.01	2.8	0.0
2024	5.1	5.1	0.0	5.1	0.0
2276	13.9	13.9	0.0	13.9	0.0
2545	11.8	12.2	0.4	12.0	0.2
3050	1.0	1.0	0.0	1.0	0.0
3194	1.1	1.1	0.0	1.1	0.0
3479	12.7	12.7	0.0	12.7	0.0

Table 23
Results of Low Flow Salinity Test W4

Station	Base Slinity (ppt)	Plan 7		Plan 13		Plan 14		Plan 15		Plan 16		Plan 18	
		Salinity (ppt)	Change (ppt)	Salinity (ppt)	Change (ppt)	Salinity (ppt)	Change (ppt)	Salinity (ppt)	Change (ppt)	Salinity (ppt)	Change (ppt)	Salinity (ppt)	Change (ppt)
354	18.5	18.8	0.3	18.7	0.2	-	-	18.8	0.3	18.7	0.2	-	-
432	7.0	4.9	-2.1	7.3	0.3	6.9	-0.1	4.9	-2.1	7.3	0.3	6.9	-0.1
805	2.3	2.1	-0.2	2.3	0.0	2.2	-0.1	2.1	-0.2	2.3	0.0	2.2	-0.1
1375	2.9	2.5	-0.4	2.7	-0.2	2.0	-0.9	2.5	-0.4	2.7	-0.2	2.0	-0.9
1744	5.7	5.8	0.1	6.0	0.3	5.7	0.0	5.8	0.1	6.0	0.3	5.7	0.0
1870	8.6	18.1	9.5	8.4	-0.2	14.2	5.6	18.1	9.5	8.4	-0.2	14.2	5.6
1906	23.9	24.7	0.8	24.1	0.2	23.9	0.0	24.7	0.8	24.1	0.2	23.9	0.0
1998	2.8	2.8	0.0	3.0	0.2	-	-	2.8	0.0	3.0	0.2	-	-
2024	4.7	4.7	0.0	4.9	0.0	4.9	0.2	4.7	0.0	4.9	0.0	4.9	0.2
2276	13.7	13.7	0.0	13.7	0.0	-	-	13.7	0.0	13.7	0.0	-	-
2545	11.3	12.3	1.0	11.9	0.6	12.0	0.7	12.3	1.0	11.9	0.6	12.0	0.7
3050	7.7	10.2	2.5	9.6	1.9	7.6	-0.1	10.2	2.5	9.6	1.9	7.6	-0.1
3194	1.1	1.1	0.0	1.9	0.8	1.1	0.0	1.1	0.0	1.9	0.8	1.1	0.0
3479	12.5	12.5	0.0	12.5	0.0	12.7	0.2	12.5	0.0	12.5	0.0	12.7	0.2

Table 24
Results of Low Flow Salinity Test W5

Station	Base Slinity (ppt)	Plan 7		Plan 12		Plan 13		Plan 14		Plan 15		Plan 18	
		Salinity (ppt)	Change (ppt)	Salinity (ppt)	Change (ppt)	Salinity (ppt)	Change (ppt)	Salinity (ppt)	Change (ppt)	Salinity (ppt)	Change (ppt)	Salinity (ppt)	Change (ppt)
354	16.9	18.1	1.2	16.6	-0.3	17.2	0.3	16.8	-0.1	16.7	-0.2	-	-
432	3.8	7.26	3.4	3.2	-0.6	4.0	0.2	2.7	-1.1	2.4	-1.4	3.8	0.0
805	2.1	2.3	0.2	2.1	0.0	2.1	0.0	2.1	-0.02	1.8	-0.3	2.1	0.0
1375	1.1	1.5	0.4	1.1	0.0	1.1	0.0	1.1	0.04	1.0	-0.1	1.1	0.0
1744	3.0	5.0	2.0	2.6	-0.4	3.1	0.1	2.6	-0.4	2.4	-0.6	2.9	-0.1
1870	1.1	15.0	13.9	1.1	0.0	1.1	0.0	1.1	0.0	1.0	-0.1	1.0	-0.1
1906	1.9	23.6	21.7	21.0	19.1	2.2	0.3	2.9	1.0	2.8	0.9	1.9	0.0
1998	2.1	2.3	0.2	2.2	0.1	2.2	0.1	2.2	0.1	2.0	-0.1	-	-
2024	5.0	5.0	0.0	5.1	0.1	5.1	0.1	5.1	0.1	4.4	-0.6	4.4	-0.6
2276	13.1	13.1	0.0	13.1	0.0	-	-	13.1	0.0	13.5	0.4	-	-
2545	8.3	12.8	4.5	7.5	-0.8	8.6	0.3	8.0	-0.3	7.7	-0.6	8.2	-0.1
3050	1.0	3.9	2.9	1.2	0.2	1.2	0.2	1.2	0.2	1.0	0.0	1.0	0.0
3194	0.9	1.0	0.1	0.9	0.0	0.9	0.0	0.9	0.0	0.9	0.0	0.9	0.0
3479	12.0	12.0	0.0	12.0	0.0	12.0	0.0	12.0	0.0	12.4	0.4	12.3	0.3

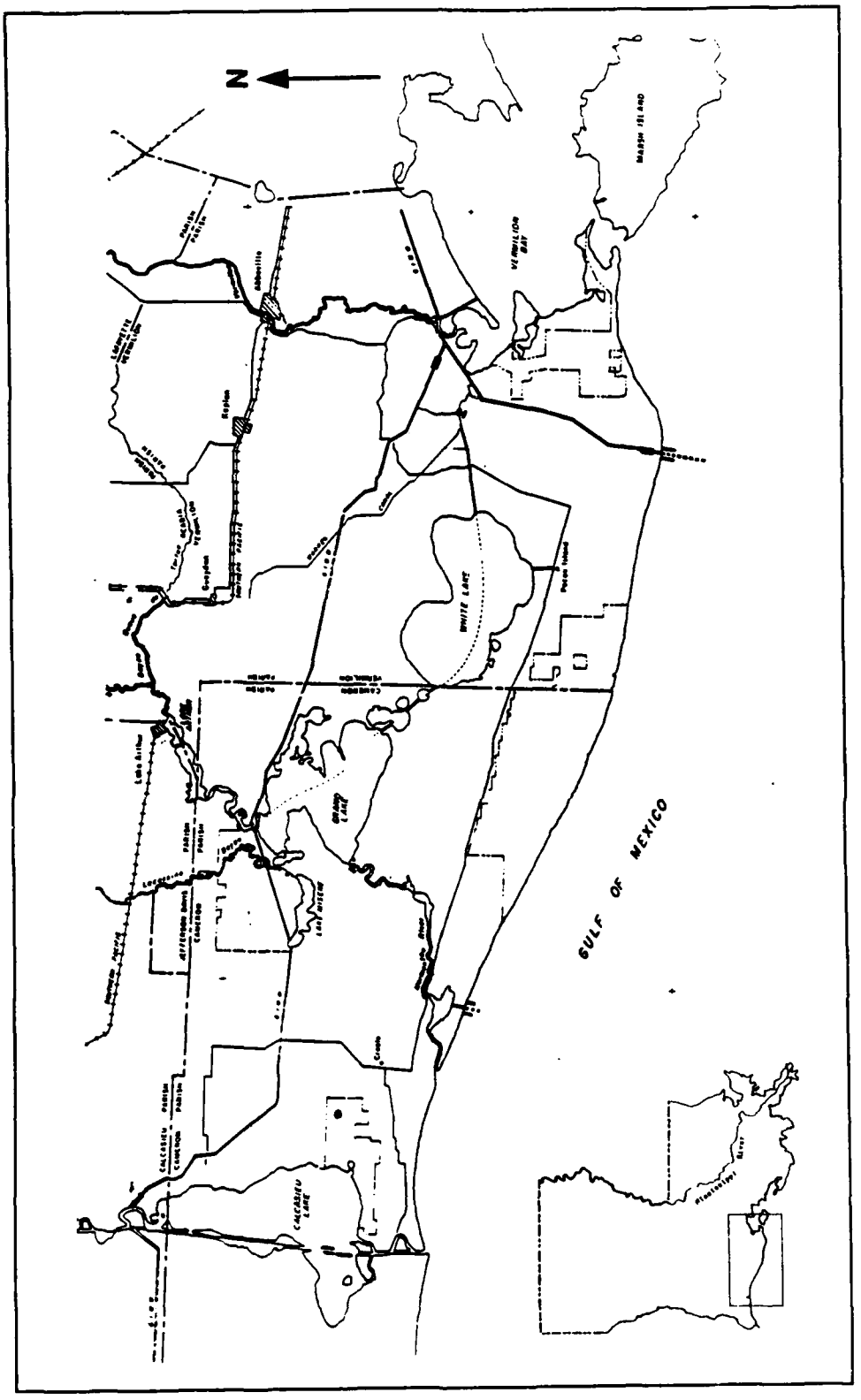

Figure 1. Project location map

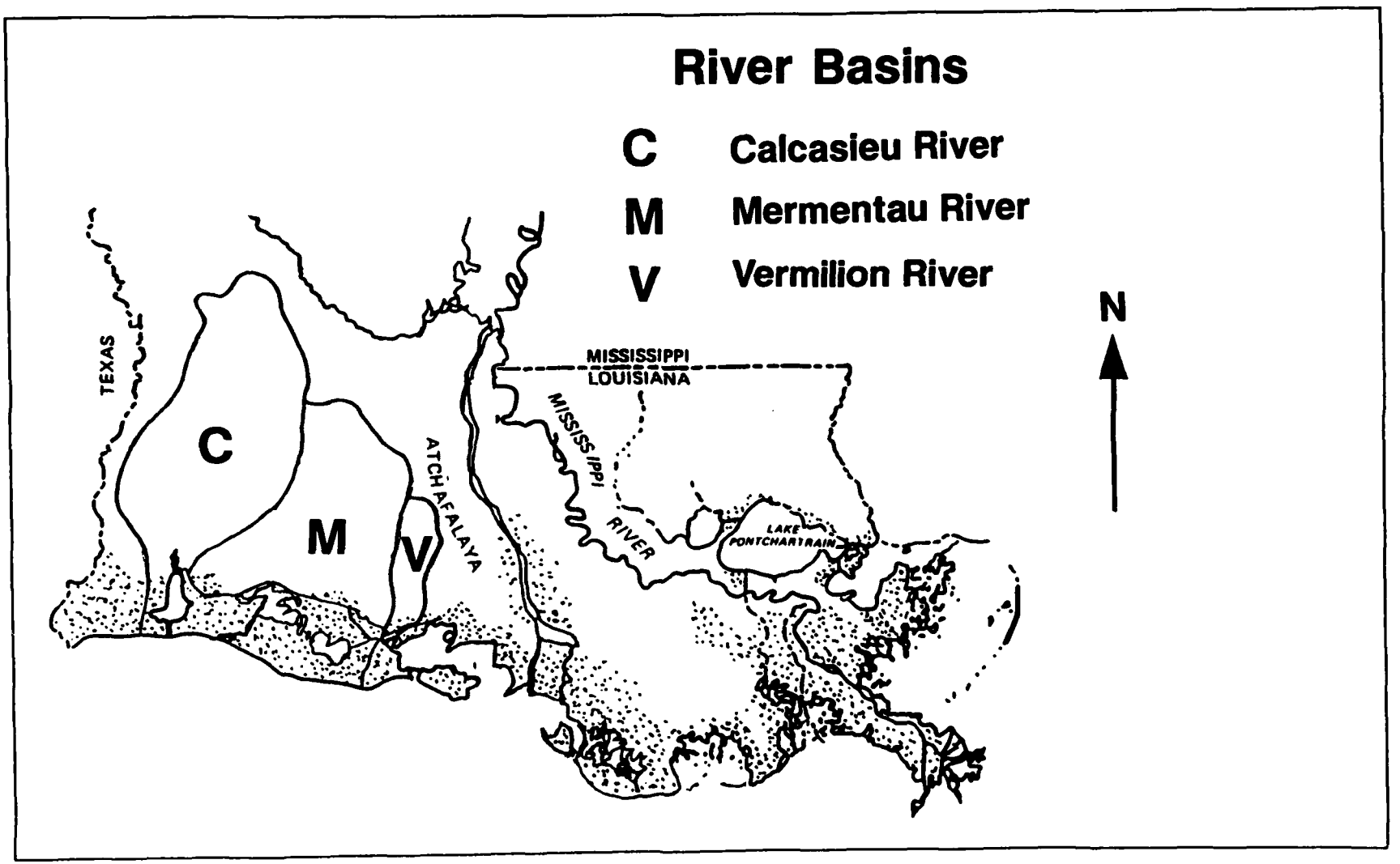

Figure 2. Mermentau River drainage area

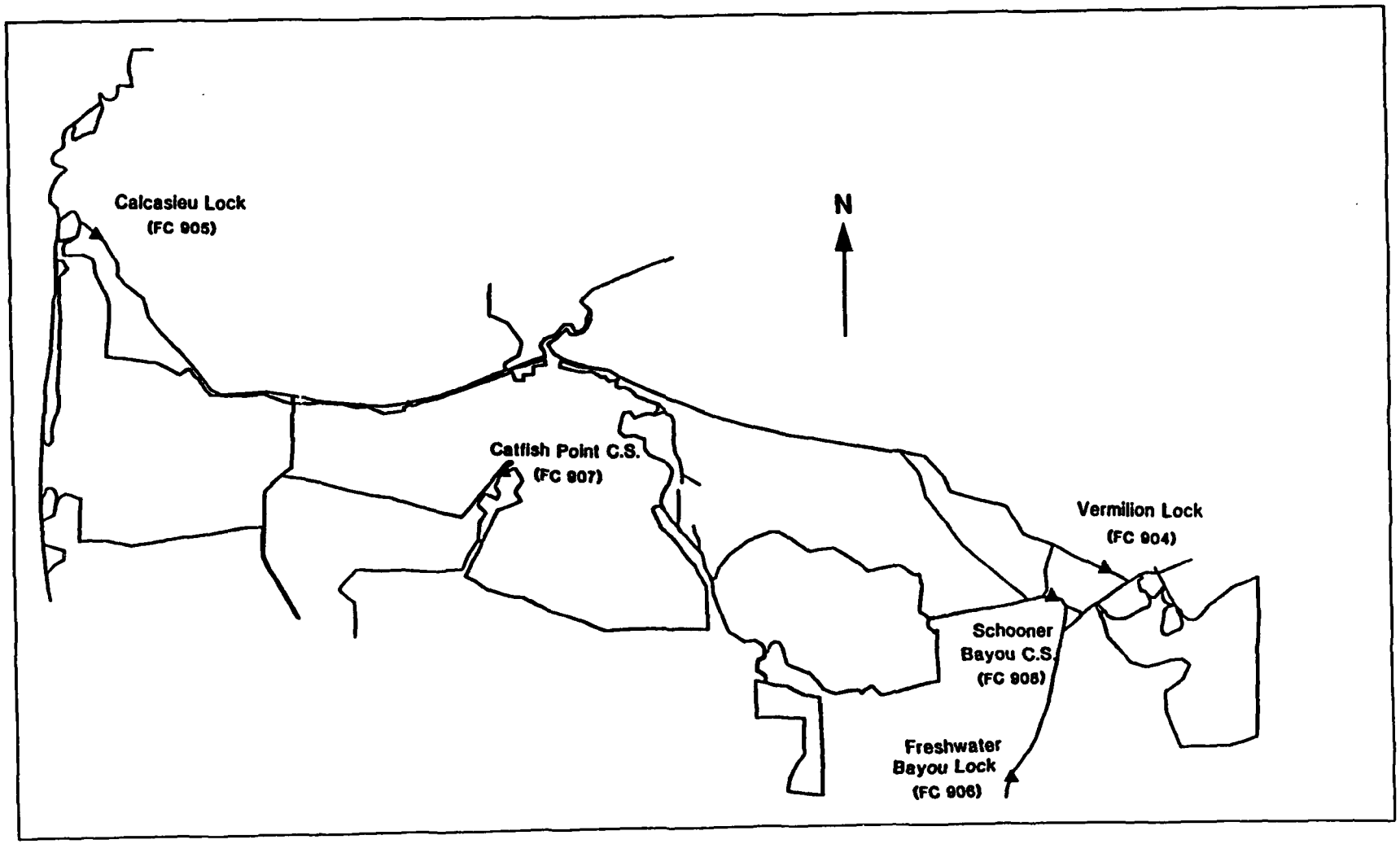

Figure 3. Location of flow control structures and locks in high-flow case network. The label in parentheses refers to the flow controller identification used in the model

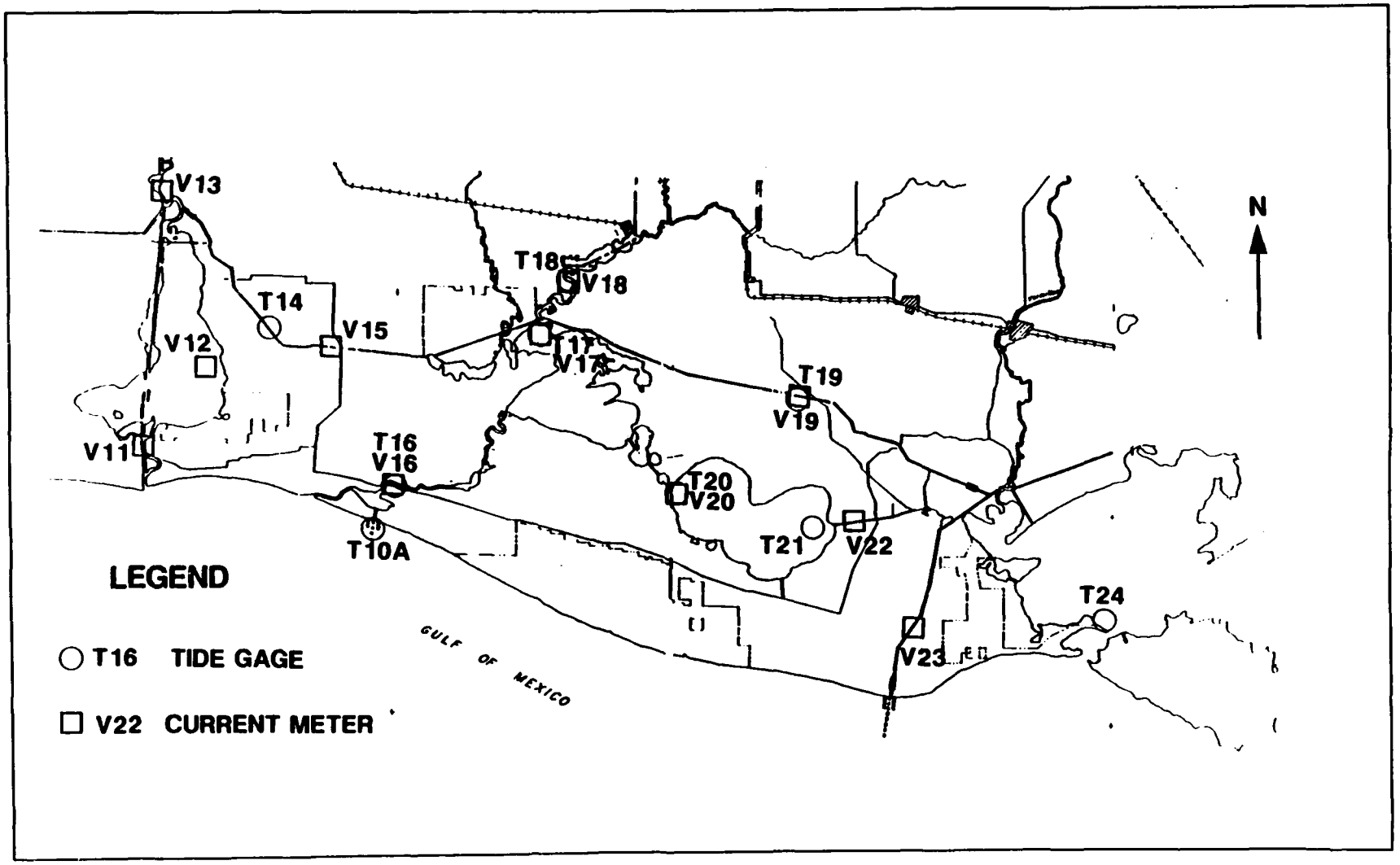

Figure 4. Water level and current meter monitoring stations

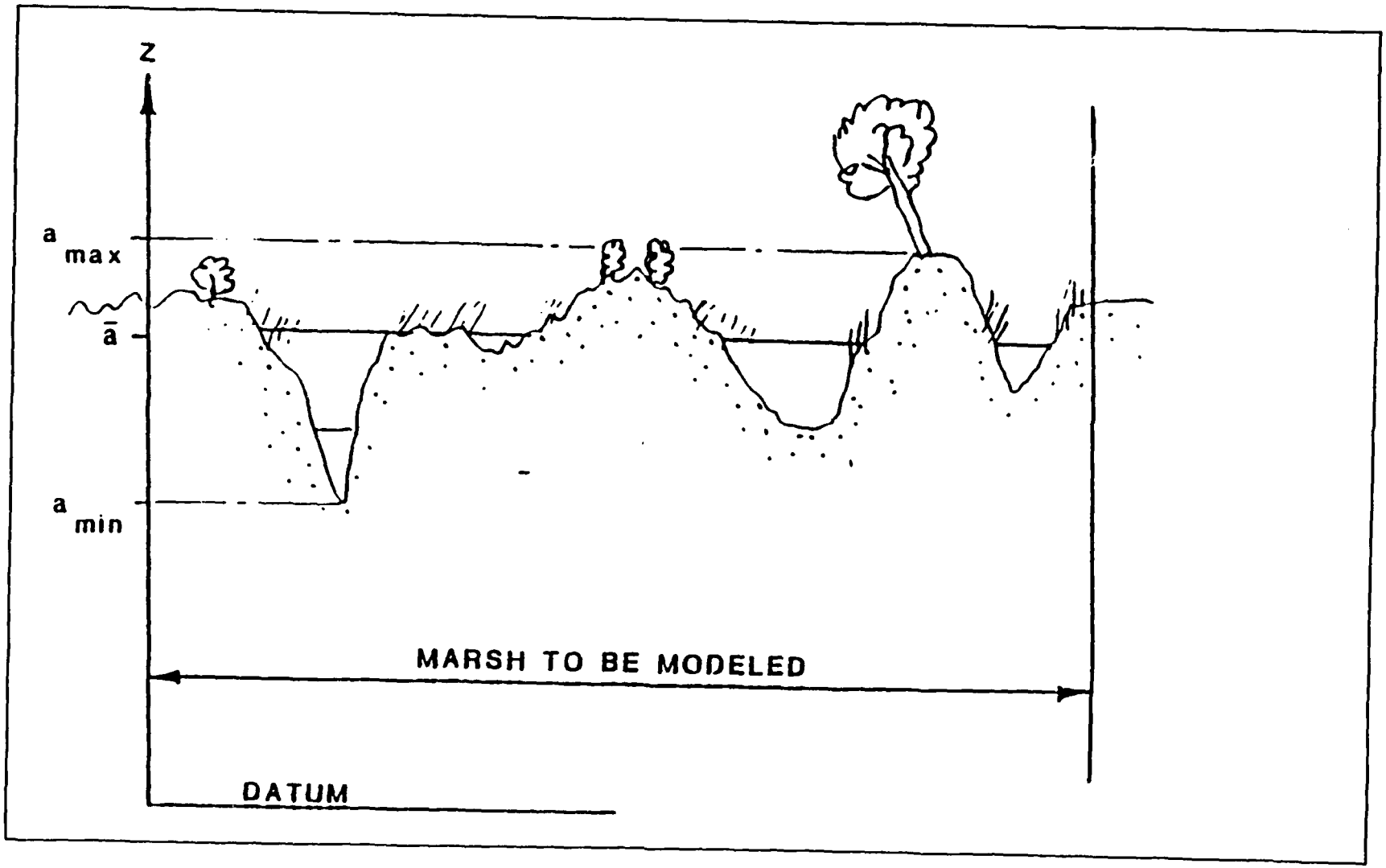

Figure 5. Illustration of marsh to be modeled

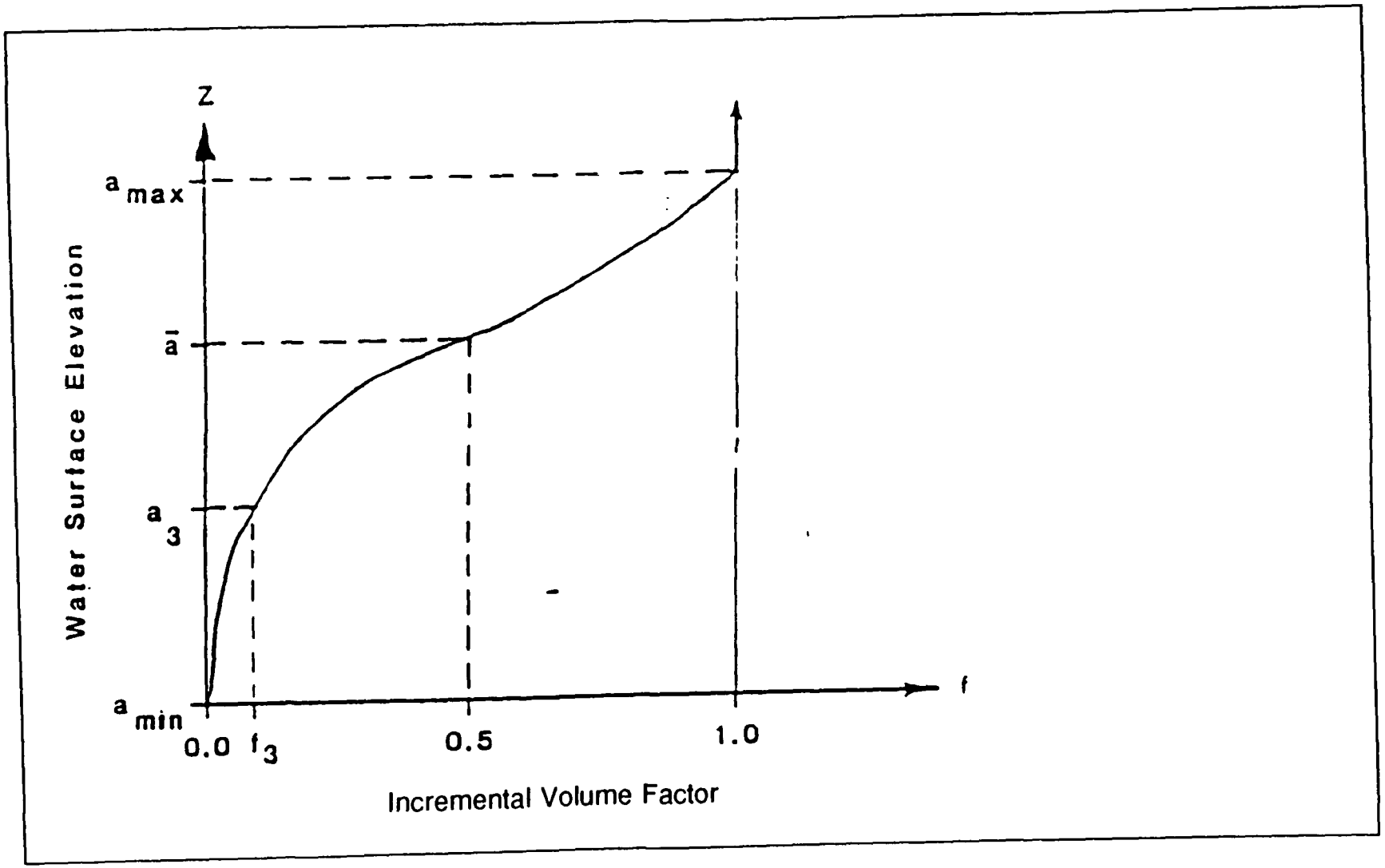

Figure 6. Plot of incremental volume factor vs water surface elevation

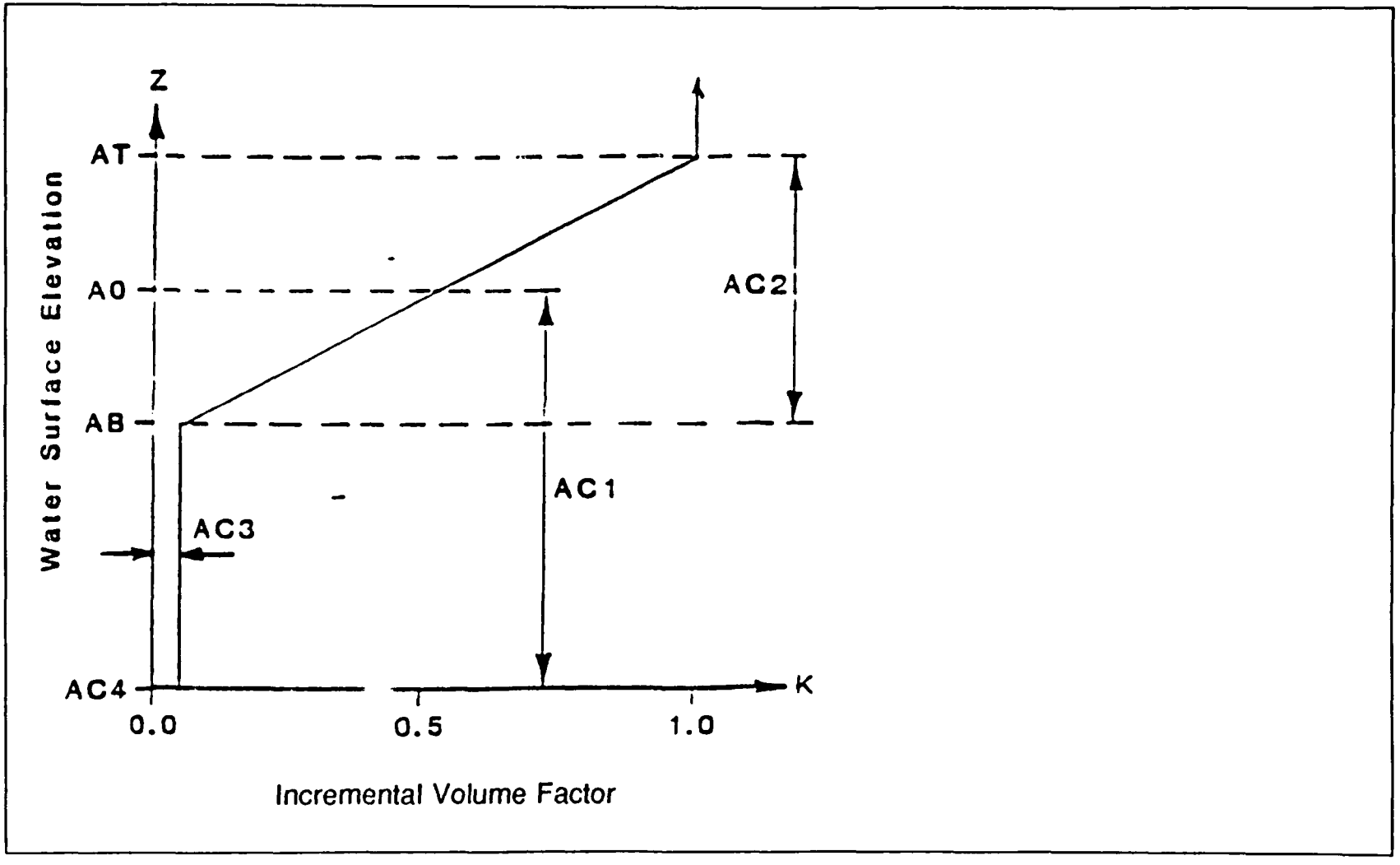

Figure 7. Schematized plot of incremental volume factor vs water surface elevation

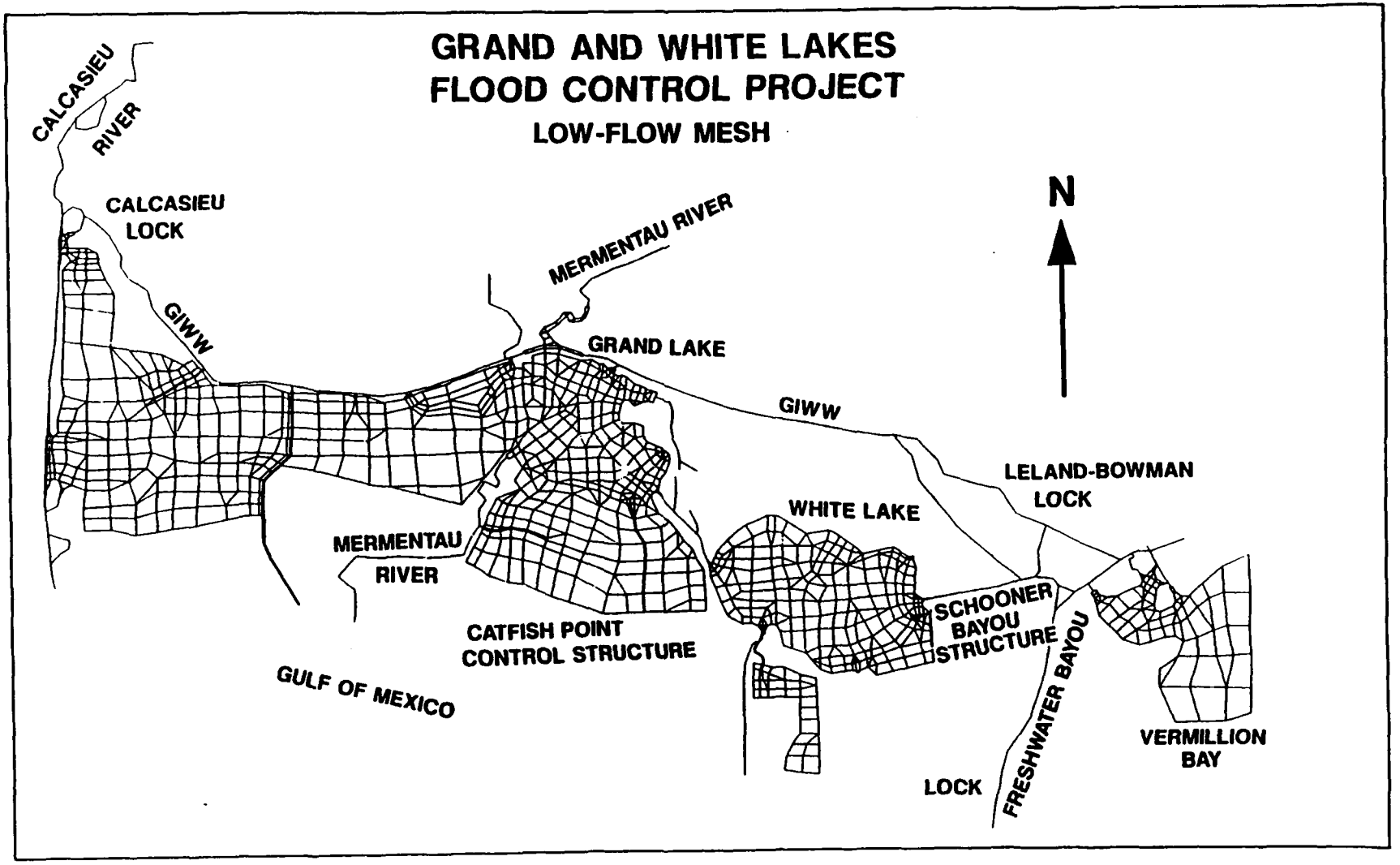

Figure 8. Numerical model low-flow mesh of Grand and White Lakes project

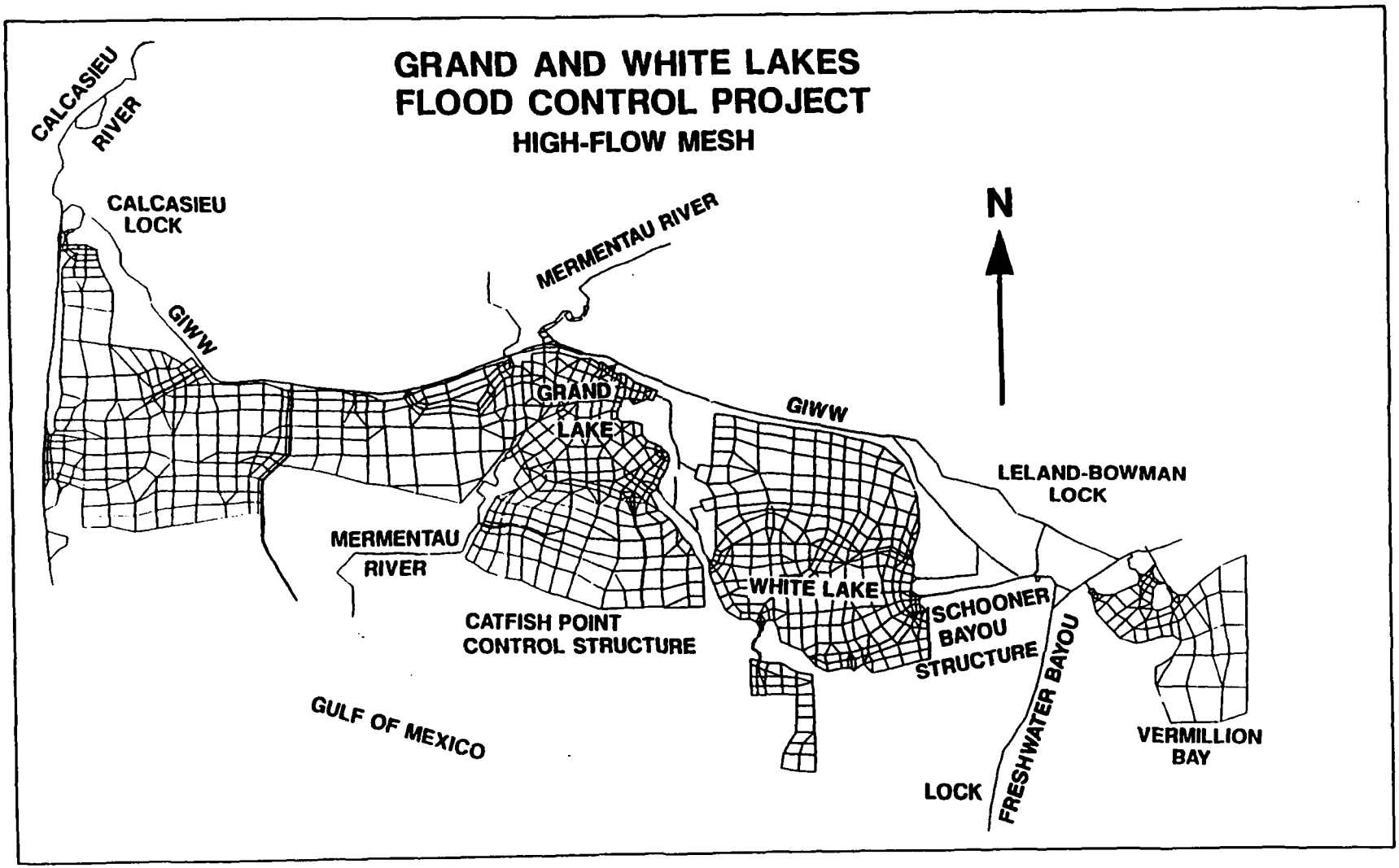

Figure 9. Numerical model high-flow mesh of Grand and White Lakes project

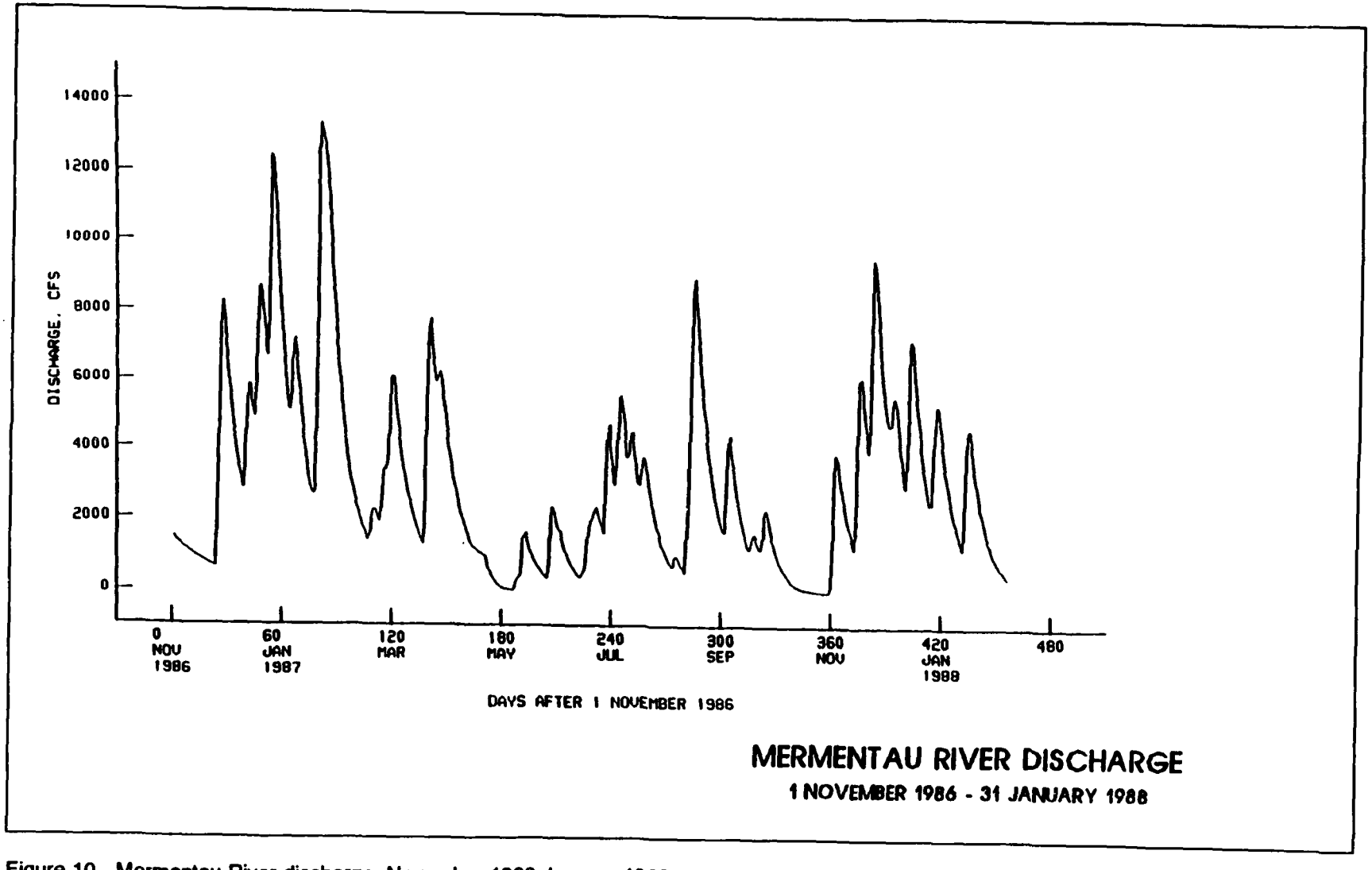

Figure 10. Mermentau River discharge, November 1986-January 1988

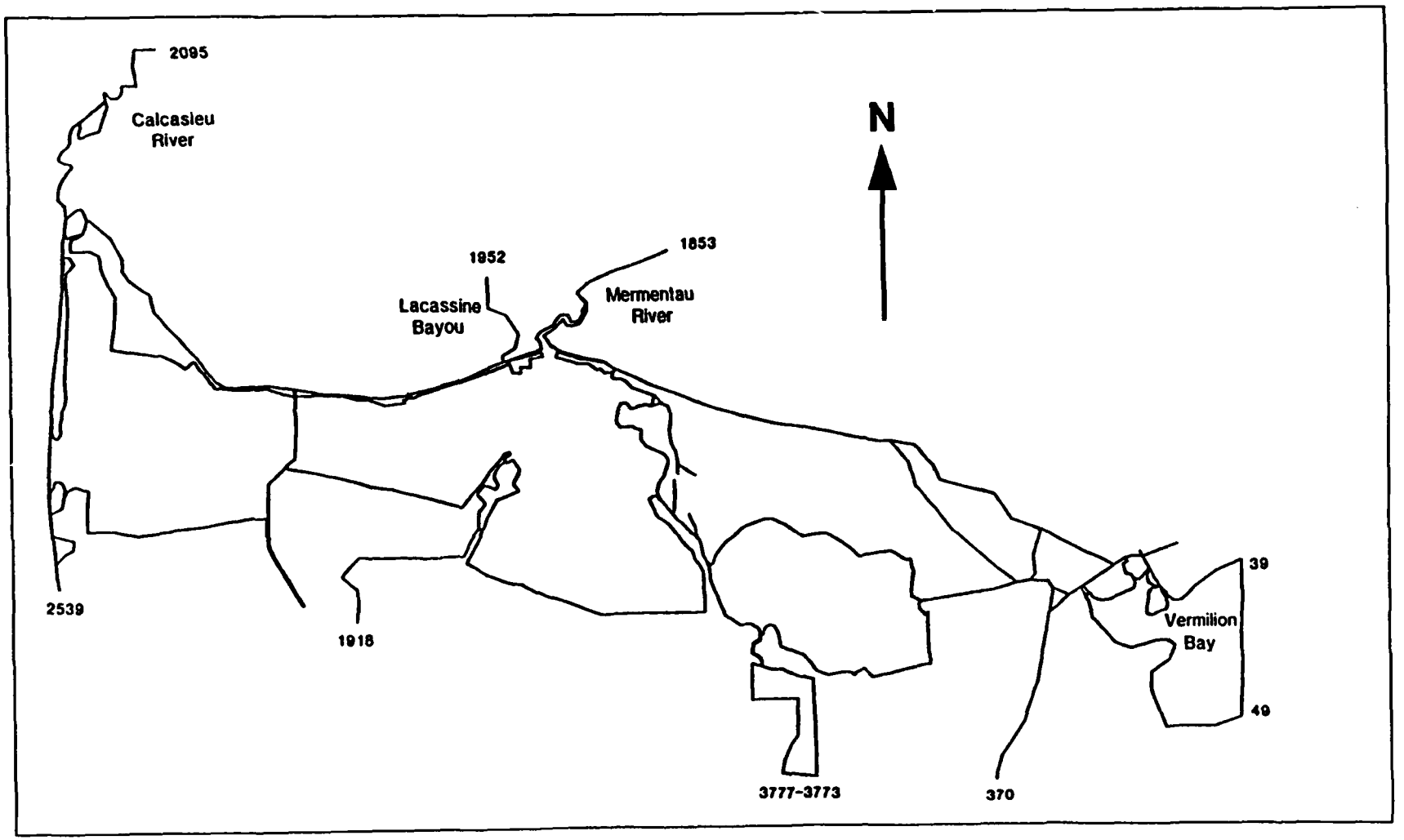

Figure 11. Location of boundary condition stations for the verification simulation. Stations 2095, 1952, and 1853 are flow boundary conditions. Stations 2539, 1918, 3777-3733, 370, and 39-49 are tidal stage boundary conditions

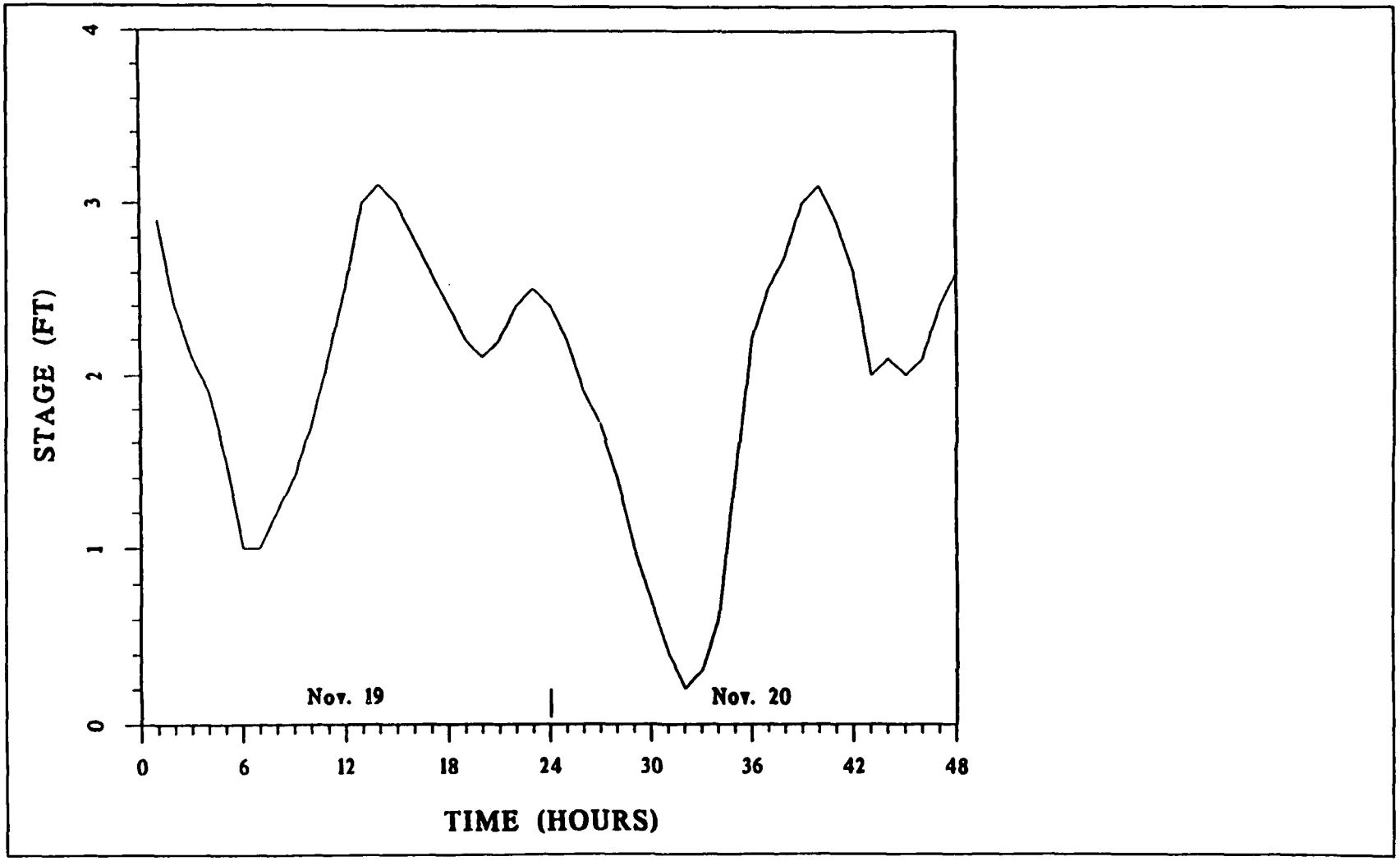

Figure 12. Tidal stage used in verification for Gulf boundary stations

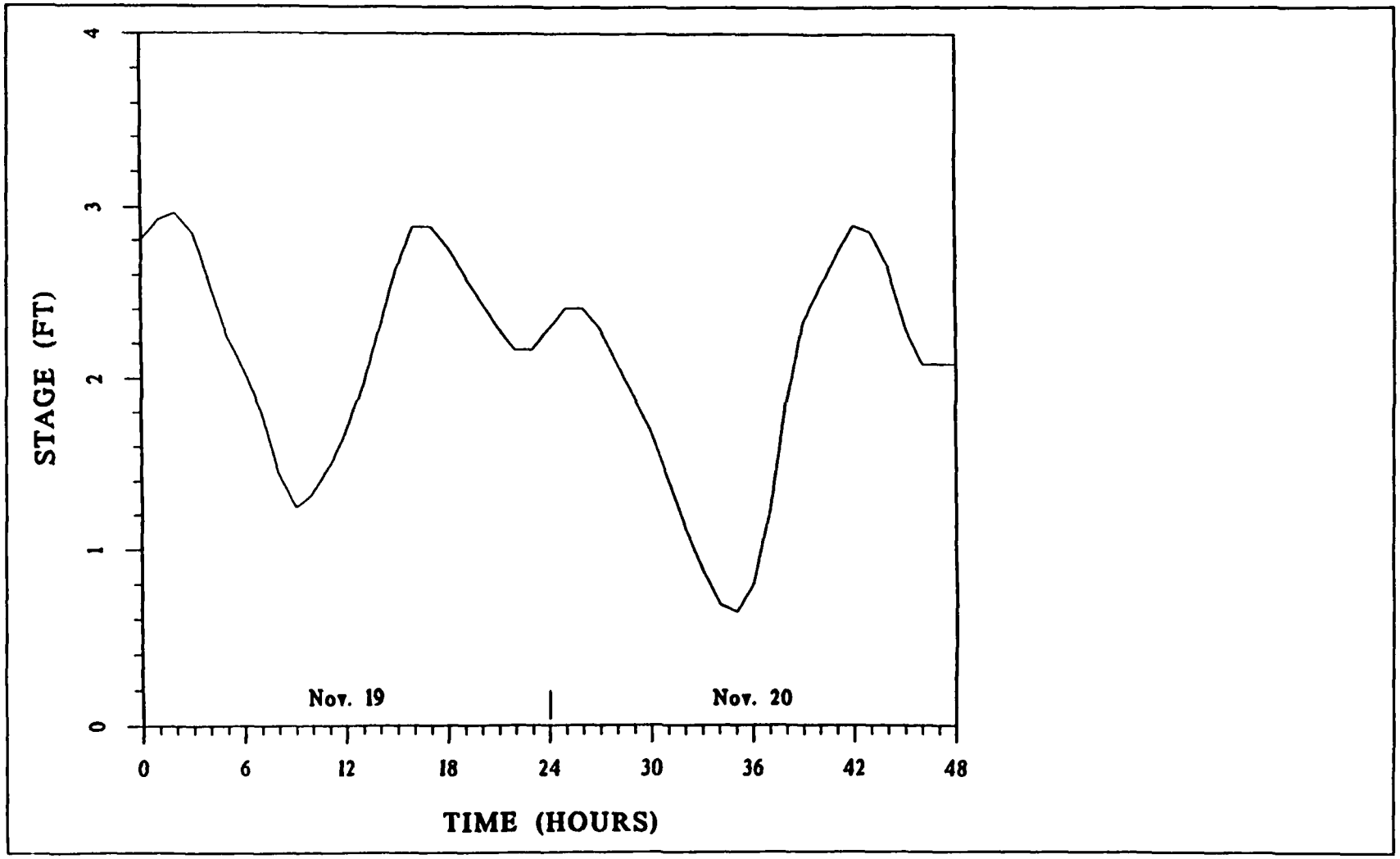

Figure 13. Tidal stage used in verification at Vermillion Bay boundary stations

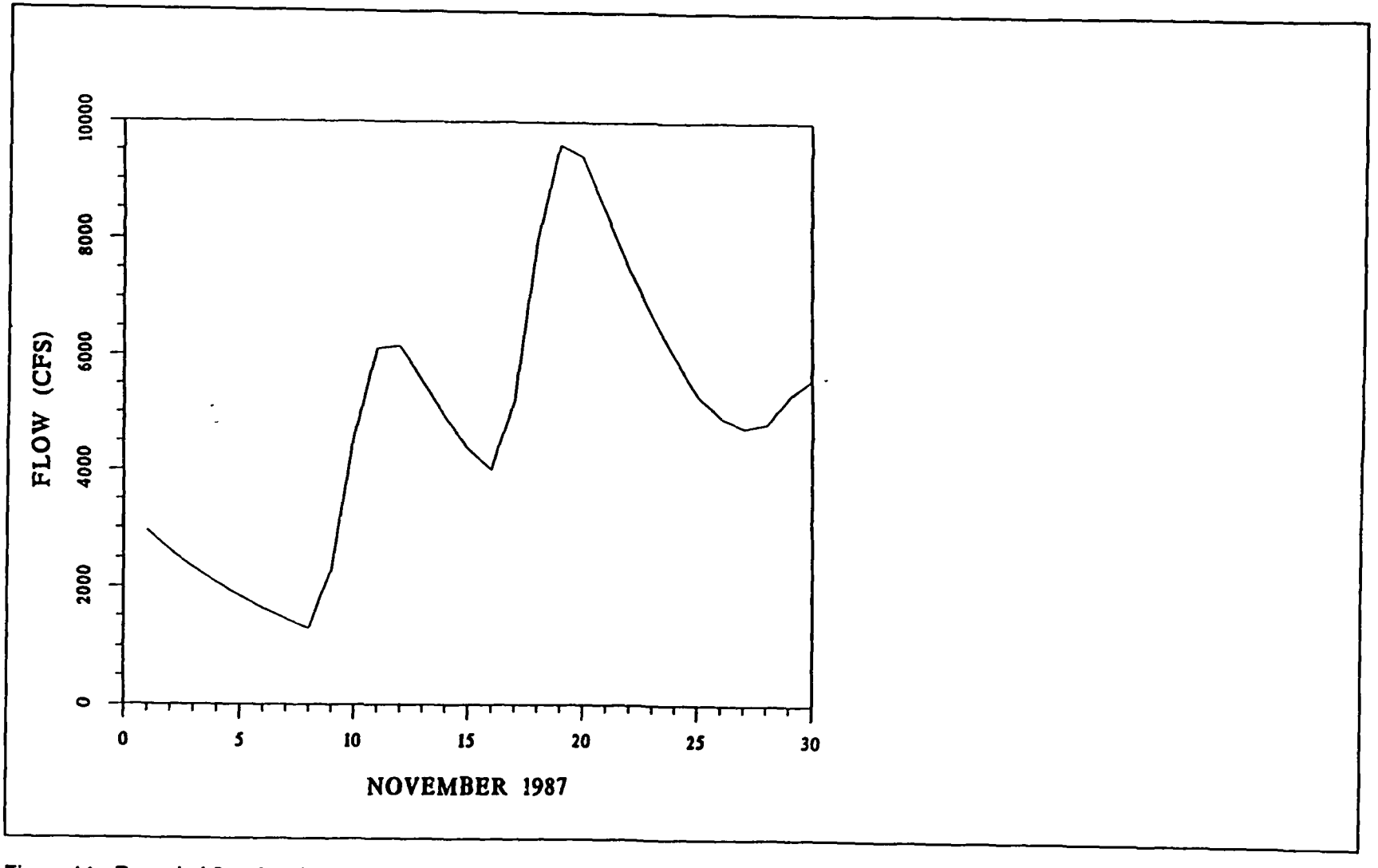

Figure 14. Recorded flow for Mermentau River and Lacassine Bayou at Grand Lake for November 1987

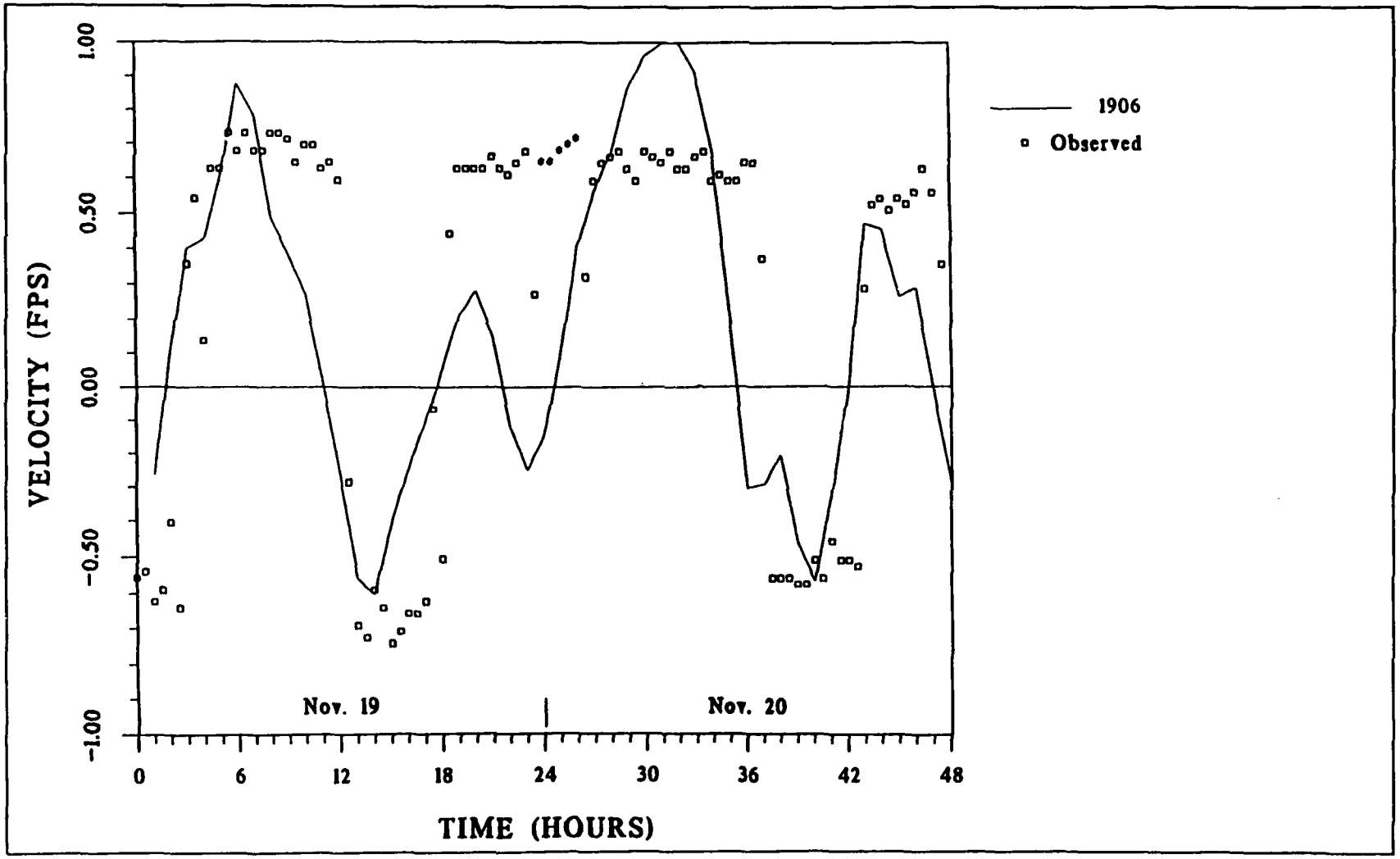

Figure 15. Observed vs. simulated velocities for Station 1744. Positive velocity represents flow towards Gulf

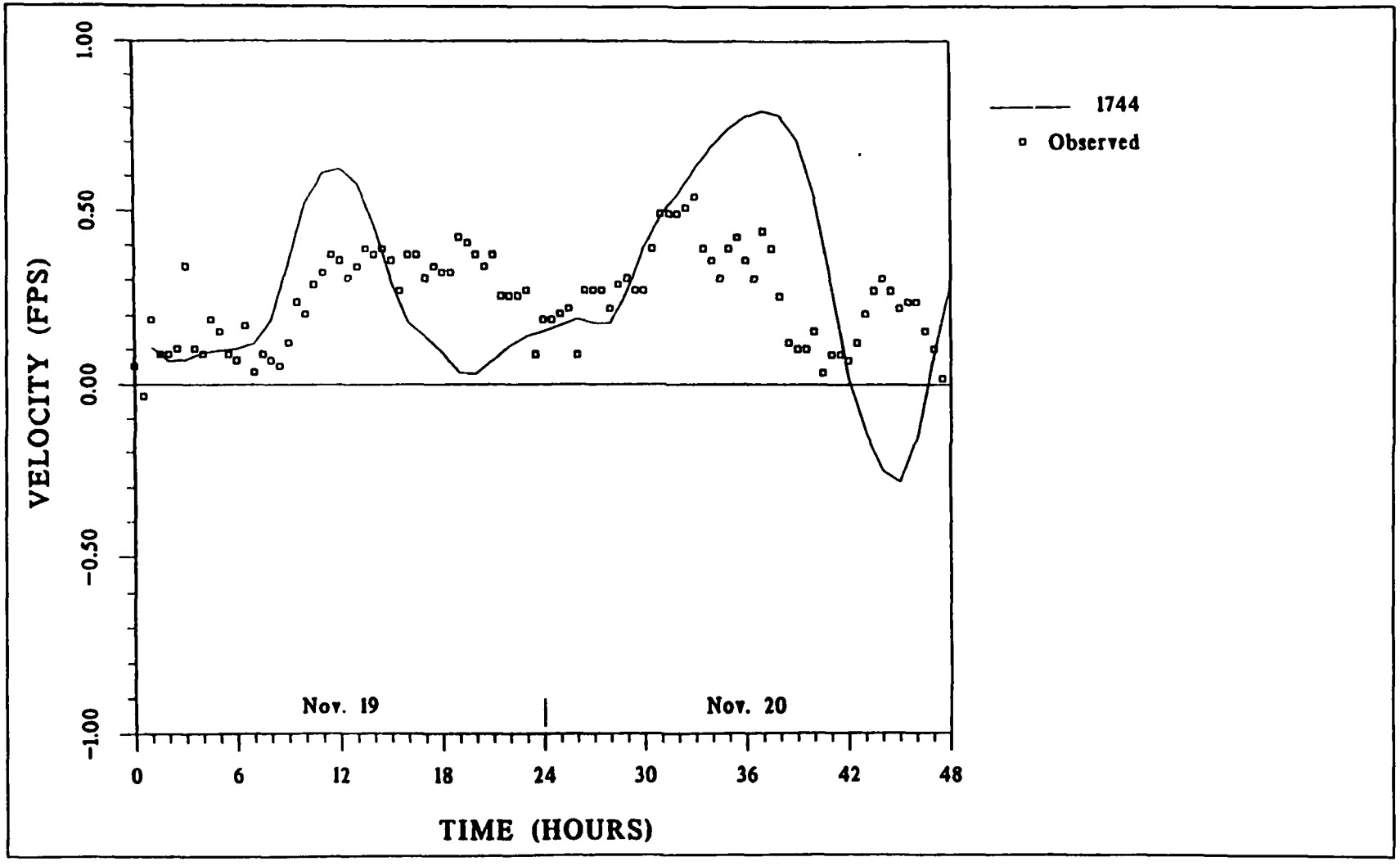

Figure 16. Observed vs. simulated velocities for Station 1744. Positive velocity represents flow towards Gulf

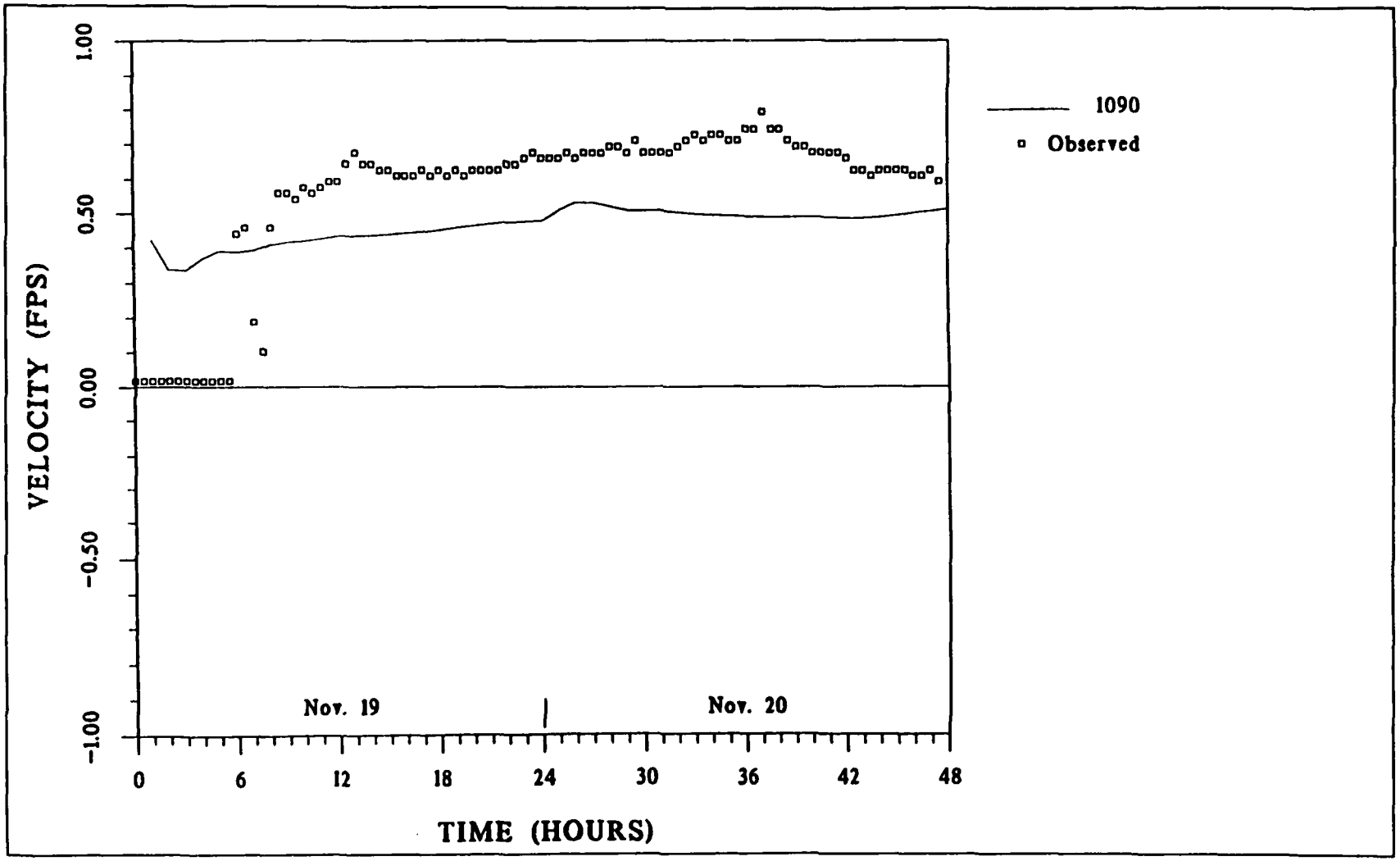

Figure 17. Observed vs. simulated velocities for Station 1090. Positive velocity represents flow towards Gulf

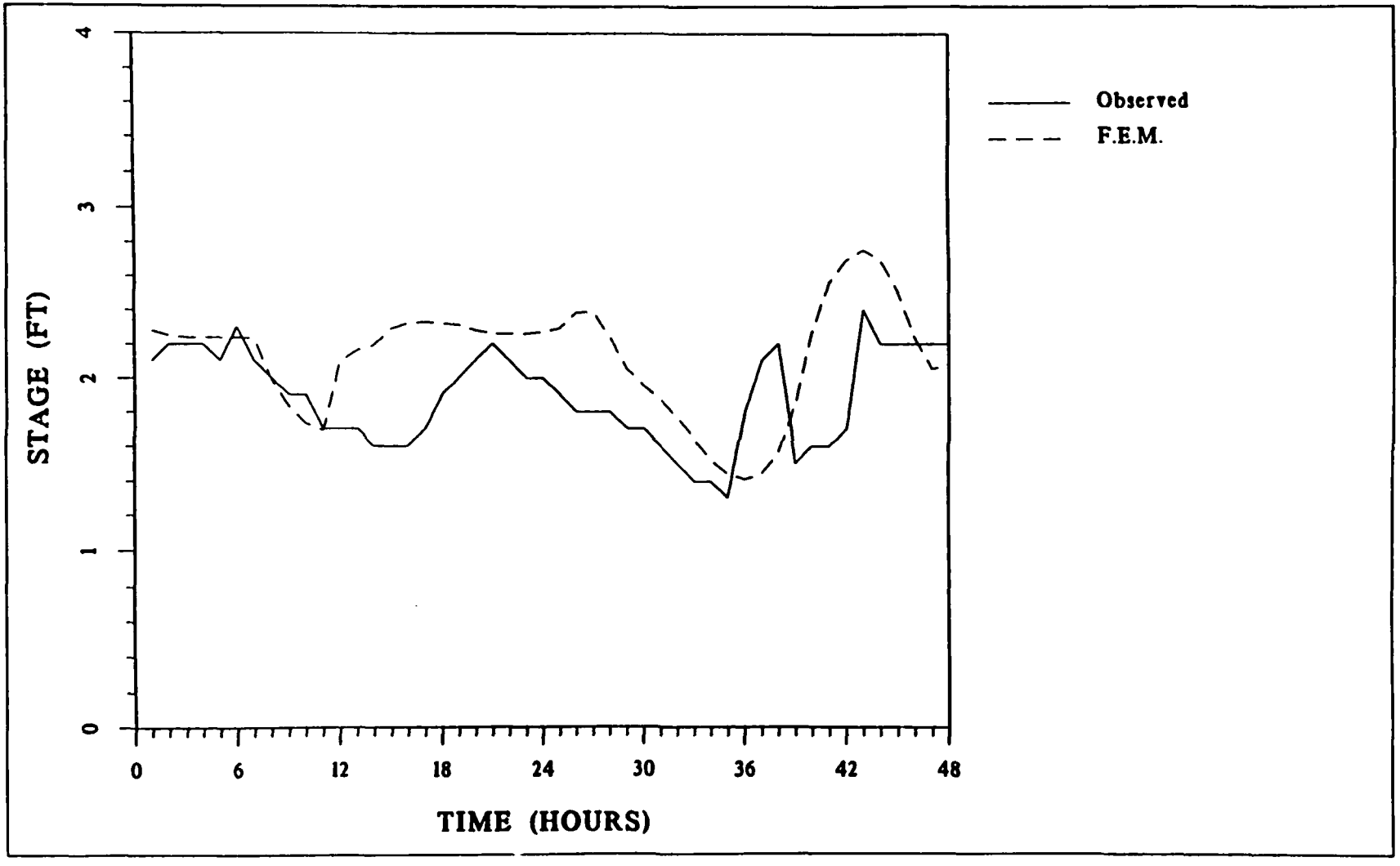

Figure 18. Comparison of observed and model stage at the west end of the Schooner Bayou control structure

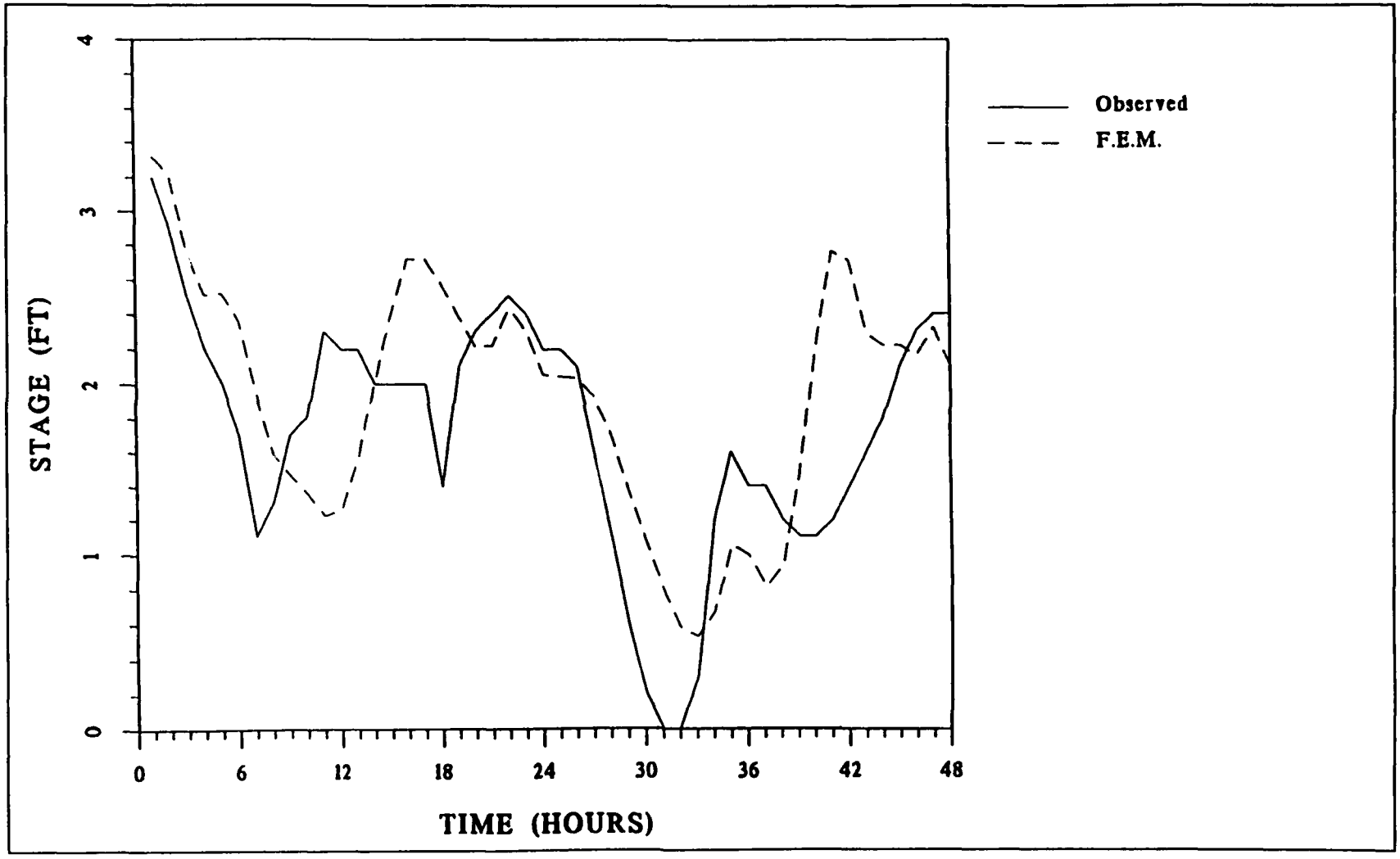

Figure 19. Comparison of observed and model stage at the north end of Freshwater Bayou Lock

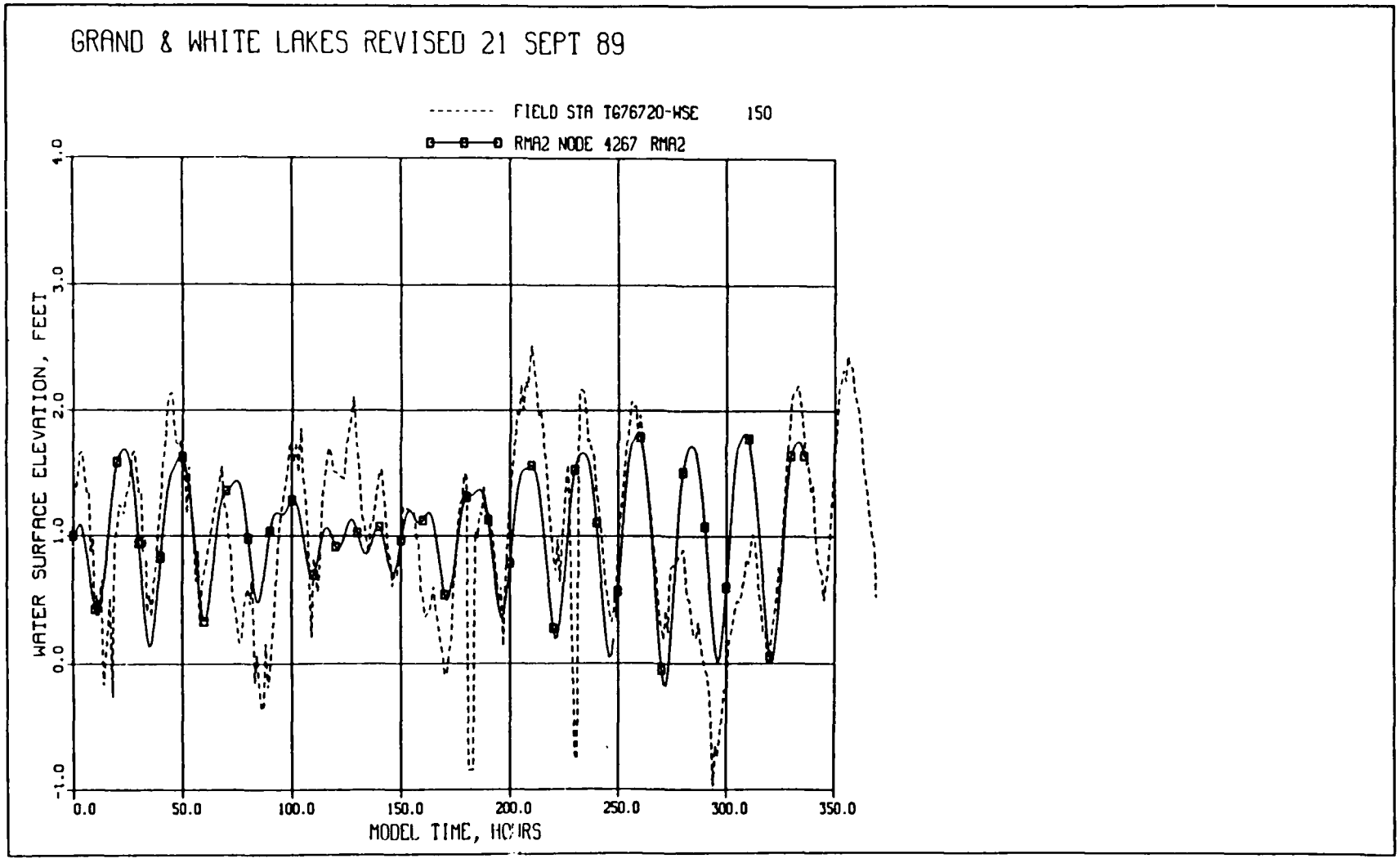

Figure 20. Comparison of field and model water surface elevations at Station 4267 near the downstream end of Vermillion Lock

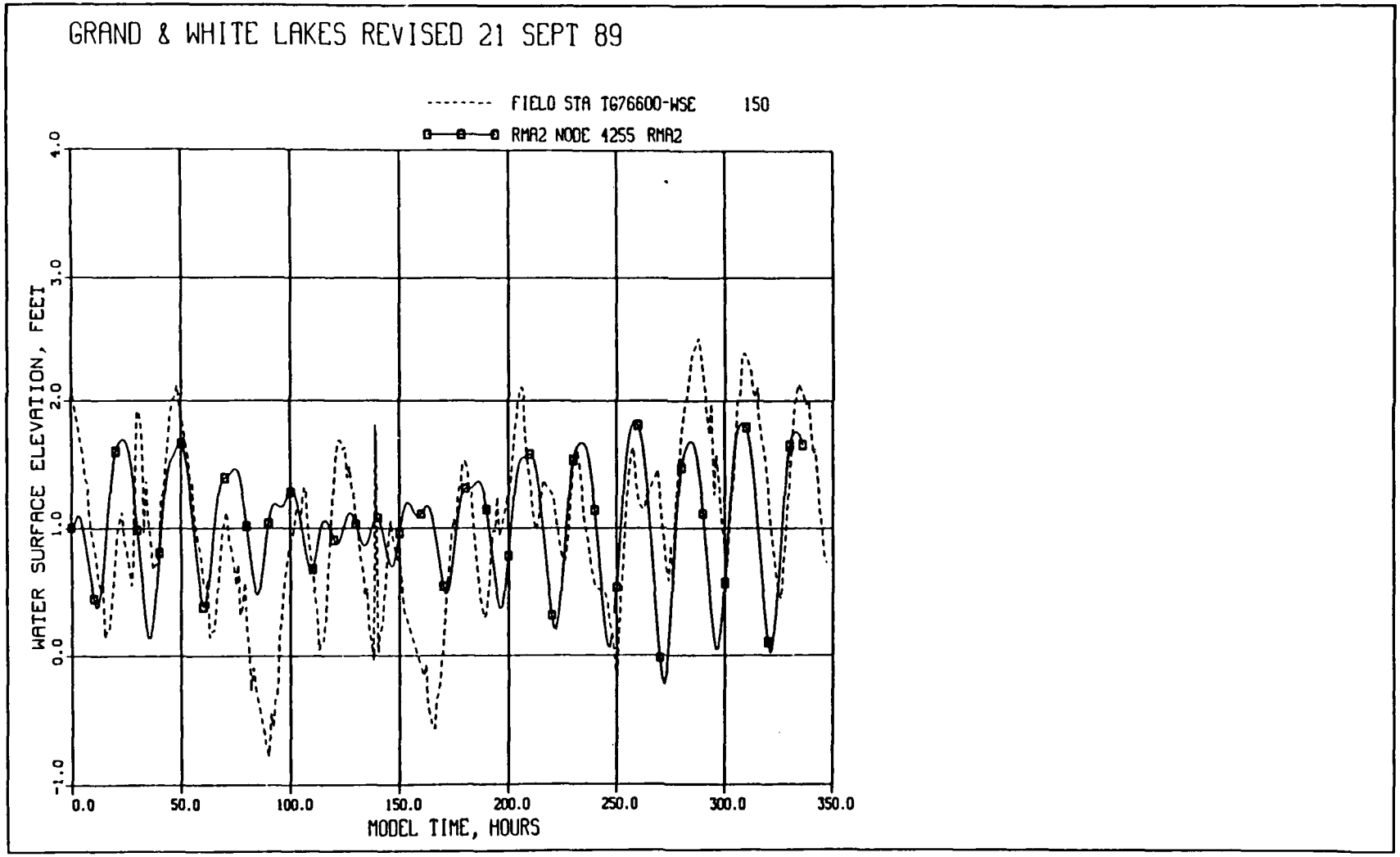

Figure 21. Comparison of field and model water surface elevations at Station 4255 near the downstream end of Schooner Bayou Lock

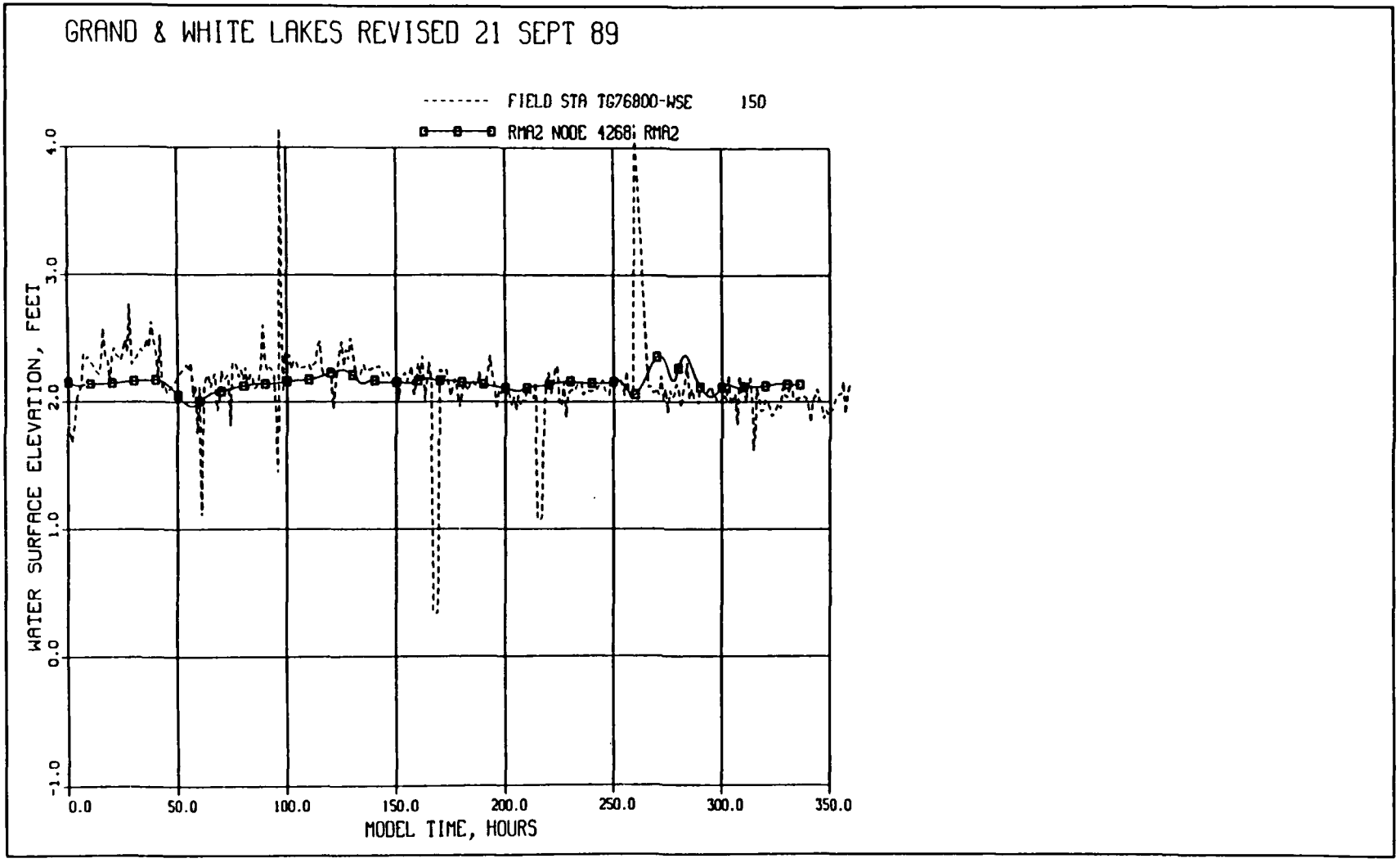

Figure 22. Comparison of field and model water surface elevations at Station 4286 near the upstream end of Vermillion Lock

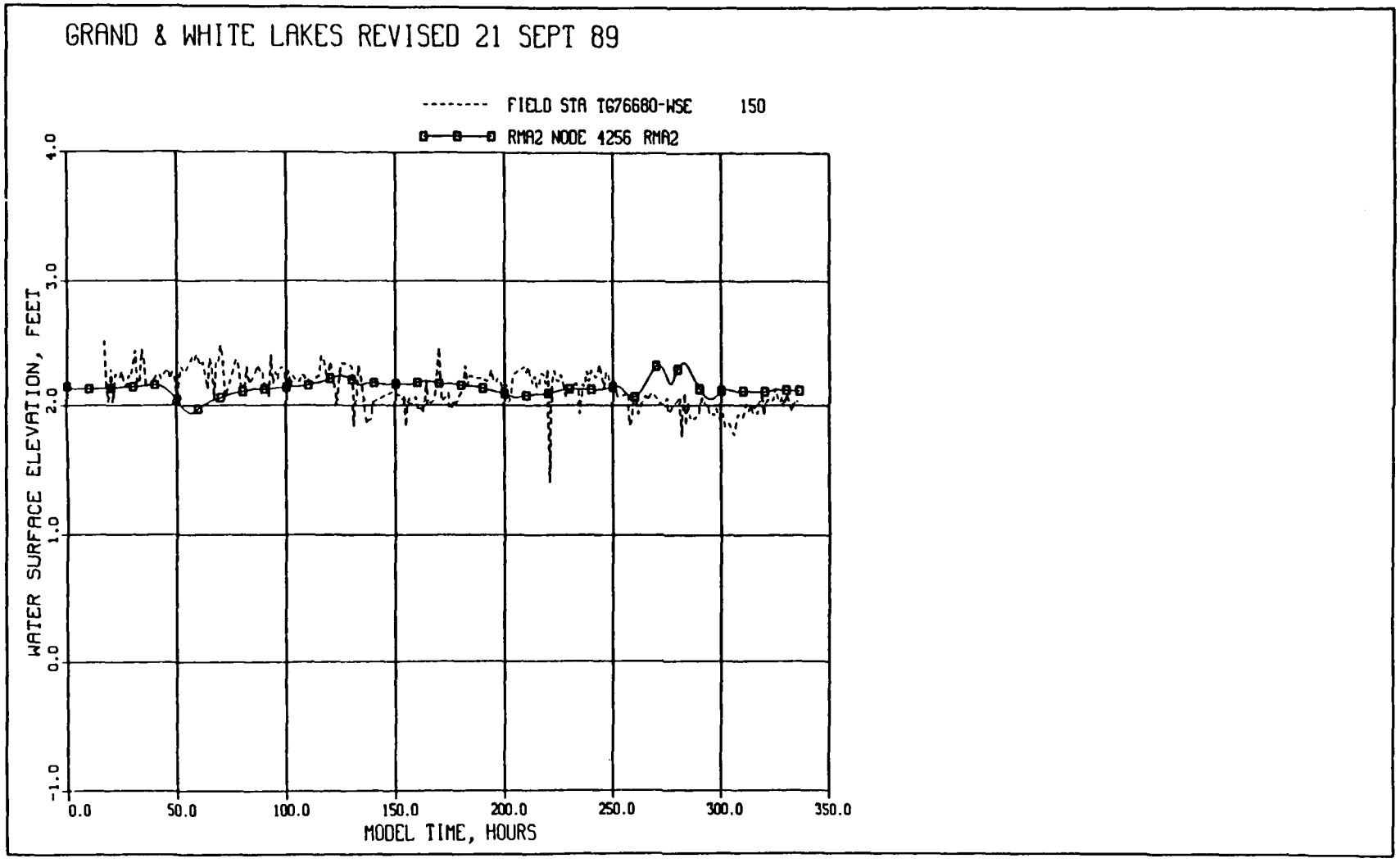

Figure 23. Comparison of field and model water surface elevations at Station 4256 near the upstream end of Schooner Bayou Lock

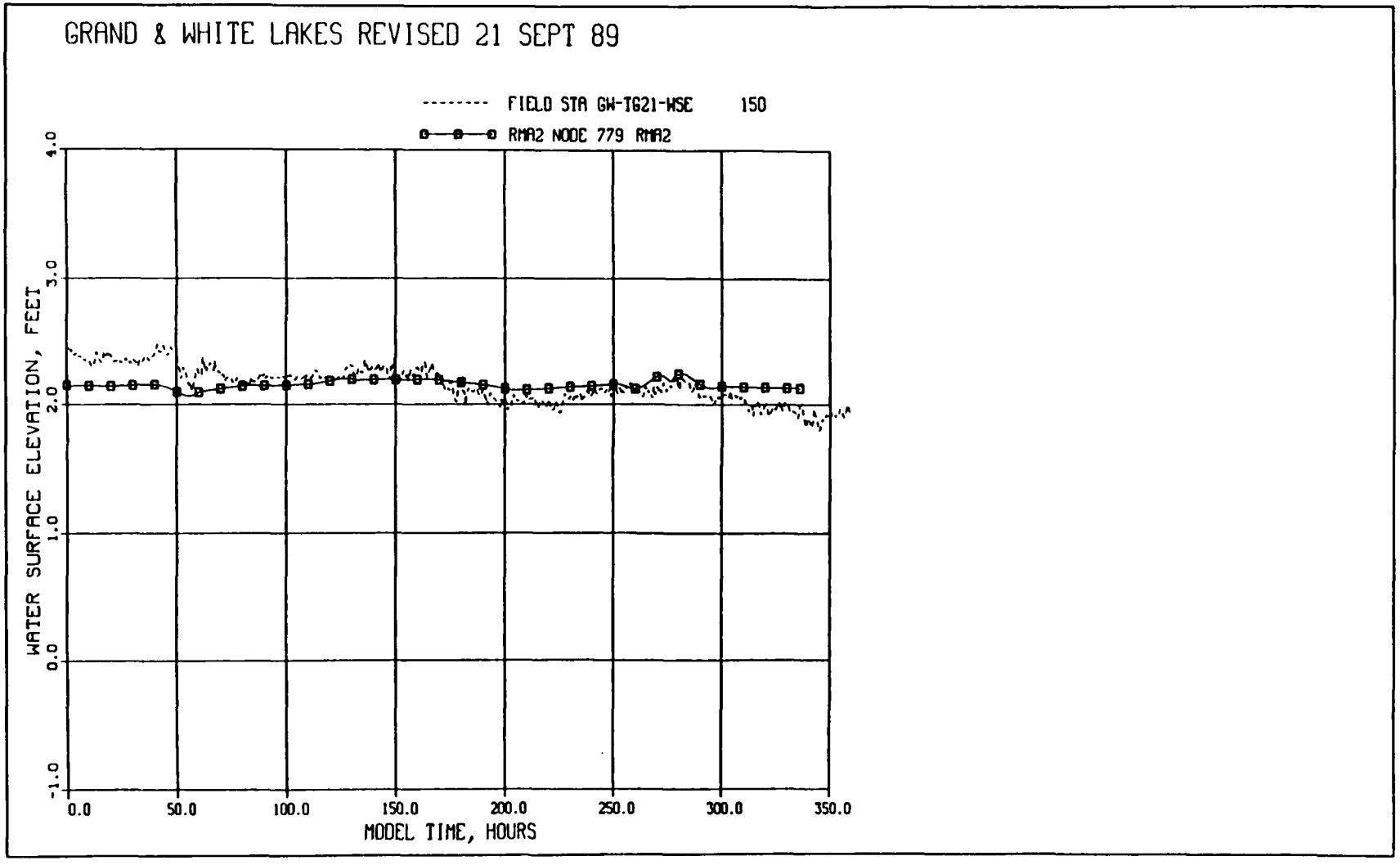

Figure 24. Comparison of field and model water surface elevations at Station 779 in White Lake

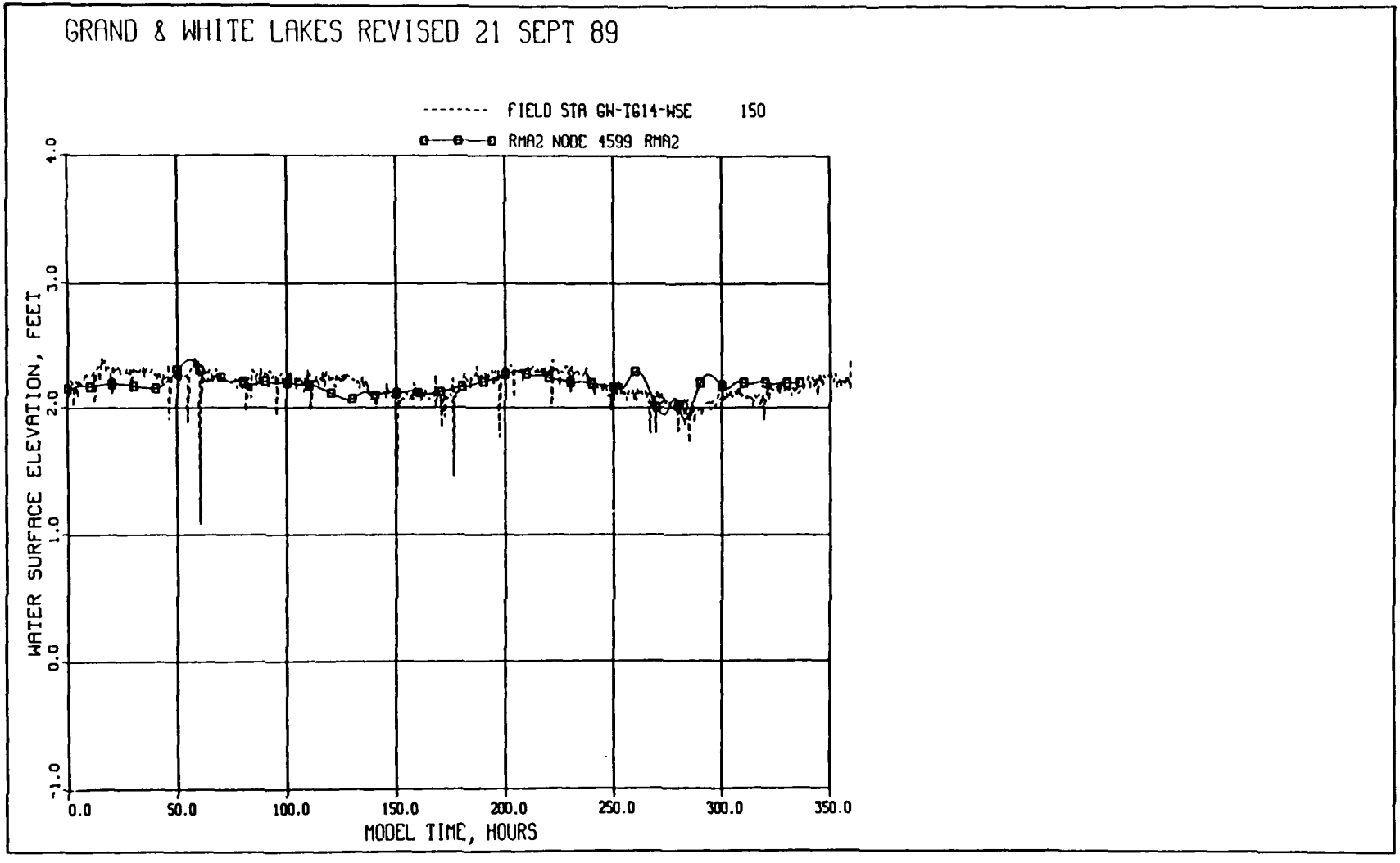

Figure 25. Comparison of field and model water surface elevations at Station 4599 in GIWW west of Grand Lake

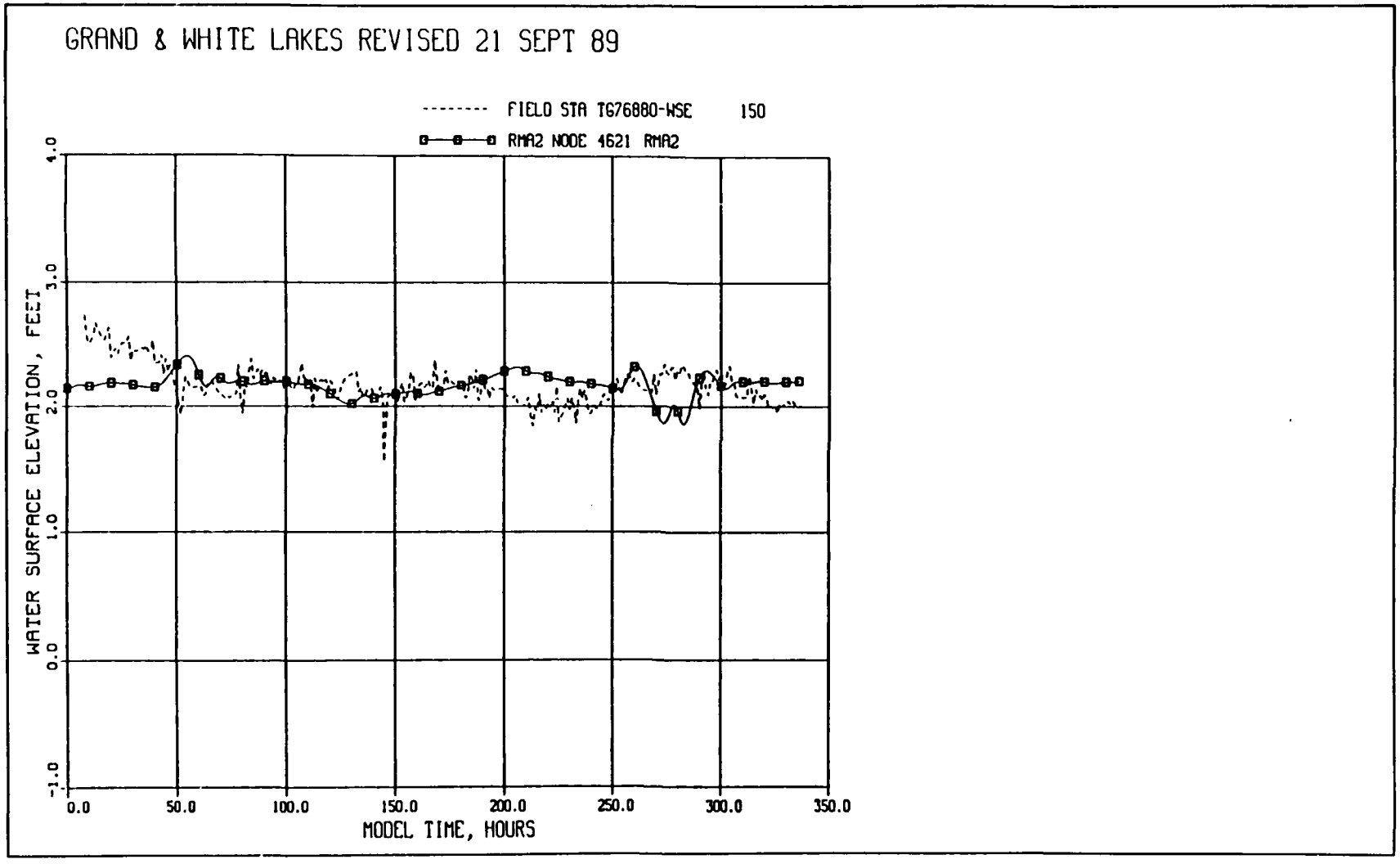

Figure 26. Comparison of field and model water surface elevations at Station 4621 at east end of Calcaiseau Lock

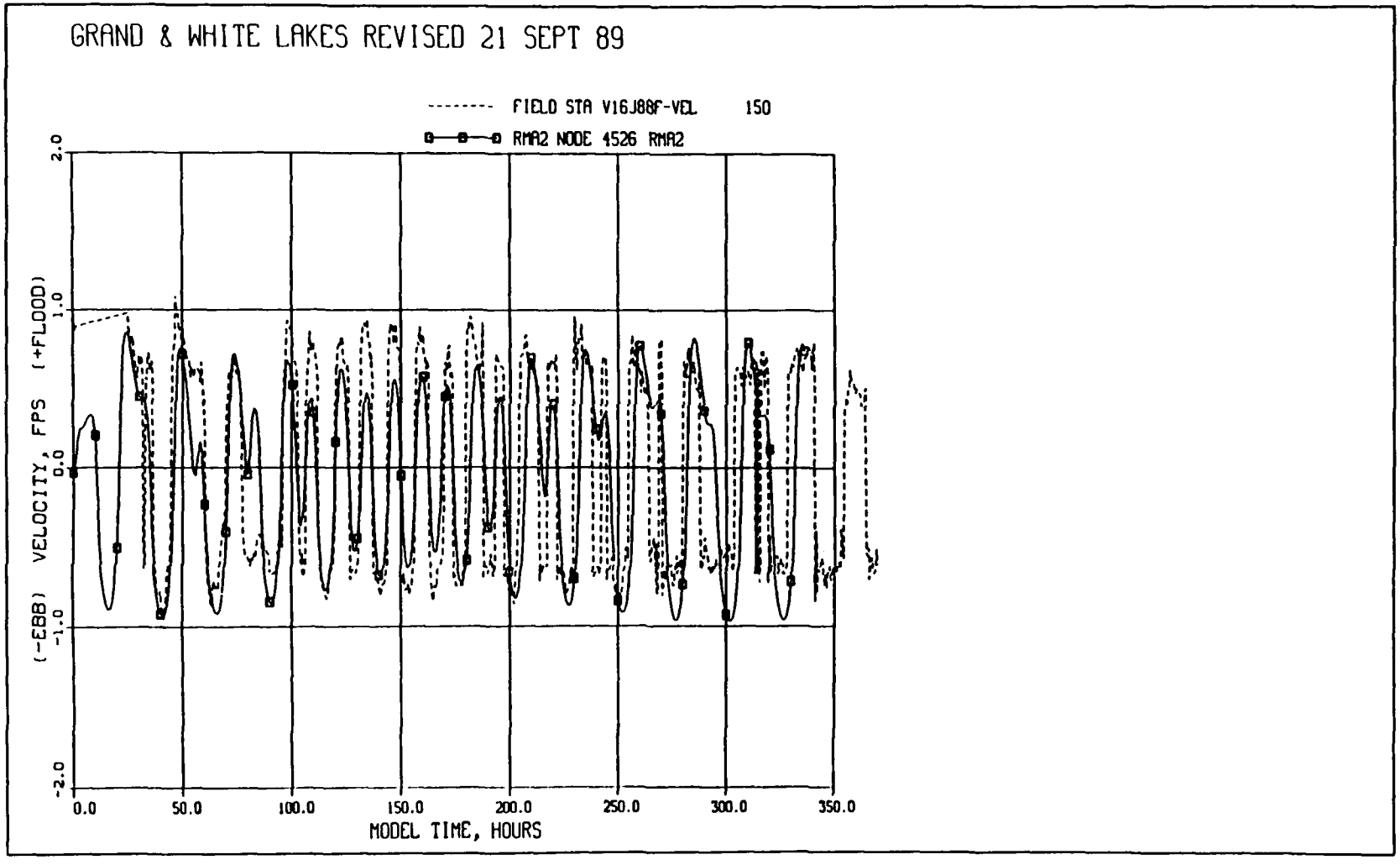

Figure 27. Comparison of field and model current velocities at Station 4526 in lower Mermentau River for low flow conditions

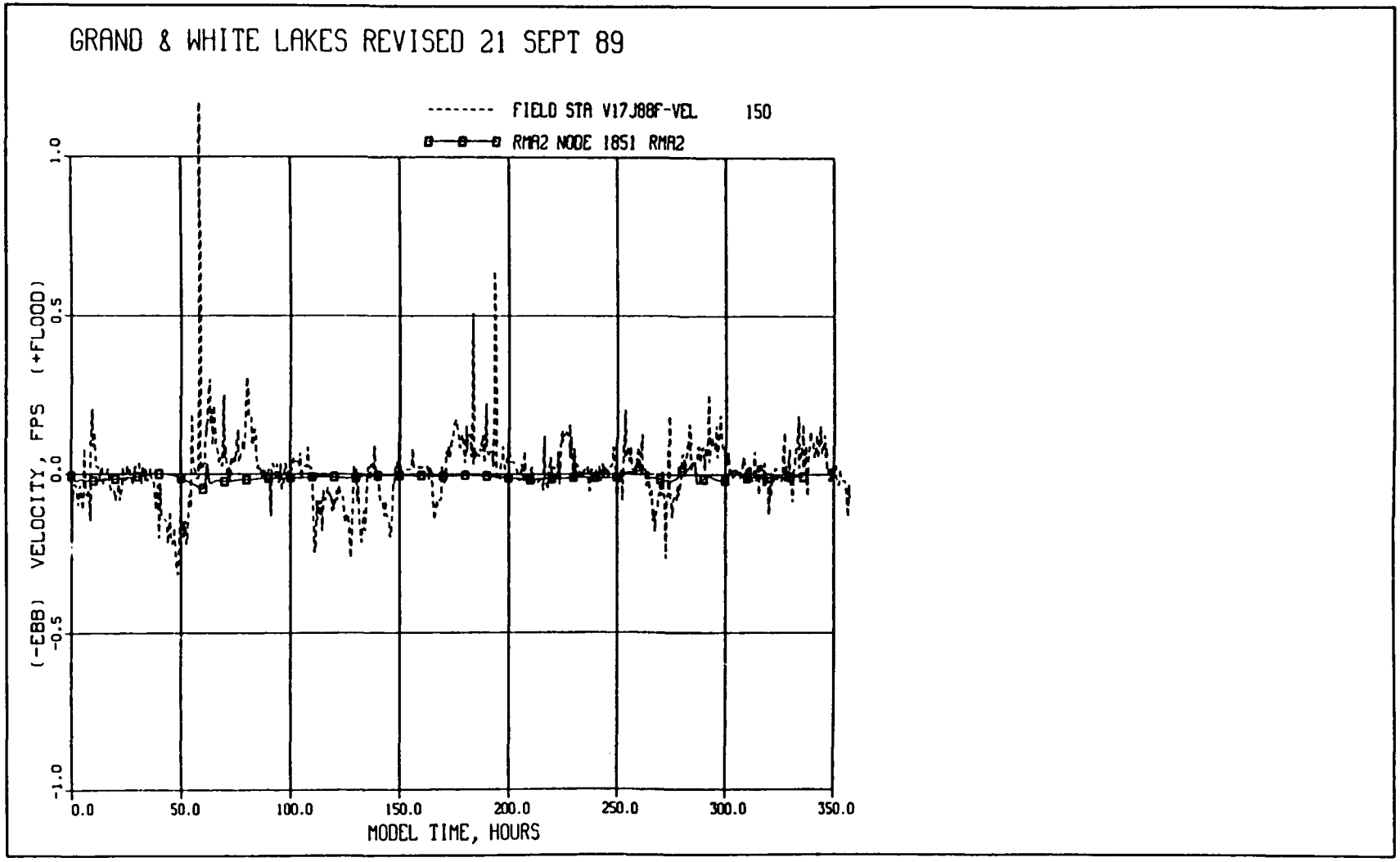

Figure 28. Comparison of field and model current velocities at Station 1851 in mouth of upper Mermentau River for low flow conditions

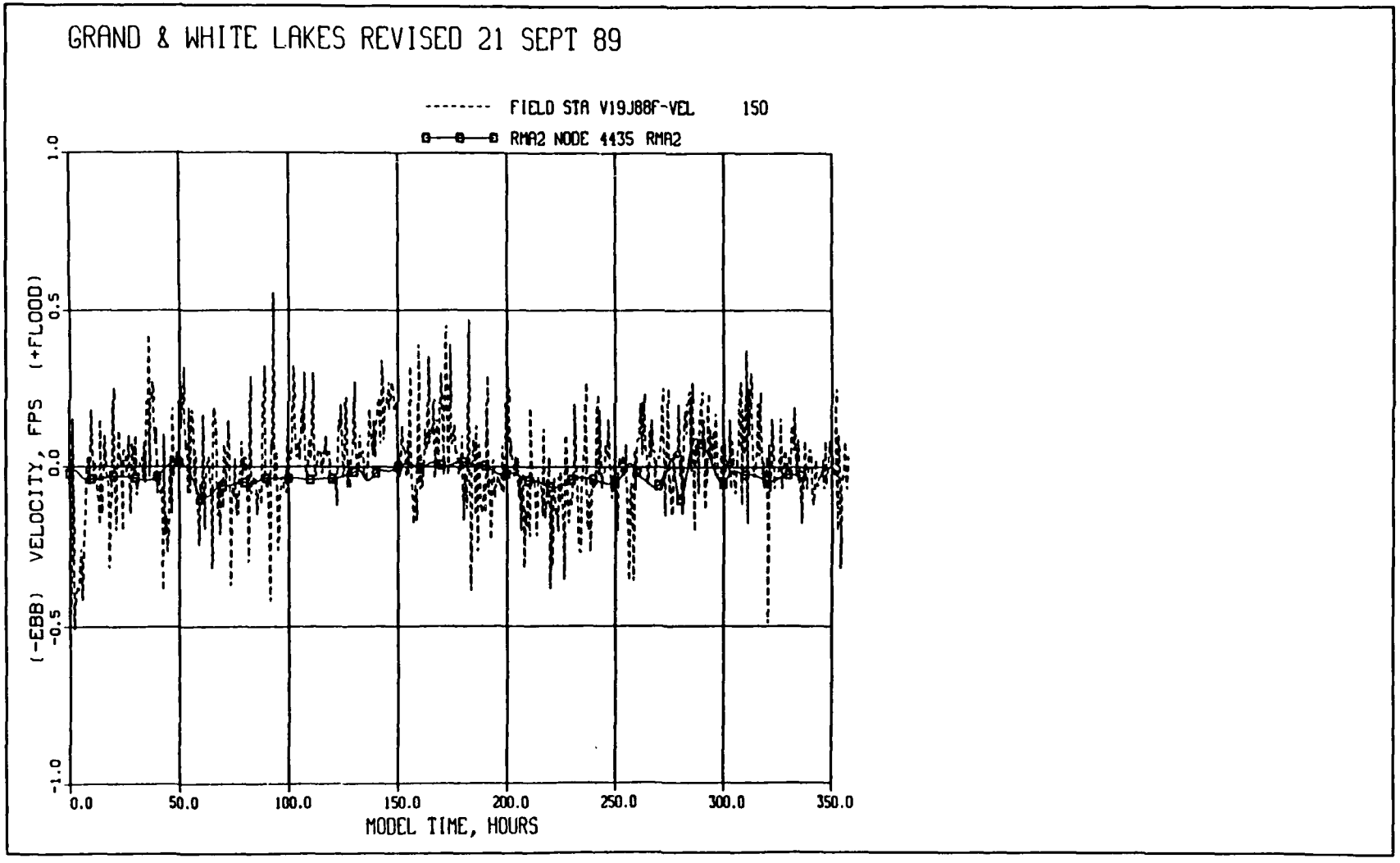

Figure 29. Comparison of field and model current velocities at Station 4435 in the GIWW, north of White Lake, for low flow conditions

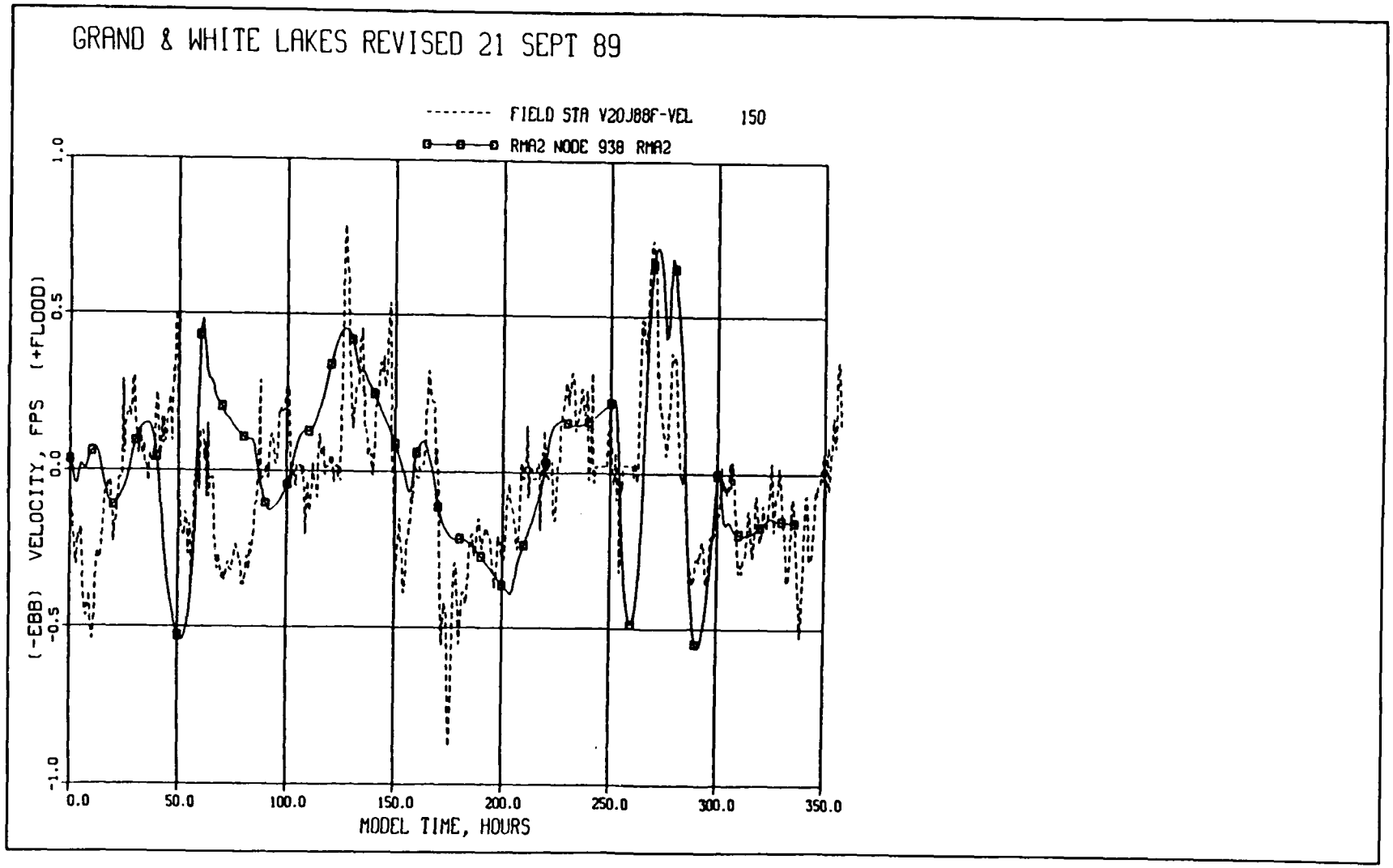

Figure 30. Comparison of field and model current velocities at Station 0938 in the west end of White Lake, for low flow conditions

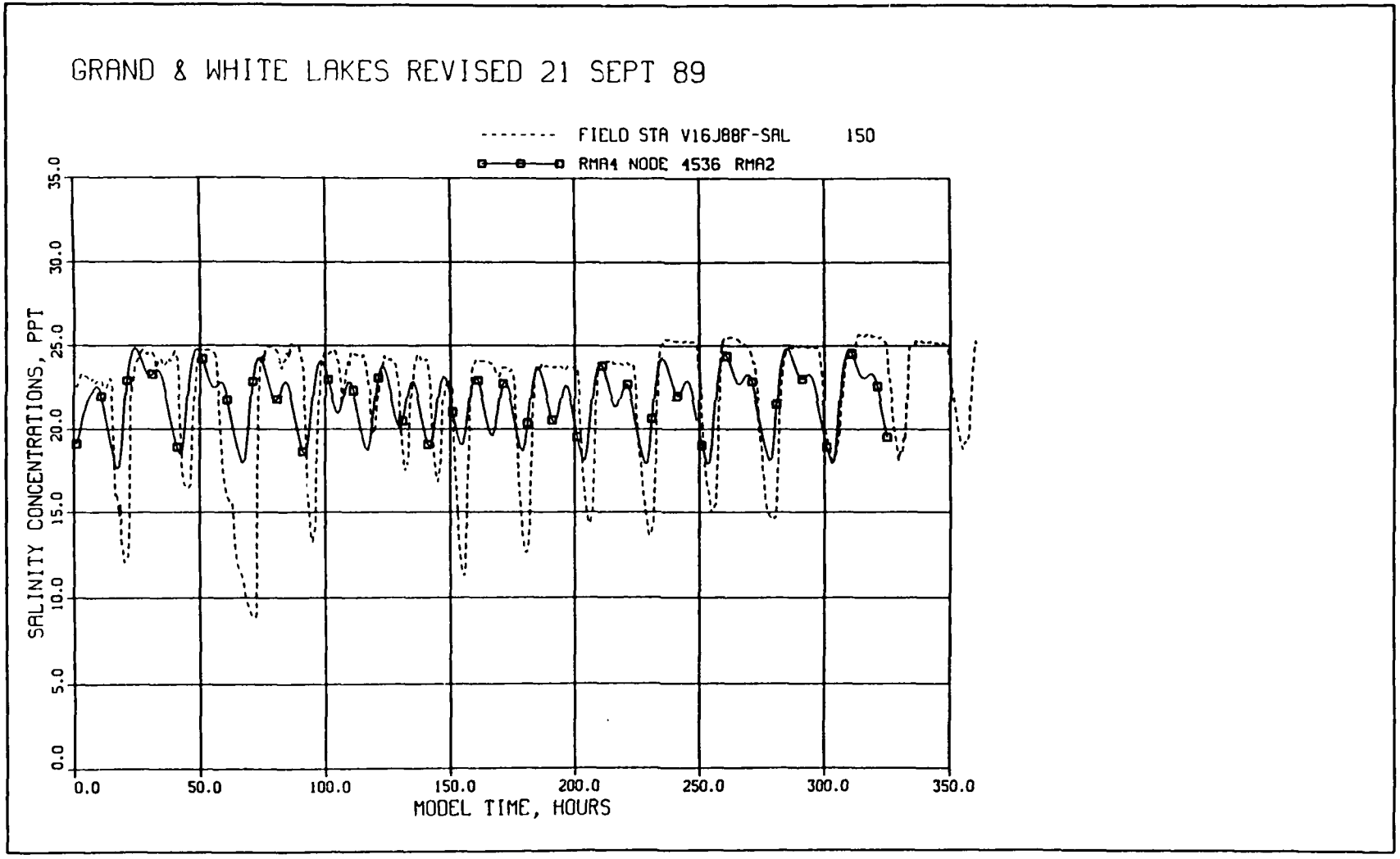

Figure 31. Comparison of field and model salinity concentrations at Station 4536 on lower Mermentau River

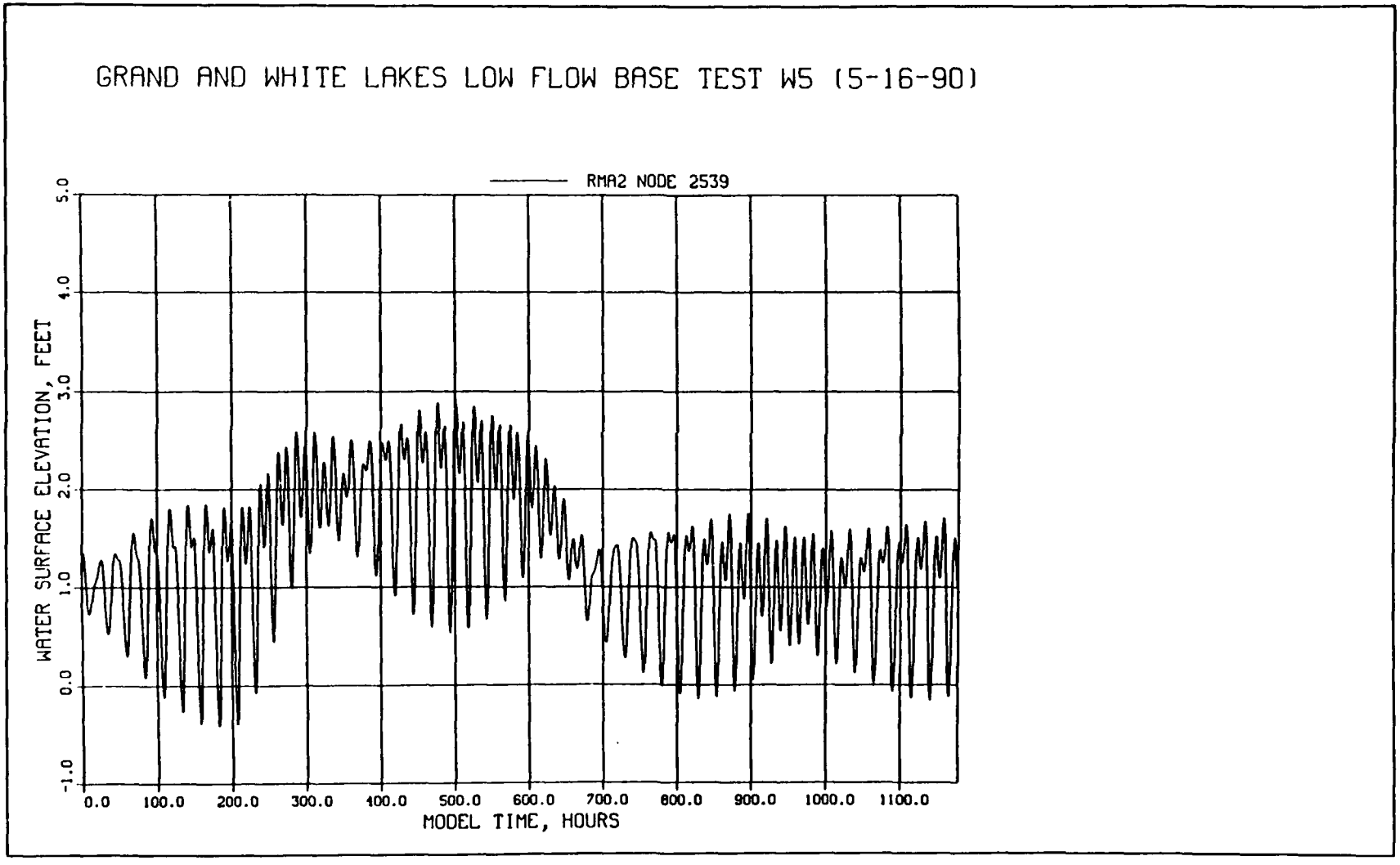

Figure 32. Water surface elevations for low flow base model Test W5 at Station 2539 (Gulf boundary condition)

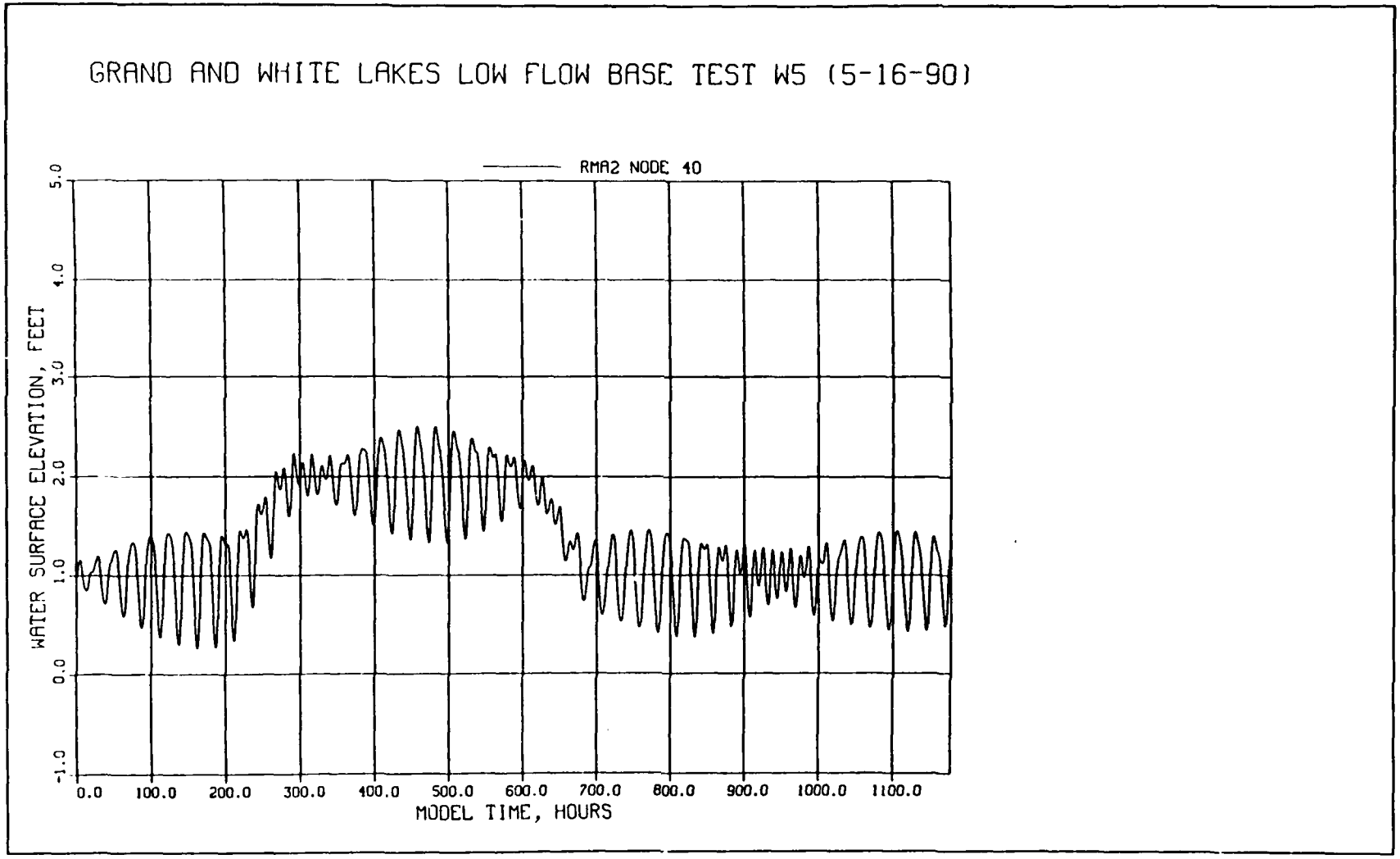

Figure 33. Water surface elevations for low flow base model Test W5 at Station 40 (Vermillion Bay boundary condition)

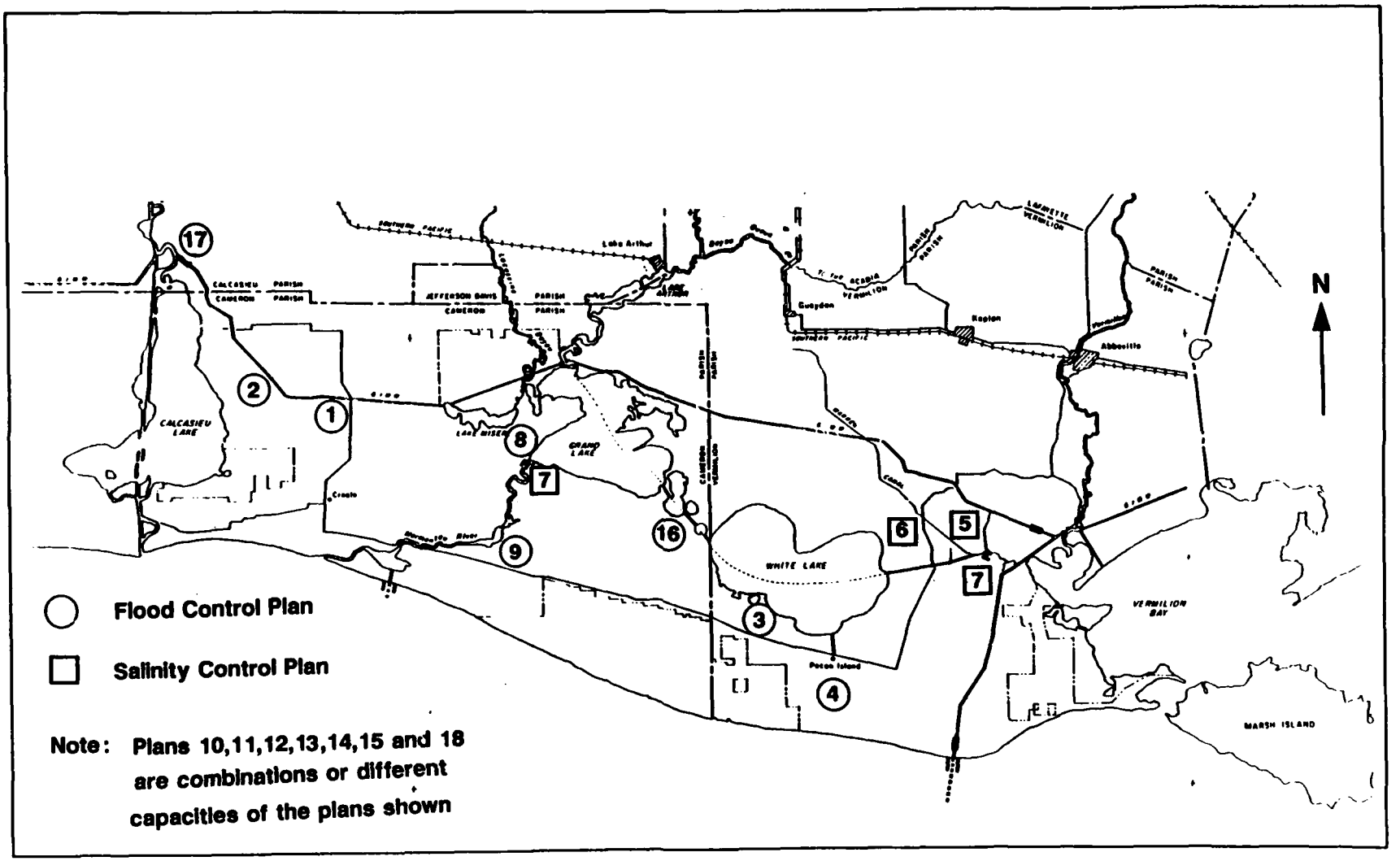

Figure 34. Location of Plan Alternatives

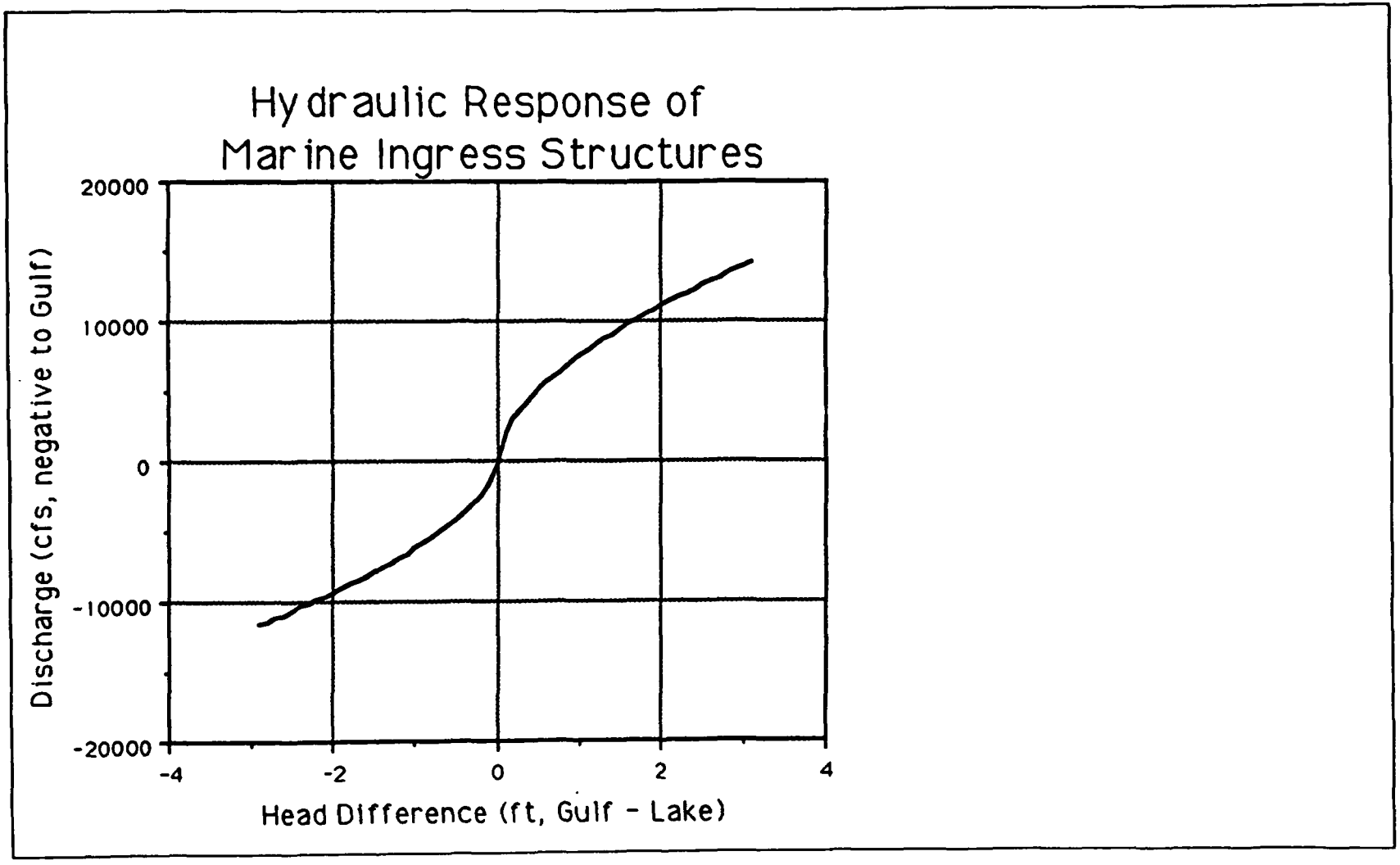

Figure 35. Hydraulic response of marine ingress structures

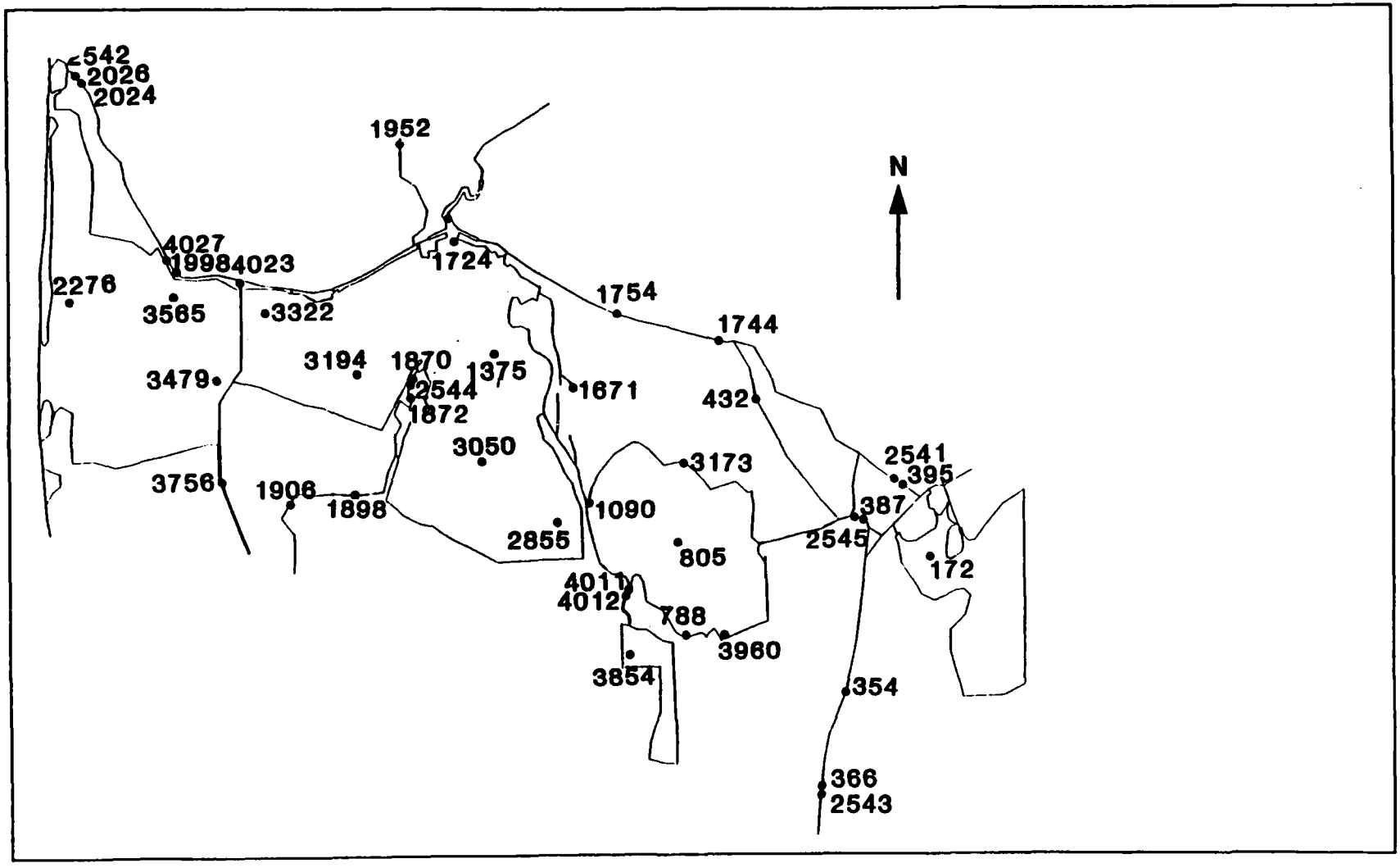

Figure 36. Numerical model Station locations

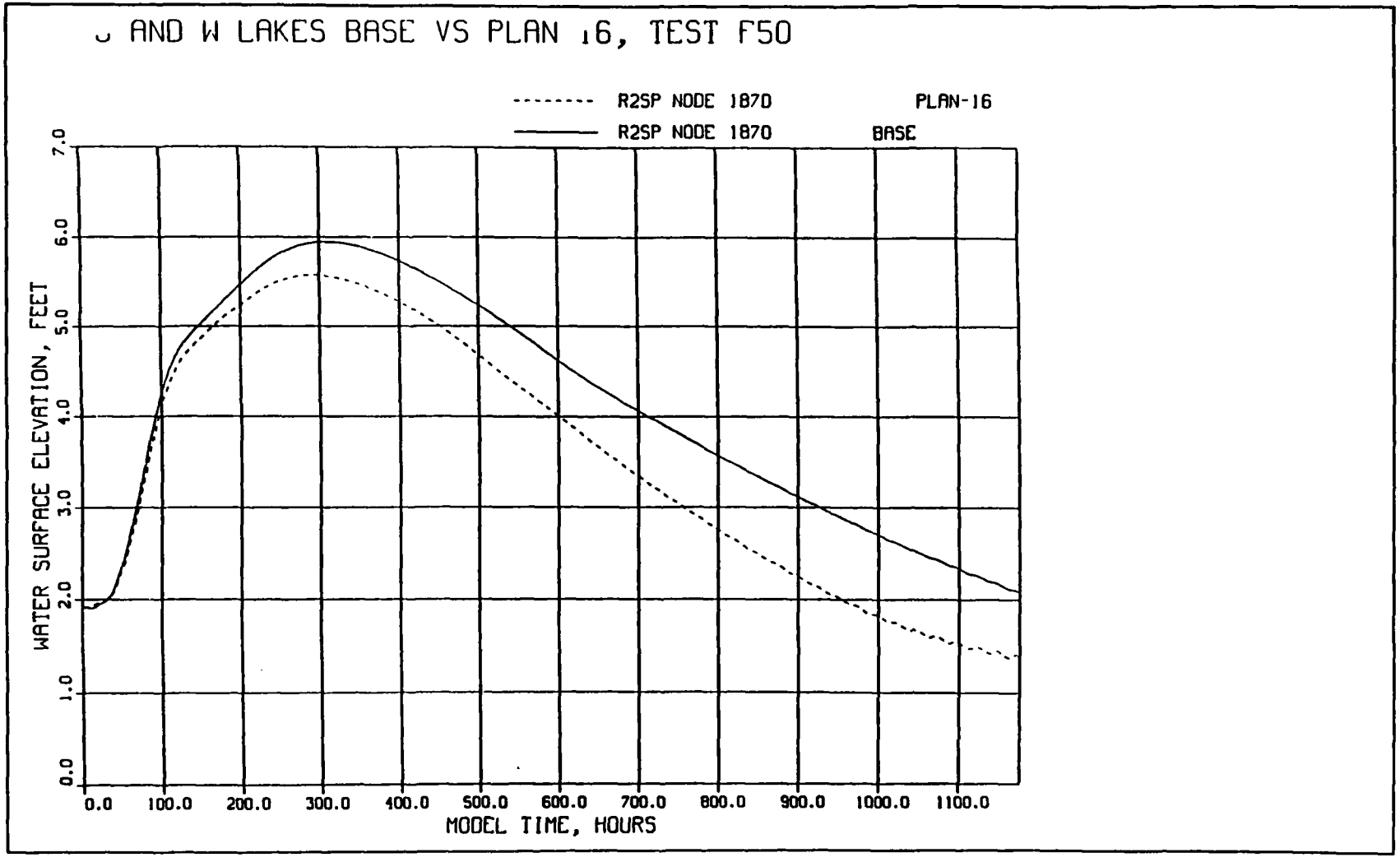

Figure 37. Comparison of water surface elevations for base vs plan 16 at Station 1870 (50 yr flood event)

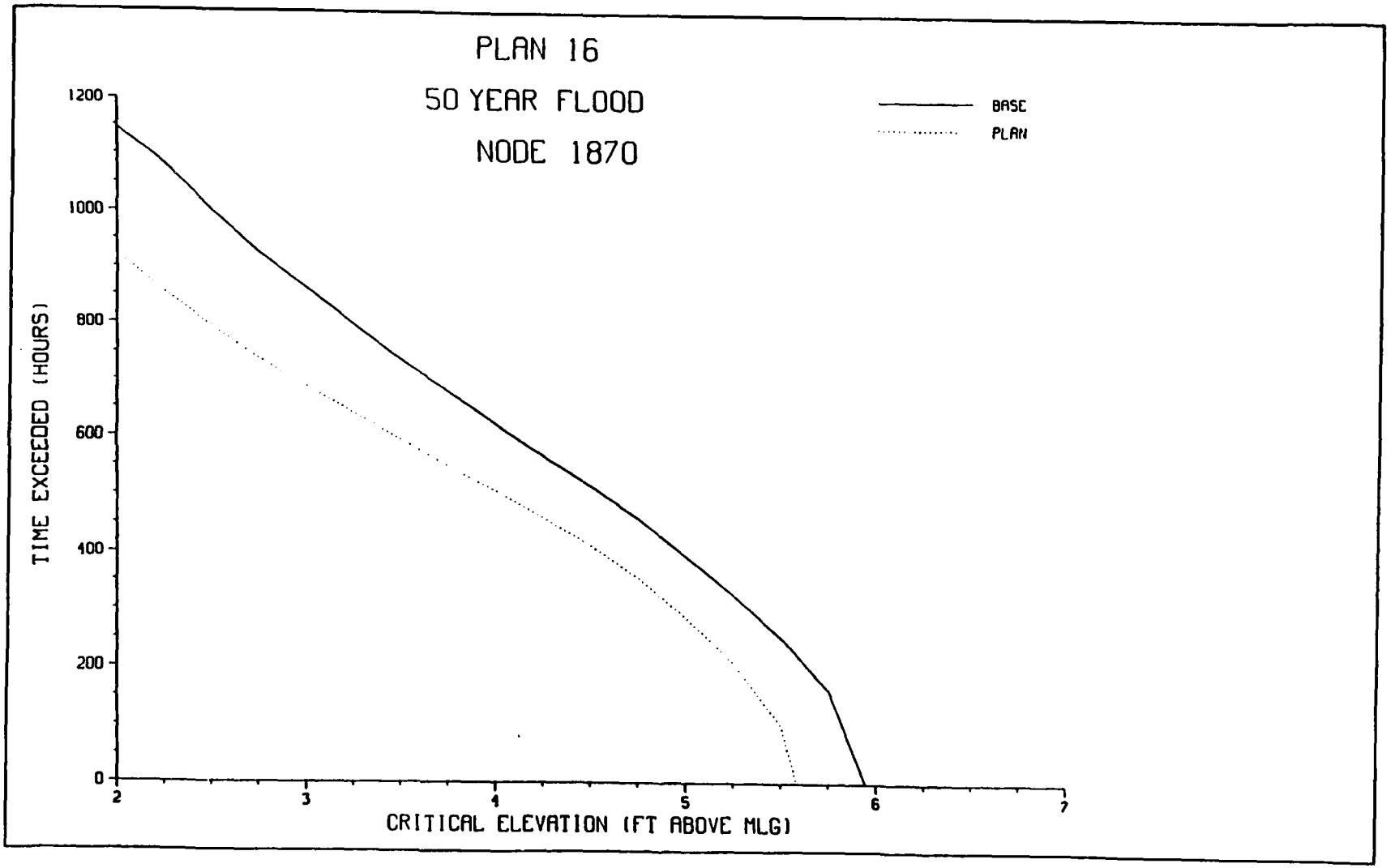

Figure 38. Comparison of water surface exceedence interval for base vs plan 16 at Station 1870 (50 yr flood event)

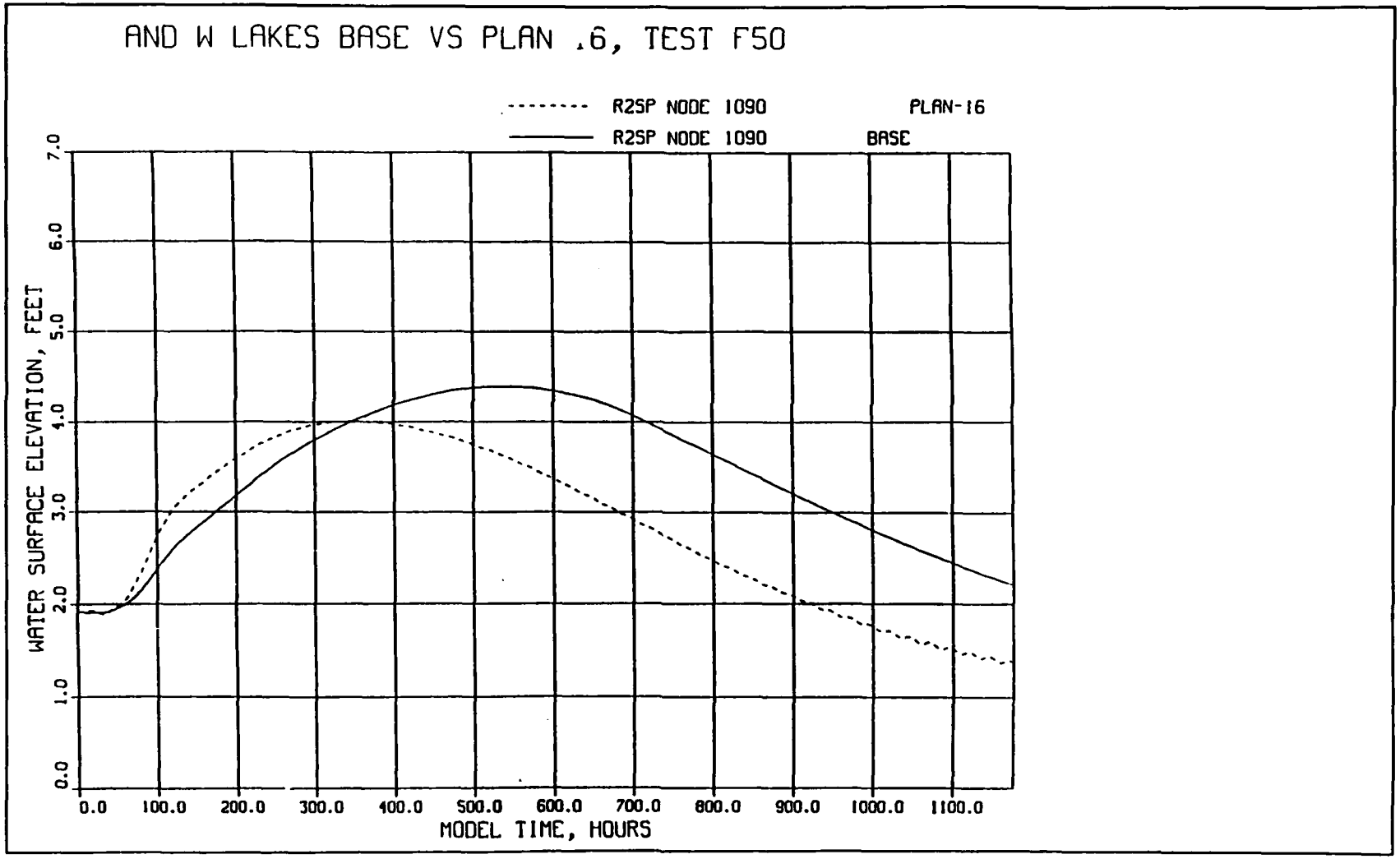

Figure 39. Comparison of water surface elevations for base vs plan 16 at Station 1090 (50 yr flood event)

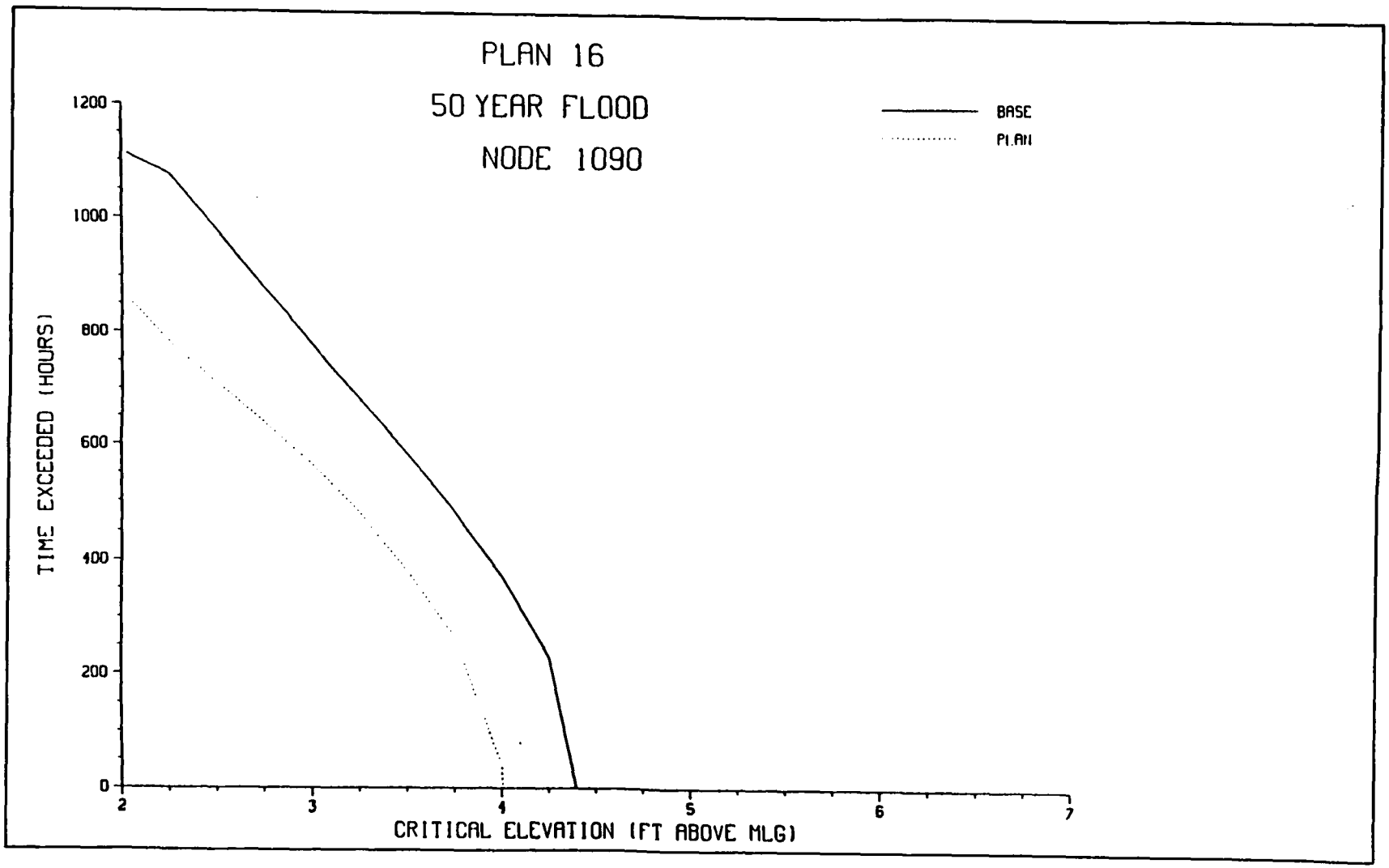

Figure 40. Comparison of water surface exceedence interval for base vs plan 16 at Station 1090 (50 yr flood event)

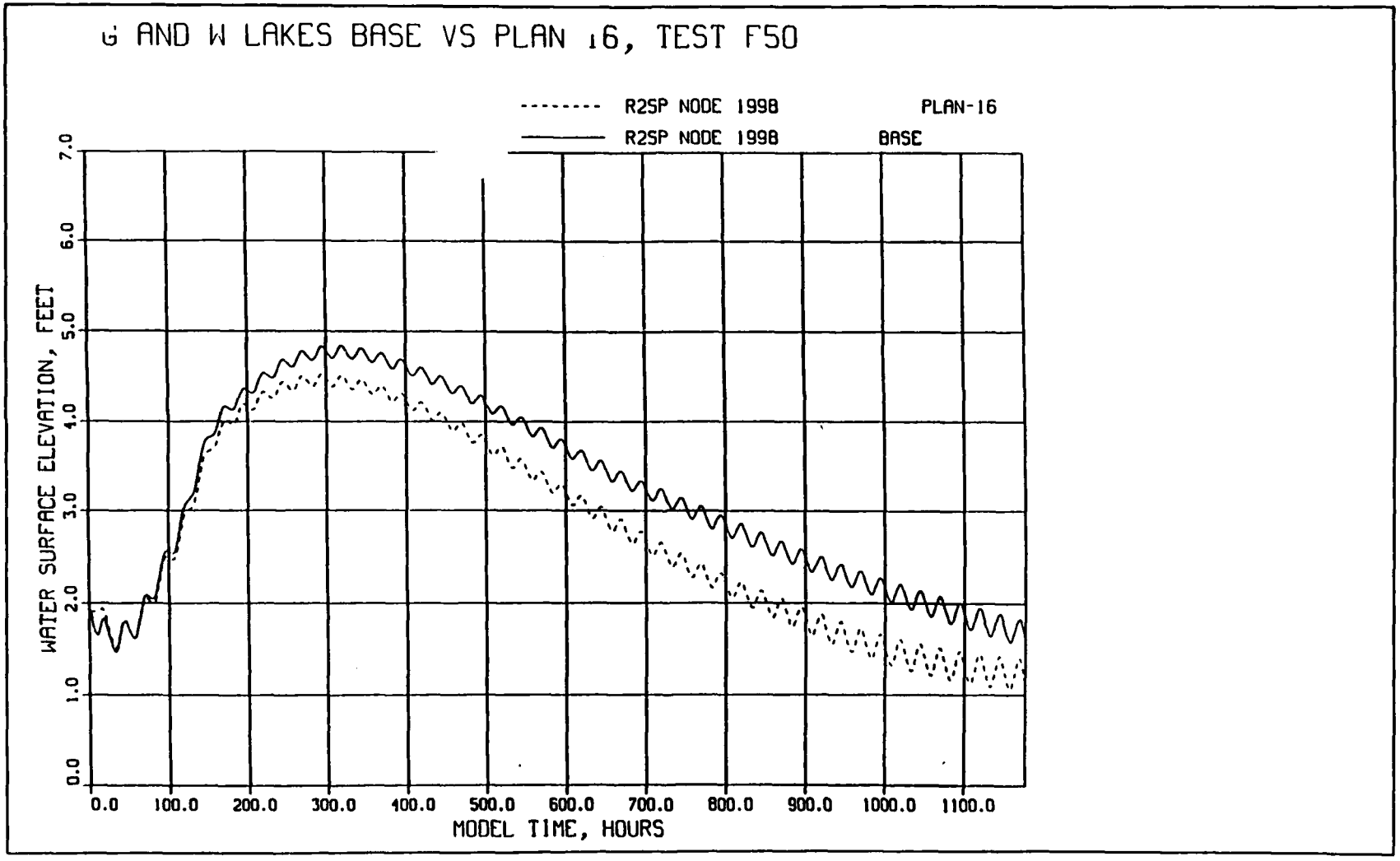

Figure 41. Comparison of water surface elevations for base vs plan 16 at Station 1998 (50 yr flood event)

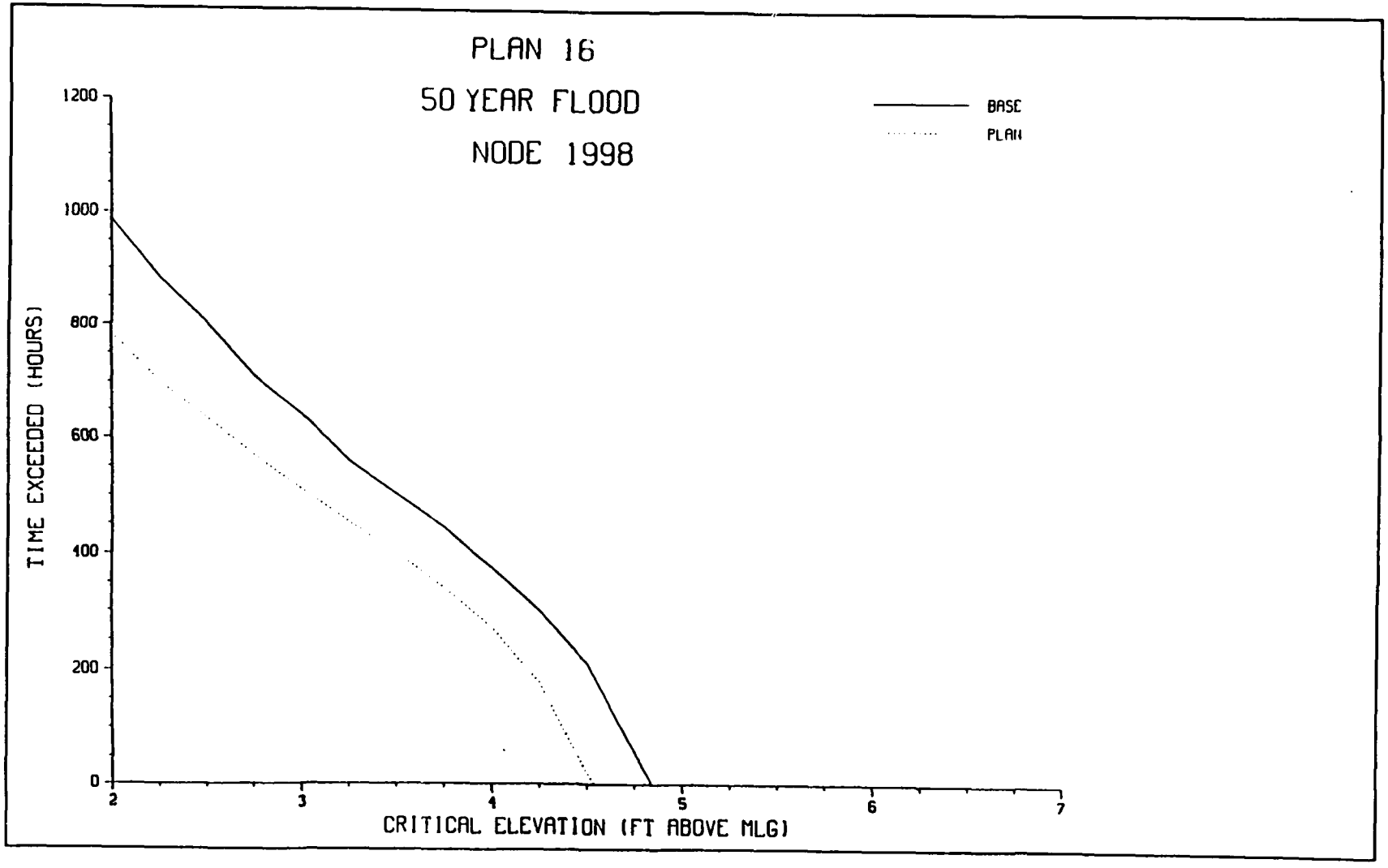

Figure 42. Comparison of water surface exceedence interval for base vs plan 16 at Station 1998 (50 yr flood event)

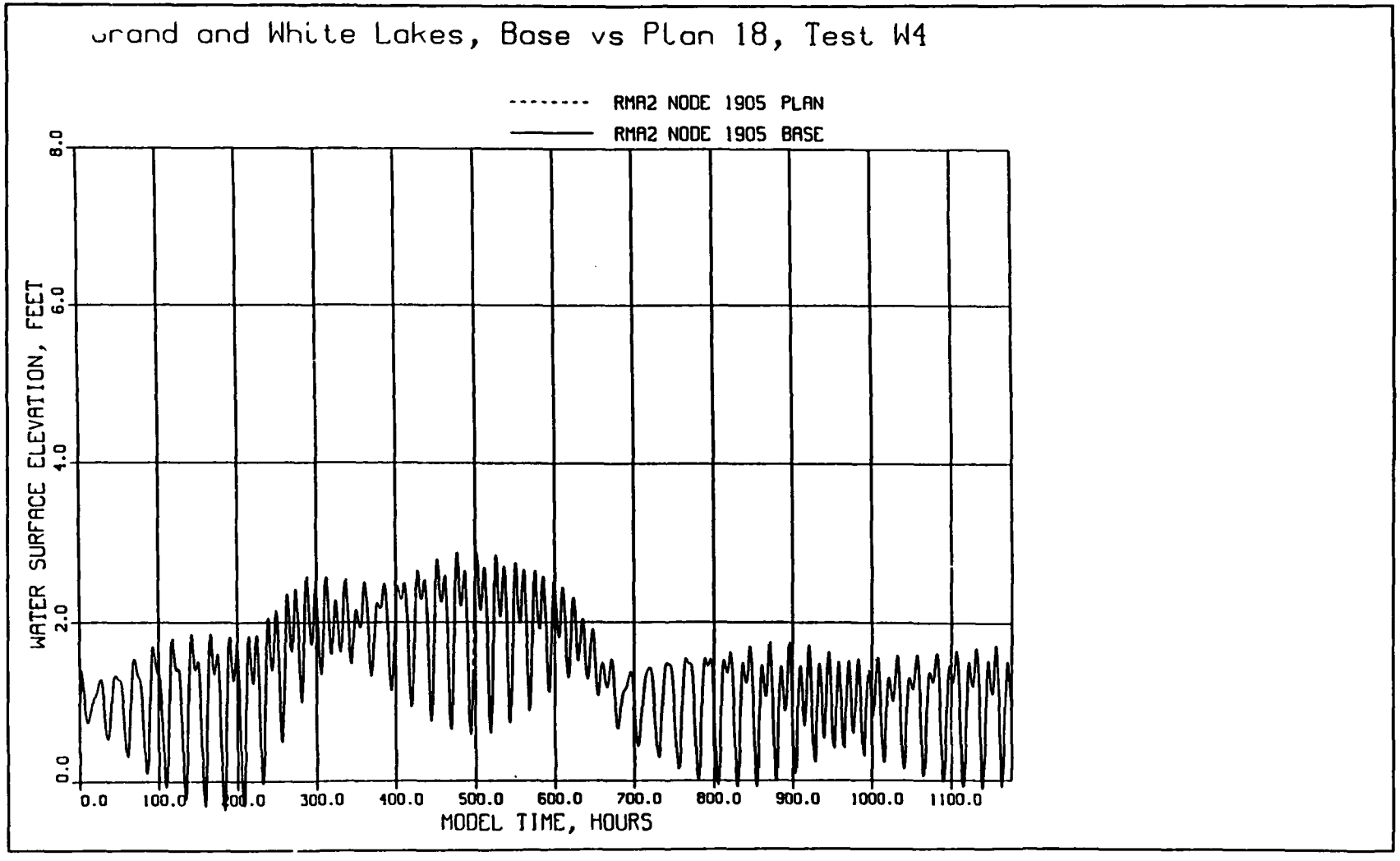

Figure 43. Comparison of water surface elevations for base vs plan 18 at Station 1905 (Test W4)

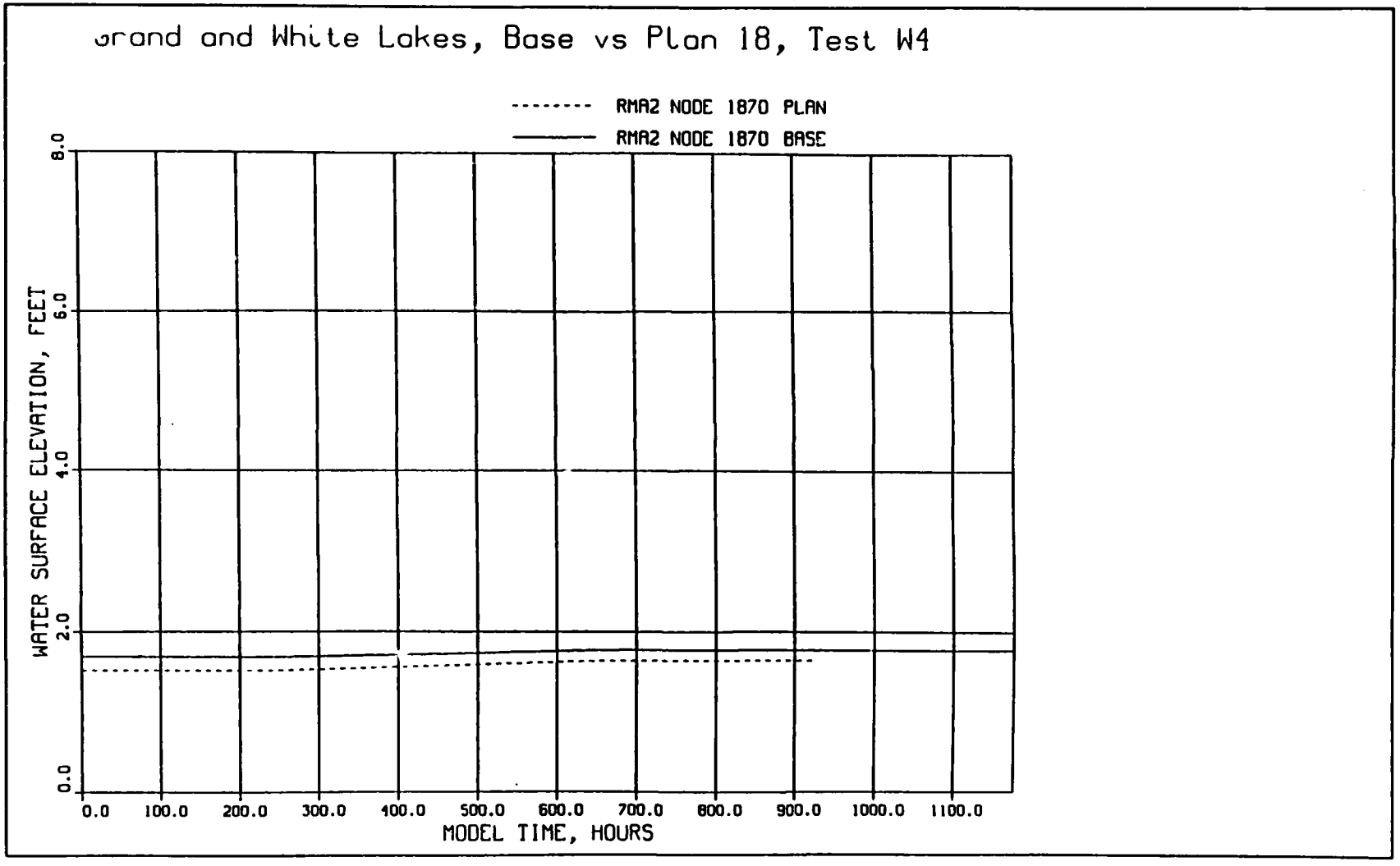

Figure 44. Comparison of water surface elevations for base vs plan 18 at Station 1870 (Test W4)

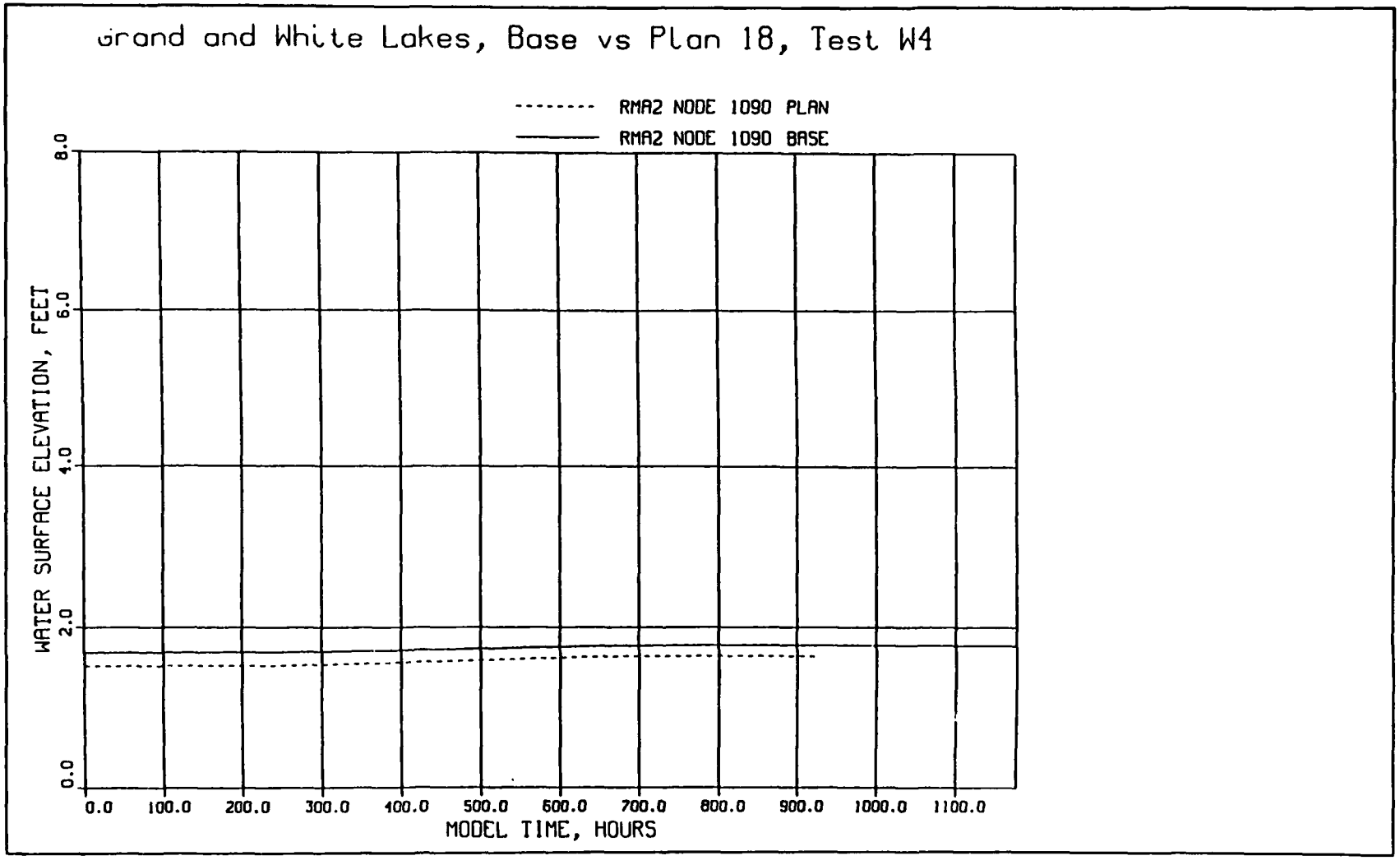

Figure 45. Comparison of water surface elevations for base vs plan 18 at Station 1090 (Test W4)

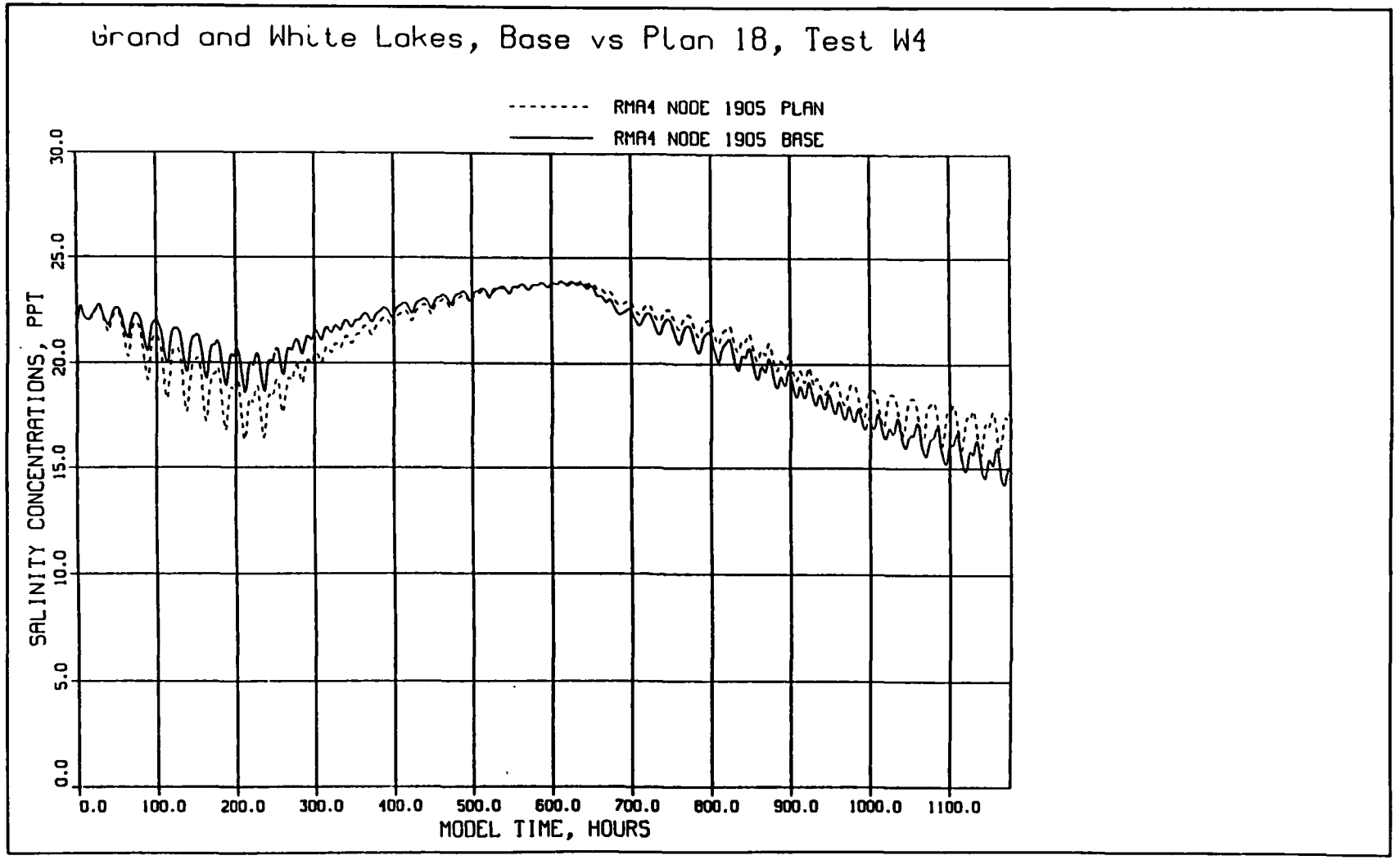

Figure 46. Comparison of salinity concentrations for base vs plan 18 at Station 1905 (Test W4)

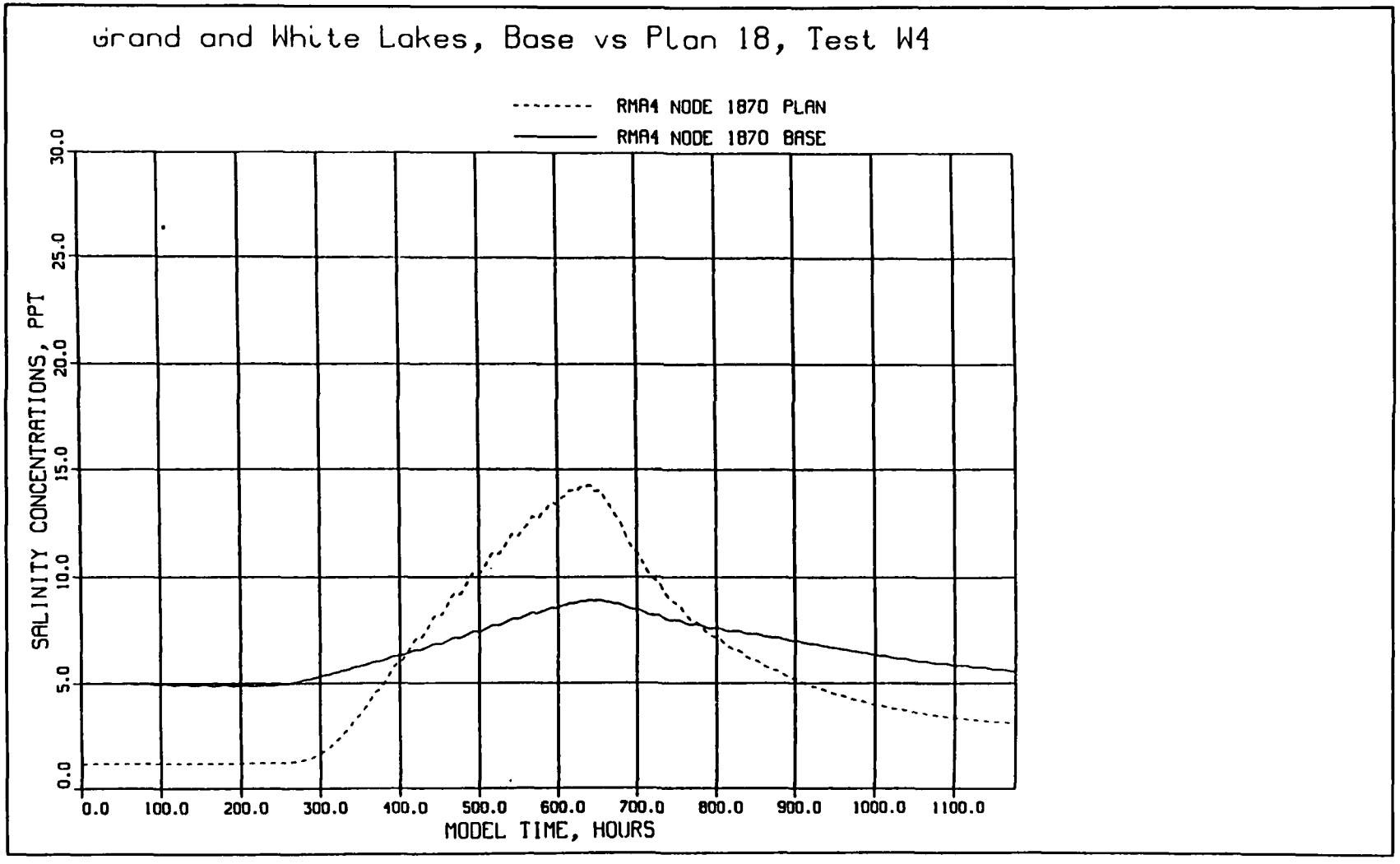

Figure 47. Comparison of salinity concentrations for base vs plan 18 at Station 1870 (Test W4)

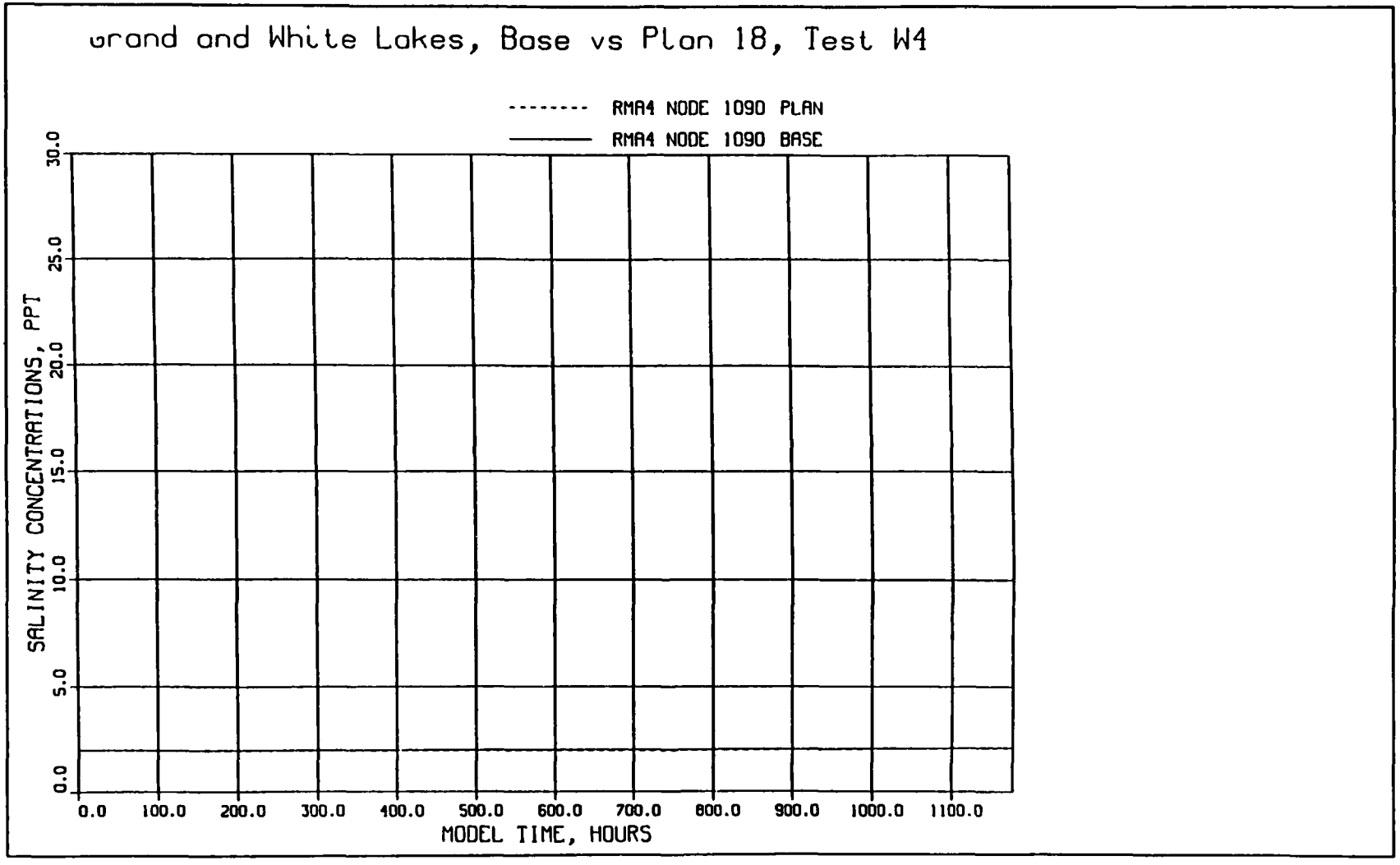

Figure 48. Comparison of salinity concentrations for base vs plan 18 at Station 1090 (Test W4)

Appendix A
The TABS-MD System

TABS-MD is a collection of generalized computer programs and utility codes integrated into a numerical modeling system for studying two-dimensional hydrodynamics, sedimentation, and transport problems in rivers, reservoirs, bays, and estuaries. A schematic representation of the system is shown in Figure A1. It can be used either as a stand-alone solution technique or as a step in the hybrid modeling approach. The basic concept is to calculate water-surface elevations, current patterns, sediment erosion, transport and deposition, the resulting bed surface elevations, and the feedback to hydraulics. Existing and proposed geometry can be analyzed to determine the impact on sedimentation of project designs and to determine the impact of project designs on salinity and on the stream system. The system is described in detail by Thomas and McAnally (1985).

The three basic components of the system are as follows:

a. "A Two-Dimensional Model for Free Surface Flows," RMA-2V.

b. "Sediment Transport in Unsteady 2-Dimensional Flows, Horizontal Plane," STUDH.

c. "Two-Dimensional Finite Element Program for Water Quality," RMA-4.

RMA-2V is a finite element solution of the Reynolds form of the Navier-Stokes equations for turbulent flows. Friction is calculated with Manning's equation and eddy viscosity coefficients are used to define the turbulent losses. A velocity form of the basic equation is used with side boundaries treated as either slip or static. The model automatically recognizes dry elements and corrects the mesh accordingly. Boundary conditions may be water-surface elevations, velocities, or discharges and may occur inside the mesh as well as along the edges.

The sedimentation model, STUDH, solves the convection-diffusion equation with bed source terms. These terms are structured for either sand or cohesive sediments. The Ackers-White (1973) procedure is used to calculate a sediment transport potential for the sands from which the actual transport is calculated

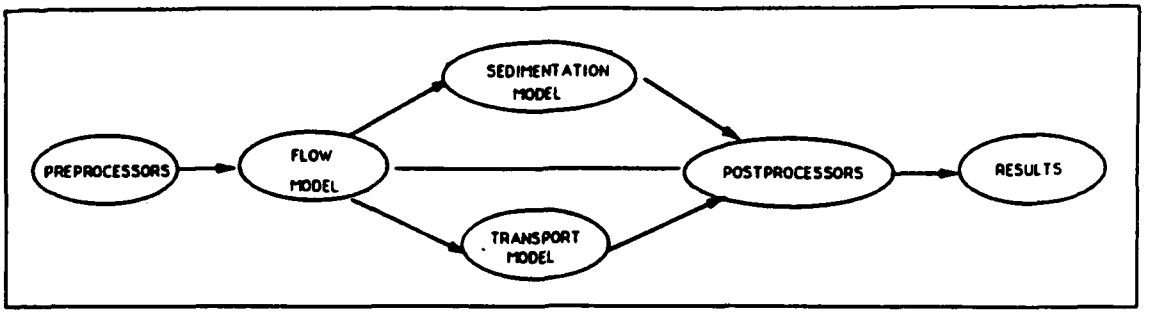

Figure A1. TABS-2 schematic

based on availability. Clay erosion is based on work by Partheniades (1962) and Ariathurai and the deposition of clay utilizes Krone's equations (Ariathurai, MacArthur, and Krone 1977). Deposited material forms layers, as shown in Figure A2, and bookkeeping allows up to 10 layers at each node for maintaining separate material types, deposit thickness, and age. The code uses the same mesh as RMA-2V.

Salinity calculations, RMA-4, are made with a form of the convective-diffusion equation which has general source-sink terms. Up to seven conservative substances or substances requiring a decay term can be routed. The code uses the same mesh as RMA-2V.

Each of these generalized computer codes can be used as a stand-alone program, but to facilitate the preparation of input data and to aid in analyzing results, a family of utility programs was developed for the following purposes:

a. Digitizing

b. Mesh generation

c. Spatial data management

d. Graphical output

e. Output analysis

f. File management

g. Interfaces

h. Job control language

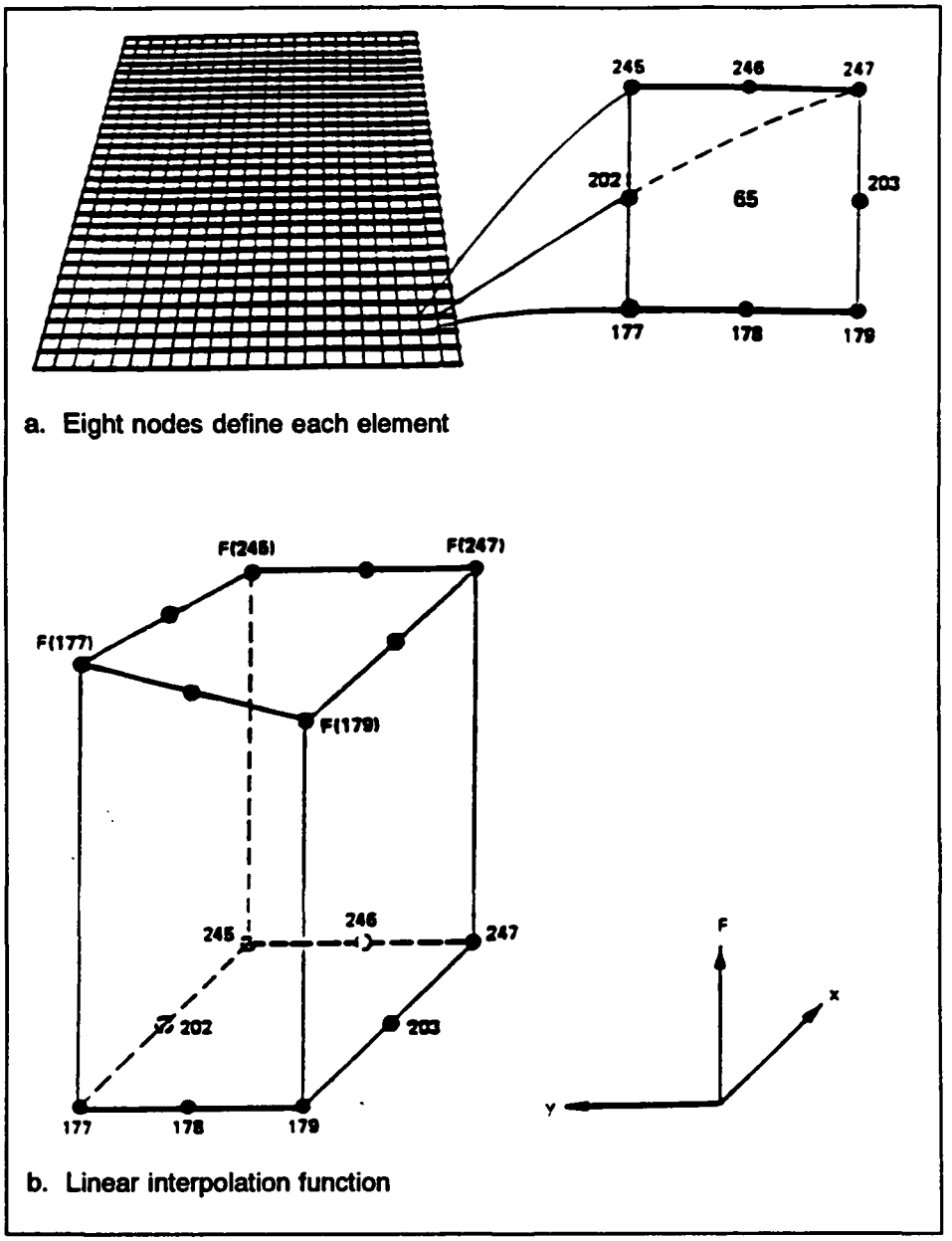

Figure A2. Two-dimensional finite element mesh

Finite Element Modeling

The TABS-2 numerical models used in this effort employ the finite element method to solve the governing equations. To help those who are unfamiliar with the method to better understand this report, a brief description of the method is given here.

The finite element method approximates a solution to equations by dividing the area of interest into smaller subareas, which are called elements. The dependent variables (e.g., water-surface elevations and sediment concentrations) are approximated over each element by continuous functions which interpolate in terms of unknown point (node) values of the variables. An error, defined as the deviation of the approximation solution from the correct solution, is minimized. Then, when boundary conditions are imposed, a set of solvable simultaneous equations is created. The solution is continuous over the area of interest.

In one-dimensional problems, elements are line segments. In twodimensional problems, the elements are polygons, usually either triangles or quadrilaterals. Nodes are located on the edges of elements and occasionally inside the elements. The interpolating functions may be linear or higher order polynomials. Figure A2 illustrates a quadrilateral element with eight nodes and a linear solution surface where F is the interpolating function.

Most water resource applications of the finite element method use the Galerkin method of weighted residuals to minimize error. In this method the residual, the total error between the approximate and correct solutions, is weighted by a function that is identical with the interpolating function and then minimized. Minimization results in a set of simultaneous equations in terms of nodal values of the dependent variable (e.g. water-surface elevations or sediment concentration). The time portion of time-dependent problems can be solved by the finite element method, but it is generally more efficient to express derivatives with respect to time in finite difference form.

The Hydrodynamic Model, RMA-2V

Applications

This program is designed for far-field problems in which vertical accelerations are negligible and the velocity vectors at a node generally point in the same directions over the entire depth of the water column at any instant of time. It expects a homogeneous fluid with a free surface. Both steady and unsteady state problems can be analyzed. A surface wind stress can be imposed.

The program has been applied to calculate flow distribution around islands; flow at bridges having one or more relief openings, in contracting and expanding reaches, into and out of off-channel hydropower plants, at river junctions, and into and out of pumping plant channels; and general flow patterns in rivers, reservoirs, and estuaries.

Limitations

This program is not designed for near-field problems where flowstructure interactions (such as vortices, vibrations, or vertical accelerations) are of interest. Areas of vertically stratified flow are beyond this program's capability unless it is used in a hybrid modeling approach. It is two-dimensional in the horizontal plane, and zones where the bottom current is in a different direction from the surface current must be analyzed with considerable subjective judgment regarding long-term energy considerations. It is a free-surface calculation for subcritical flow problems.

Governing equations

The generalized computer program RMA-2V solves the depth-integrated equations of fluid mass and momentum conservation in two horizontal directions. The form of the solved equations is

$$h\frac{\partial u}{\partial t} + hu\frac{\partial u}{\partial x} + hv\frac{\partial u}{\partial y} - \frac{h}{\rho}\left(\varepsilon_{xx}\frac{\partial^2 u}{\partial x^2} + \varepsilon_{xy}\frac{\partial^2 u}{\partial y^2}\right) + gh\left(\frac{\partial a}{\partial x} + \frac{\partial h}{\partial x}\right) + \frac{gun^2}{\left(1.486h^{1/6}\right)^2}\left(u^2 + v^2\right)^{1/2} - \zeta V_a^2 \cos\psi - 2h\omega v \sin\phi = 0 \qquad \text{(A1)}$$

$$h\frac{\partial v}{\partial t} + hu\frac{\partial v}{\partial x} + hv\frac{\partial v}{\partial y} - \frac{h}{\rho}\left(\varepsilon_{yx}\frac{\partial^2 v}{\partial x^2} + \varepsilon_{yy}\frac{\partial^2 v}{\partial y^2}\right) + gh\left(\frac{\partial a}{\partial y} + \frac{\partial h}{\partial y}\right) + \frac{gvn^2}{\left(1.486h^{1/6}\right)^2}\left(u^2 + v^2\right)^{1/2} - \zeta V_a^2 \cos\psi - 2\omega hu \sin\phi = 0 \qquad \text{(A2)}$$

$$\frac{\partial h}{\partial t} + h\left(\frac{\partial u}{\partial x} + \frac{\partial v}{\partial y}\right) + u\frac{\partial h}{\partial x} + v\frac{\partial h}{\partial y} = 0 \qquad \text{(A3)}$$

where

h = depth
u,v = velocities in the Cartesian directions
x,y,t = Cartesian coordinates and time
ρ = density

ε = eddy viscosity coefficient, for xx = normal direction on x-axis surface; yy = normal direction on y-axis surface; xy and yx = shear direction on each surface
g = acceleration due to gravity
a = elevation of bottom
n = Manning's n value
1.486 = conversion from SI to non-SI units
ζ = empirical wind shear coefficient
V_a = wind speed
ψ = wind direction
ω = rate of earth's angular rotation
ϕ = local latitude

Equations A1, A2, and A3 are solved by the finite element method using Galerkin weighted residuals. The elements may be either quadrilaterals or triangles and may have curved (parabolic) sides. The shape functions are quadratic for flow and linear for depth. Integration in space is performed by Gaussian integration. Derivatives in time are replaced by a nonlinear finite difference approximation. Variables are assumed to vary over each time interval in the form

$$f(t) = f(0) + at + bt^{c} \qquad t_0 \le t < t \tag{A4}$$

which is differentiated with respect to time, and cast in finite difference form. Letters a, b, and c are constants. It has been found by experiment that the best value for c is 1.5 (Norton and King 1977).

The solution is fully implicit and the set of simultaneous equations is solved by Newton-Raphson iteration. The computer code executes the solution by means of a front-type solver that assembles a portion of the matrix and solves it before assembling the next portion of the matrix. The front solver's efficiency is largely independent of bandwidth and thus does not require as much care in formation of the computational mesh as do traditional solvers.

The code RMA-2V is based on the earlier version RMA-2 (Norton and King 1977) but differs from it in several ways. It is formulated in terms of velocity (v) instead of unit discharge (vh), which improves some aspects of the code's behavior; it permits drying and wetting of areas within the grid; and it permits specification of turbulent exchange coefficients in directions other than along the x- and z-axes. For a more complete description, see Appendix F of Thomas and McAnally (1985).

The Sediment Transport Model, STUDH

Applications

STUDH can be applied to clay and/or sand bed sediments where flow velocities can be considered two-dimensional (i.e., the speed and direction can be satisfactorily represented as a depth-averaged velocity). It is useful for both deposition and erosion studies and, to a limited extent, for stream width studies. The program treats two categories of sediment: noncohesive, which is referred to as sand here, and cohesive, which is referred to as clay.

Limitations

Both clay and sand may be analyzed, but the model considers a single, effective grain size for each and treats each separately. Fall velocity must be prescribed along with the water-surface elevations, x-velocity, y-velocity, diffusion coefficients, bed density, critical shear stresses for erosion, erosion rate constants, and critical shear stress for deposition.

Many applications cannot use long simulation periods because of their computation cost. Study areas should be made as small as possible to avoid an excessive number of elements when dynamic runs are contemplated yet must be large enough to permit proper posing of boundary conditions. The same computation time interval must be satisfactory for both the transverse and longitudinal flow directions.

The program does not compute water-surface elevations or velocities; therefore these data must be provided. For complicated geometries, the numerical model for hydrodynamic computations, RMA-2V, is used.

Governing equations

The generalized computer program STUDH solves the depth-integrated convection-dispersion equation in two horizontal dimensions for a single sediment constituent. For a more complete description, see Appendix G of Thomas and McAnally (1985). The form of the solved equation is

$$\frac{\partial C}{\partial t} + u\frac{\partial C}{\partial x} + v\frac{\partial C}{\partial y} = \frac{\partial}{\partial x}\left(D_x\frac{\partial C}{\partial x}\right) + \frac{\partial}{\partial y}\left(D_y\frac{\partial C}{\partial y}\right) + \alpha_1 C_2 + \alpha = 0 \qquad \text{(A5)}$$

where

C = concentration of sediment

u = depth-integrated velocity in x-direction

v = depth-integrated velocity in y-direction
D_x = dispersion coefficient in x-direction
D_y = dispersion coefficient in y-direction
α_1 = coefficient of concentration-dependent source/sink term
α_2 = coefficient of source/sink term

The source/sink terms in Equation B5 are computed in routines that treat the interaction of the flow and the bed. Separate sections of the code handle computations for clay bed and sand bed problems.

Sand transport

The source/sink terms are evaluated by first computing a potential sand transport capacity for the specified flow conditions, comparing that capacity with amount of sand actually being transported, and then eroding from or depositing to the bed at a rate that would approach the equilibrium value after sufficient elapsed time.

The potential sand transport capacity in the model is computed by the method of Ackers and White (1973), which uses a transport power (work rate) approach. It has been shown to provide superior results for transport under steady-flow conditions (White, Milli, and Crabbe 1975) and for combined waves and currents (Swart 1976). Flume tests at the U.S. Army Engineer Waterways Experiment Station have shown that the concept is valid for transport by estuarine currents.

The total load transport function of Ackers and White is based upon a dimensionless grain size

$$D_{gr} = D\left[\frac{g(s-1)}{\nu^2}\right]^{1/3} \tag{A6}$$

where
D = sediment particle diameter
s = specific gravity of the sediment
ν = kinematic viscosity of the fluid

and a sediment mobility parameter

$$F_{gr} = \left[\frac{\tau^{n'}\tau'^{(1-n')}}{\rho g D(s-1)}\right]^{1/2} \tag{A7}$$

where

τ = total boundary shear stress

n' = a coefficient expressing the relative importance of bed-load and suspended-load transport, given in Equation A9

τ' = boundary surface shear stress

The surface shear stress is that part of the total shear stress which is due to the rough surface of the bed only, i.e., not including that part due to bed forms and geometry. It therefore corresponds to that shear stress that the flow would exert on a plane bed.

The total sediment transport is expressed as an effective concentration

$$G_p = C \left[\frac{F_{gr}}{A} - 1 \right]^m \frac{sD}{h} \left[\sqrt{\frac{\rho}{\tau}} \, U \right]^{n'} \tag{A8}$$

where U is the average flow speed, and for $1 < D_{gr} \leq 60$

$$n' = 1.00 - 0.56 \log D_{gr} \tag{A9}$$

$$A = \frac{0.23}{\sqrt{D_{gr}}} + 0.14 \tag{A10}$$

$$\log C = 2.86 \log D_{gr} - (\log D_{gr})^2 - 3.53 \tag{A11}$$

$$m = \frac{9.66}{D_{gr}} + 1.34 \tag{A12}$$

For $D_{gr} < 60$

$$n' = 0.00 \tag{A13}$$

$$A = 0.17 \tag{A14}$$

$$C = 0.025 \tag{A15}$$

$$m = 1.5 \tag{A16}$$

Equations A6-A16 result in a potential sediment concentration G_p. This value is the depth averaged concentration of sediment that will occur if an equilibrium transport rate is reached with a nonlimited supply of sediment. The rate of sediment deposition (or erosion) is then computed as

$$R = \frac{G_p - C}{t_c} \tag{A17}$$

where

C = present sediment concentration
t_c = time constant

For deposition, the time constant is

$$t_c = \text{larger of} \begin{cases} \Delta t \\ \text{or} \\ \dfrac{C_d h}{V_s} \end{cases} \tag{A18}$$

and for erosion it is

$$t_c = \text{larger of} \begin{cases} \Delta t \\ \text{or} \\ \dfrac{C_e h}{U} \end{cases} \tag{A19}$$

where

Δt = computational time-step
C_d = response time coefficient for deposition
V_s = sediment settling velocity
C_e = response time coefficient for erosion

The sand bed has a specified initial thickness which limits the amount of erosion to that thickness.

Cohesive sediments transport

Cohesive sediments (usually clays and some silts) are considered to be depositional if the bed shear stress exerted by the flow is less than a critical value τ_d. When that value occurs, the deposition rate is given by Krone's (1962) equation

$$S = \begin{cases} -\frac{2V_s}{h} C \left(1 - \frac{\tau}{\tau_d}\right) \text{ for } C < C_c & \text{(A20)} \\ -\frac{2V_s}{hC_c^{4/3}} C^{5/3} \left(1 - \frac{\tau}{\tau_d}\right) \text{ for } C > C_c & \text{(A21)} \end{cases}$$

where

S = source term
V_s = fall velocity of a sediment particle
h = flow depth
C = sediment concentration in water column
τ = bed shear stress
τ_d = critical shear stress for deposition
C_c = critical concentration = 300 mg/ℓ

If the bed shear stress is greater than the critical value for particle erosion τ_e, material is removed from the bed. The source term is then computed by Ariathurai's (Ariathurai, MacArthur, and Krone 1977) adaptation of Partheniades' (1962) findings:

$$S = \frac{P}{h}\left(\frac{\tau}{\tau_e} - 1\right) \text{ for } \tau > \tau_e \qquad \text{(A22)}$$

where P is the erosion rate constant, unless the shear stress is also greater than the critical value for mass erosion. When this value is exceeded, mass failure of a sediment layer occurs and

$$S = \frac{T_L P_L}{h\Delta T} \text{ for } \tau > \tau_s \qquad \text{(A23)}$$

where

T_L = thickness of the failed layer

P_L = density of the failed layer
Δt = time interval over which failure occurs
τ_s = bulk shear strength of the layer

The cohesive sediment bed consists of 1 to 10 layers, each with a distinct density and erosion resistance. The layers consolidate with overburden and time.

Bed shear stress

Bed shear stresses are calculated from the flow speed according to one of four optional equations: the smooth-wall log velocity profile or Manning equation for flows alone; and a smooth bed or rippled bed equation for combined currents and wind waves. Shear stresses are calculated using the shear velocity concept where

$$\tau_b = \rho u_*^2 \tag{A24}$$

where
τ_b = bed shear stress
u_* = shear velocity

and the shear velocity is calculated by one of four methods:

a. Smooth-wall log velocity profiles

$$\frac{\bar{u}}{u_*} = 5.75 \log\left(3.32 \frac{u_* h}{\nu}\right) \tag{A25}$$

which is applicable to the lower 15 percent of the boundary layer when

$$\frac{u_* h}{\nu} > 30$$

where u is the mean flow velocity (resultant of u and v components)

b. The Manning shear stress equation

$$u_* = \frac{(\bar{u}n)\sqrt{g}}{CME\ (h)^{1/6}} \tag{A26}$$

where *CME* is a coefficient of 1 for SI (metric) units and 1.486 for non-SI units of measurement.

c. A Jonsson-type equation for surface shear stress (plane beds) caused by waves and currents

$$u_* = \sqrt{\frac{1}{2}\left(\frac{f_w u_{om} + f_c \bar{u}}{u_{om} + \bar{u}}\right)(\bar{u} + u_{om})^2} \tag{A27}$$

where

f_w = shear stress coefficient for waves
u_{om} = maximum orbital velocity of waves
f_c = shear stress coefficient for currents

d. A Bijker-type equation for total shear stress caused by waves and current

$$u_* = \sqrt{\frac{1}{2} f_c \bar{u}^2 + \frac{1}{4} f_w u_{om}^2} \tag{A28}$$

Solution method

Equation A5 is solved by the finite element method using Galerkin weighted residuals. Like RMA-2V, which uses the same general solution technique, elements are quadrilateral and may have parabolic sides. Shape functions are quadratic. Integration in space is Gaussian. Time-stepping is performed by a Crank-Nicholson approach with a weighting factor (θ) of 0.66. A front-type solver similar to that in RMA-2V is used to solve the simultaneous equations.

The Water Quality Transport Model, RMA4

Applications

The water quality model, RMA4, is designed to simulate the depth-average convection-diffusion process in most water bodies with a free surface. The model is used for investigating the physical processes of migration and mixing of a soluble substance in reservoirs, rivers, bays, estuaries and coastal zones. The model is useful for evaluation of the basic processes or for defining the effectiveness of remedial measures. For complex geometries the model uses the depth-averaged hydrodynamics from RMA2.

The water quality model has been applied to define horizontal salinity distribution; to trace temperature effects from power plants; to calculate residence times of harbors or basins; to optimize the placement of outfalls; to identify potential critical areas for oil spills or other pollutants spread; to evaluate turbidity plume extent; and to monitor other water quality criteria within game and fish habitats.

Limitations

The formulation of RMA4 is limited to one-dimensional (cross-sectionally averaged) and two-dimensional (depth-averaged) situations in which the concentration is fairly well-mixed in the vertical. It will not provide accurate concentrations for stratified situations in which the constituent concentration influences the density of the fluid. In addition, the accuracy of the transport model is dependent on the accuracy of the hydrodynamics (e.g. as supplied from RMA2).

Governing Equations

The CEWES version of RMA4 is a revised version of RMA4 as developed by King (1989). The generalized computer program solves the depth-integrated equations of the transport and mixing process. The form of the equations solved is:

$$h\left(\frac{\partial c}{\partial t} + u\frac{\partial c}{\partial x} + v\frac{\partial c}{\partial y} - \frac{\partial}{\partial x}D_x\frac{\partial c}{\partial x} - \frac{\partial}{\partial y}D_y\frac{\partial}{\partial y} - \sigma + kc\right) = 0 \qquad \text{(A29)}$$

where

h = water depth
c = constituent concentration
t = time
u, v, = velocity components

D_x, D_y, = turbulent mixing coefficients
k = first order decay
σ = source/sink of constituent

Note that the basic governing equation for RMA4 is the same as for the sediment transport model, STUDH. The differences between the two models lies in the source/sink terms and bed modeling in STUDH.

Equation A29 is solved by the finite element method using Galerkin weighted residuals. As with the hydrodynamic model, RMA2, the transport model RMA4 handles one-dimensional segments or two-dimensional quadrilaterals or triangles with the option for curved sides. Spatial integration of the equations is performed by Gaussian techniques and the temporal variations are handled by nonlinear finite differences, consistent with the method described in paragraph 15, above. The frontal solution method is also used in RMA4, as with the other programs in the TABS-MD system, to provide an efficient solution algorithm.

The boundary conditions for RMA4 are specified in several optional ways. The boundary concentration may be specified absolutely at a certain level regardless of the flow direction; the concentration can be specified to be applied only when the water is leaving the model; or a mixing zone may be specified just beyond the model boundary to provide the possibility of reentrainment of constituent into the model that may have crossed the boundary earlier. For a more detailed description of the constituent transport model, RMA4, see King and Rachiele (1989).

Within the one-dimensional formulation of the model, there is a provision for defining the constituent concentration mixing and transport at control structures as they may have been specified in RMA2. These allow for either a flow-through condition, as for example for a weir type flow, or for a mixing chamber type of flux, which would be appropriate for a navigation lock.

References

Ackers, P., and White, W. R. 1973. (Nov). "Sediment Transport: New Approach and Analysis," *Journal, Hydraulics Division, American Society of Civil Engineers*, Vol 99, No. HY-11, pp 2041-2060.

Ariathurai, R., MacArthur, R. D., and Krone, R. C. 1977 (Oct). "Mathe-- matical Model of Estuarial Sediment Transport," Technical Report D-77-12, U.S. Army Engineer Waterways Experiment Station, Vicksburg, MS.

King, Ian P., December 1988, "Program Documentation: RMA2- A Two-Dimensional Finite Element Model for Flow in Estuaries and Streams; Version 4.2," Resource Management Associates, Lafayette, Ca.

Krone, R. B. 1962. "Flume Studies of Transport of Sediment in Estuarial Shoaling Processes," Final Report, Hydraulics Engineering Research Laboratory, University of California, Berkeley, CA.

Norton, W. R., and King, I. P. 1977 (Feb). "Operating Instructions for the Computer Program RMA-2V," Resource Management Associates, Lafayette, CA.

Partheniades, E. 1962. "A Study of Erosion and Deposition of Cohesive Soils in Salt Water," Ph.D. Dissertation, University of California, Berkeley, CA.

Swart, D. H. 1976 (Sep). "Coastal Sediment Transport, Computation of Longshore Transport," R968, Part 1, Delft Hydraulics Laboratory, The Netherlands.

Thomas, W. A., and McAnally, W. H., Jr. 1985 (Aug). "User's Manual for the Generalized Computer Program System; Open-Channel Flow and Sedimentation, TABS-2, Main Text and Appendices A through O," Instruction Report HL-85-1, U.S. Army Engineer Waterways Experiment Station, Vicksburg, MS.

White, W. R., Milli, H., and Crabbe, A. D. 1975. "Sediment Transport Theories: An Appraisal of Available Methods," Report Int 119, Vols 1 and 2, Hydraulics Research Station, Wallingford, England.

REPORT DOCUMENTATION PAGE

Form Approved
OMB No. 0704-0188

1. AGENCY USE ONLY (Leave blank)	2. REPORT DATE	3. REPORT TYPE AND DATES COVERED
	August 1993	Final report

4. TITLE AND SUBTITLE

Grand and White Lakes Flood Control Project; Numerical Model Investigation

5. FUNDING NUMBERS

6. AUTHOR(S)

Joseph V. Letter, Jr.

7. PERFORMING ORGANIZATION NAME(S) AND ADDRESS(ES)

U.S. Army Engineer Waterways Experiment Station
Hydraulics Laboratory
3909 Halls Ferry Road, Vicksburg, MS 39180-6199

8. PERFORMING ORGANIZATION REPORT NUMBER

Technical Report
HL-93-11

9. SPONSORING/MONITORING AGENCY NAME(S) AND ADDRESS(ES)

U.S. Army Engineer District, New Orleans
P.O. Box 60267
New Orleans, LA 70160-0267

10. SPONSORING/MONITORING AGENCY REPORT NUMBER

11. SUPPLEMENTARY NOTES

Available from National Technical Information Service, 5285 Port Royal Road, Springfield, VA 22161.

12a. DISTRIBUTION/AVAILABILITY STATEMENT

Approved for public release; distribution is unlimited.

12b. DISTRIBUTION CODE

13. ABSTRACT *(Maximum 200 words)*

The Grand and White Lakes flood control project provides protection over a broad portion of the Louisiana coastline. The study area involves a wide variety of wetlands and complex canals and waterways. The area supports many economic interests with potentially conflicting desires for management of the water resources. The project required the capability of quantitatively estimating the relative performance of a large number of design alternatives.

Numerical modeling techniques capable of addressing the flood routing and salinity intrusion processes required to evaluate project alternatives were developed. These techniques included the specification of control structures within the one-dimensional finite element formulation, utilization of marsh porosity, discretization of complex spatial geometric features of the wetlands, and the use of one-dimensional networking in conjunction with the two-dimensional finite element formulation.

Numerical testing was performed for eighteen separate design alternatives for the system. Flood events with 2-, 5-, 10-, 25- and 50-year return intervals were simulated and stage exceedance curves generated. Salinity

(Continued)

14. SUBJECT TERMS		15. NUMBER OF PAGES
Flood control	Mermentau River	124
Grand and White Lakes	Multidimensional modeling	16. PRICE CODE
Marsh porosity	Salinity intrusion	

17. SECURITY CLASSIFICATION OF REPORT	18. SECURITY CLASSIFICATION OF THIS PAGE	19. SECURITY CLASSIFICATION OF ABSTRACT	20. LIMITATION OF ABSTRACT
UNCLASSIFIED	UNCLASSIFIED		

13. (Concluded).

intrusion testing was performed for the influence of marine organism ingress structures on the upstream basin. The results of the testing showed that the marine ingress structures should be very modest in size if salinity intrusion problems are to be avoided. The flood control testing suggested that the optimum location of the increased flow capacity should be near the mouth of the primary tributary, the Mermentau River, or else extensive channelization would have to accompany an alternate location.